

Universidade do Minho
Escola de Ciências

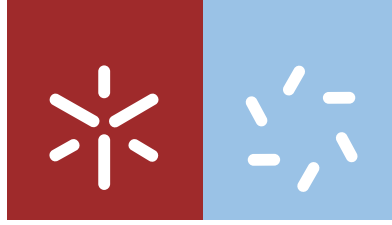
Ana Rita Sobreiro Almeida

**Mesenchymal stem cells culture on
poly(vinylidene fluoride)
piezoelectric microspheres**

Ana Rita Sobreiro Almeida **Mesenchymal stem cells culture on poly(vinylidene fluoride) piezoelectric microspheres**

UMinho | 2015

outubro de 2015



Universidade do Minho
Escola de Ciências

Ana Rita Sobreiro Almeida

**Mesenchymal stem cells culture on
poly(vinylidene fluoride)
piezoelectric microspheres**

Dissertação de Mestrado
Mestrado em Biofísica e Bionanossistemas

Trabalho efetuado sob a orientação do
Professor Doutor José Luis Gómez-Ribelles
e do
Professor Doutor Senentxu Lanceros-Méndez

outubro de 2015

DECLARAÇÃO

Nome

Ana Rita Sobreiro Almeida

Endereço de correio eletrónico: rita.isaias.almeida@hotmail.com

Telefone: 916630635

Número de identificação civil: 14171142

Título da dissertação de mestrado

“Mesenchymal stem cells culture on poly(vinylidene fluoride) piezoelectric microspheres”

Orientadores

Professor Doutor José Luis Gómez-Ribelles

Professor Doutor Senentxu Lanceros-Méndez

Ano de conclusão: 2015

Designação do Mestrado

Mestrado em Biofísica e Bionanossistemas

1. É AUTORIZADA A REPRODUÇÃO INTEGRAL DESTA DISSERTAÇÃO APENAS PARA EFEITOS DE INVESTIGAÇÃO, MEDIANTE DECLARAÇÃO ESCRITA, QUE A TAL SE COMPROMETE;

Universidade do Minho, 28 de Outubro de 2015

Assinatura: _____

AGRADECIMENTOS

Todo o trajeto percorrido ao longo destes dois anos de mestrado enriqueceu-me não só a nível de conhecimento mas também a nível pessoal. Por isso, quero agradecer a todas as pessoas que tornaram esta conquista possível, porque sem elas, nem 1 das 25000 palavras que compõem dissertação se ia escrever.

Primeiramente, às universidades que me acolheram, a Universidade do Minho e a Universitat Politècnica de València, desafiaram-me primeiro a viver em duas cidades novas e conseguir adaptar-me. Foram dois anos de aquisição de conhecimento, de muito esforço e desafios que permitiram testar a minha capacidade de resistência e gestão do tempo. Entre trabalhos, houve também tempo para disfrutar das melhores coisas que ofereciam, entre elas a multiculturalidade proporcionada pelo ambiente de Erasmus em que me inseri. Um obrigada a este programa igualmente!

Depois, e principalmente em ambiente de dissertação, obrigada ao Professor José Luis Gómez Ribelles por me aceitar como orientanda e por, entre o pouco tempo que tinha, conseguir dar-me o apoio necessário e discutir comigo todos os aspetos relevantes da minha dissertação. Não posso deixar de referir o entusiasmo pela ciência e a motivação que me dava nos momentos mais difíceis. Não me esqueço, também, de todo o grupo de investigação do Centro de Biomateriales y Ingeniería Tisular, incansáveis e extraordinariamente prestáveis, principalmente à Maria Noel que mesmo não sendo orientadora, agiu como tal todo o ano e com ela aprendi a trabalhar em investigação.

Também quero deixar algumas palavras de agradecimento ao Professor Senentxu Lanceros-Méndez, sempre pronto a ajudar e a orientar da melhor forma possível, uma mente brilhante que contagia de boa disposição e entusiasmo qualquer pessoa do seu grupo de trabalho, Electroactive Smart Materials, que juntos fazem com que os momentos de seriedade laboral sejam mais leves e dá gosto trabalhar assim. Deste grupo, não posso deixar de destacar a Dra. Clarisse Ribeiro, que mesmo estando longe foi um apoio incansável todo o ano, sendo uma das principais pessoas envolvidas nesta dissertação, mesmo não possuindo o título oficial de orientadora. Muito obrigada!

Ao apoio dos amigos, foram as principais pessoas a que recorri durante o meu percurso de mestrado, principalmente a Ana Lima e à Catarina Malheiro, pelos trabalhos e apresentações de grupo infinitas e pelas horas de estudo (queima de neurónios) em conjunto! Por fim, um especial obrigado

à Margarida, que me acompanhou nos bons e maus momentos desde o início de todo o percurso académico até ao último dia do programa de Erasmus. Obrigada por ouvires a descarga de frustrações ao fim do dia durante 5 anos. No fundo sabes mais de Engenharia de Tecidos que todos os teus amigos das plantas... Obrigada!

À família, são tudo para mim. Aos meus avós, principalmente. Faço isto por mim e por vocês. O principal apoio e refúgio que tenho, nunca me fecham os braços e olham para mim com tanto orgulho, que me encham o coração de força para continuar.

Finalmente, aos meus pais. Que dizer para vos agradecer, as páginas desta tese não bastam. Ao meu pai, que me transmitiu todos os princípios, teimosia e orgulho que tenho. Faz-me ser uma pessoa melhor, mais ambiciosa e dá-me força para lutar e defender-me da melhor maneira que posso em qualquer ambiente. À minha mãe, a base de toda a minha vida. Está sempre a viver todos os segundos de alegria que tenho, e se choro ela também chora por dentro. Tenho o teu espírito de guerreira em mim, tenho esta robustez, energia, resistência porque foste tu que ma incutiste. És o meu maior exemplo, a minha melhor amiga e em cada palavra que trocamos, tu descansas-me por dentro e relembras-me que consigo lutar ainda mais. Obrigada aos dois pelos conselhos, por me lembrarem de quem sou, por me fazerem esquecer o que se passa à minha volta quando chego a casa. Foram essenciais nestes dois anos. São os únicos que sabem o quanto trabalhei para chegar onde estou e que não me fico por aqui. Muito, muito obrigada!

RESUMO

Nos últimos anos, as células estaminais mesenquimais (CEM's) têm sido foco de interesse na comunidade científica devido à sua capacidade de diferenciação em diferentes linhagens celulares, tais como adipócitos, osteoblastos e condrócitos. Neste trabalho, CEM's humanas foram combinadas com poli(fluoreto de vinilideno), PVDF, um polímero piezoelétrico biocompatível, de modo a impulsionar a sua expansão e proliferação *in vitro*, com o objetivo principal de obter um substancial número de células com fenótipo osteoblástico para regeneração de tecidos.

Com este propósito, filmes de PVDF em fase α foram submetidos a *electrospray* com diferentes tempos de deposição, dando origem a dois substratos, com alta e baixa concentração de micropartículas de β -PVDF. Foram também produzidas micropartículas sem substrato com vista a criar um ambiente 3D e filmes planos de β -PVDF foram usados como referência. Antes do cultivo celular, os marcadores superficiais celulares característicos de CEM's (CD105, CD90 e CD73) foram analisados por citometria de fluxo (CF). Quatro dias depois de serem cultivadas nos biomateriais, a viabilidade celular foi examinada. Em paralelo, CF, microscopia eletrónica de varrimento (MEV) e ensaios de imunocitoquímica de vinculina foram realizados de modo a avaliar a manutenção da multipotencialidade das CEM's e a sua morfologia nos diferentes substratos. Quando a confluência celular foi atingida, foi introduzido um meio de diferenciação osteogénico e o cultivo continuou por 14 dias. Finalmente, CF e um ensaio de imunocitoquímica de osteocalcina foram realizados de modo a avaliar como as diferentes topografias dos biomateriais influenciavam a diferenciação osteogénica.

A primeira análise de CF confirmou que as células utilizadas eram CEM's humanas. No quarto dia, os resultados de MTS mostraram que a proliferação foi similar em todos os substratos. A MEV e o ensaio de imunocitoquímica de vinculina mostraram que as CEM's adotaram diferentes morfologias dependendo do biomaterial. Adicionalmente, CF mostrou uma perda de marcadores específicos das CEM's em meio de expansão e 14 dias depois da introdução de meio osteogénico, as células cultivadas nos filmes planos e com micropartículas revelaram existência de osteocalcina e perda de marcadores.

Concluindo, as novas topografias com micropartículas de PVDF permitiram um incremento na diferenciação de CEM's. As células proliferaram satisfatoriamente e a morfologia adotada nos substratos sugere aderência às microesferas. Concluindo, estes suportes mostraram induzir perda de multipotencialidade das CEM's cultivadas em meio de expansão, mesmo antes da confluência celular.

ABSTRACT

Mesenchymal Stem Cells (MSCs) have attracted great interest in the scientific community in the past few years due to their differentiation potential towards cells belonging to the musculoskeletal lineages, such as adipocytes, osteoblasts, and chondrocytes. In this work, human MSCs were combined with poly(vinylidene fluoride) (PVDF), a biocompatible piezoelectric polymer, allowing their *in vitro* expansion and proliferation, with the main goal of obtaining an important number of cells with osteoblastic phenotype for tissue regeneration.

With this purpose, α -phase PVDF films were subjected to PVDF electro spray with different deposition times, producing two substrates, with high and low concentration of β -phase PVDF microspheres. Microspheres only were also produced to create a 3D environment. Flat β -phase films were used as reference. Before cell seeding, the characteristic cell surface markers of MSCs (CD105, CD90 and CD73) were analyzed by flow cytometry (FC). Cells were cultured onto the biomaterials and viability was assessed after 4 days. In parallel, FC, Scanning Electron Microscopy (SEM) and immunocytochemistry of vinculin were performed in order to evaluate the maintenance of MSCs multipotentiality and their morphology on the different substrates. When the confluence was reached, osteogenic differentiation medium was introduced and the culture was continued for 14 days. Finally, FC and an osteocalcin immunocytochemistry were performed in order to evaluate if the different substrate morphologies influenced MSCs osteogenic differentiation.

First FC analysis confirmed that cells were actually human mesenchymal stem cells. At the fourth day, MTS results showed similar proliferation in all the substrates. SEM and vinculin immunocytochemistry have shown that a different morphology was adopted by MSCs depending on the substrate. Also, FC indicated loss of specific MSCs markers in expansion medium. After 14 days of osteogenic medium introduction, cells cultured on flat films and films with microspheres revealed osteocalcin staining and again, loss of multipotentiality.

Concluding, this new shaped PVDF microspheres substrates were able to enhance hMSC's differentiation. Cells proliferated at high rate and their morphology in the substrates suggests that these cells are adhering onto microspheres. Moreover, these supports' topography induces loss of multipotentiality in MSCs cultured in expansion medium, even before reaching confluence.

TABLE OF CONTENTS

AGRADECIMENTOS	III
RESUMO	V
ABSTRACT	VII
TABLE OF CONTENTS	IX
LIST OF FIGURES	XI
LIST OF TABLES	XIII
LIST OF ABBREVIATIONS	XV
1 INTRODUCTION	1
1.1 ELECTROACTIVE POLYMERS AND “ACTIVE” TISSUE ENGINEERING	2
1.2 POLY(VINYLDIENEFLUORIDE) AS A POLYMER OF CHOICE: PROPERTIES AND HANDLING	5
1.3 DESIGN AND DEVELOPMENT OF SCAFFOLDS/BIOMATERIALS FOR TISSUE ENGINEERING APPLICATIONS	6
1.3.1 INTERACTION BETWEEN CELLS AND BIOMATERIALS	7
1.3.2 ELECTROSPRAYING	8
1.4 MESENCHYMAL STEM CELLS	10
1.4.1 MINIMAL CRITERIA FOR DEFINING MESENCHYMAL STEM CELLS	11
1.4.2 OSTEOGENIC DIFFERENTIATION	14
1.5 STATE-OF-ART	16
1.5.1 OSTEOGENIC DIFFERENTIATION ON MICROSPHERES SCAFFOLDS	16
1.5.2 OSTEOGENIC DIFFERENTIATION ON POLY(VINYLDIENEFLUORIDE)-BASED BIOMATERIALS	18
1.6 STRUCTURE OF THE THESIS	21
2 OBJECTIVES	23
3 MATERIALS & METHODS	25
3.1 PROCESSING OF POLY(VINYLDIENEFLUORIDE) MICROSPHERES	25
3.2 PROCESSING OF POLY(VINYLDIENEFLUORIDE) MICROSPHERES FILMS	26
3.3 MATERIALS STERILIZATION	26
3.4 FIBRONECTIN ADSORPTION	26
3.5 CHARACTERIZATION OF POLY(VINYLDIENEFLUORIDE) SAMPLES	26
3.5.1 FIELD EMISSION SCANNING ELECTRON MICROSCOPY	26

3.5.2	FOURIER TRANSFORM INFRARED SPECTROSCOPY	27
3.5.3	DIFFERENTIAL SCANNING CALORIMETRY	28
3.6	EXTRACTION OF HUMAN MESENCHYMAL STEM CELLS AND PRIMARY CULTURE	29
3.6.1	HUMAN BONE MARROW SAMPLE EXTRACTION	29
3.6.2	DENSITY GRADIENT CENTRIFUGATION	29
3.6.3	PRIMARY HUMAN MESENCHYMAL STEM CELLS CULTURE	29
3.7	CELL CULTURE CONDITIONS	30
3.8	STUDY OF CELL VIABILITY	31
3.9	STUDY OF CELLS ADHESION	31
3.10	STUDY OF CELLS MORPHOLOGY	32
3.11	FLOW CYTOMETRY STUDY	32
3.12	OSTEOCALCIN IMMUNOCYTOCHEMISTRY	34
4	RESULTS AND DISCUSSION	35
4.1	ELECTROSPRAYED MICROSPHERES MORPHOLOGY AND SIZE DISTRIBUTION	35
4.2	POLY(VINYLIDENEFLUORIDE) PHASE CONTENT	36
4.3	THERMAL CHARACTERIZATION	39
4.4	CELL ATTACHMENT AND MORPHOLOGY	40
4.5	CELL VIABILITY	46
4.6	FLOW CYTOMETRY ANALYSIS	47
4.7	ASSESSMENT OF HUMAN MESENCHYMAL STEM CELLS OSTEOGENIC DIFFERENTIATION	51
4.7.1	FLOW CYTOMETRY ANALYSIS	51
4.7.2	OSTEOCALCIN LOCALIZATION BY IMMUNOCYTOCHEMISTRY	55
5	CONCLUSIONS, FINAL REMARKS & FUTURE PERSPECTIVES	59
6	BIBLIOGRAPHY	61

LIST OF FIGURES

1 INTRODUCTION

- Figure 1.1** – Tissue engineering triad. Cells of interest, signals – provided chemically by growth factors or physically by a bioreactor – and the scaffold which acts as a template for tissue formation by allowing cells to migrate, adhere, and produce tissue [4]. _____ 2
- Figure 1.2** – Strategies for the new “active” tissue engineering concept with bioreactors [24]. _____ 4
- Figure 1.3** – A) Schematic representation of the chain conformation for the α , β and γ phases of PVDF [15]. B) Obtaining the β -phase conformation of PVDF. Schematic of the molecular shape change [14]. _____ 6
- Figure 1.4** – A) Schematic of the typical electro spraying setup [49]. B) The Taylor Cone, from which a jet of charged particles emanates above a threshold voltage [54]. _____ 9
- Figure 1.5** – The progeny of a MSC can be induced into one of the several mesenchymal lineage pathways [62]. _____ 10
- Figure 1.6** – The four types of cells found within the bone matrix. Osteogenic cells are undifferentiated and can develop to osteoblasts. Osteoblasts intervene in bone formation and when they get trapped within the self-calcified matrix, they become osteocytes, which have a different structure and function. They maintain the matrix mineral concentration via secretion of enzymes. Osteoclasts are very different in appearance from the other cells and develop from monocytes and macrophages. The latter resorb old bone [149]. _____ 15
- Figure 1.7** – Relative amounts of ALP activity of stem cells cultured on β -PVDF samples in two different studies. A) [116]; B) [117]. _____ 18

3 MATERIALS & METHODS

- Figure 3.1** – Representation of the electro spray equipment installation utilized in this work. _____ 25
- Figure 3.2** – Isolation of hMSC's from a BM biopsy. The whole BM is centrifuged and the mononucleated cells are separated from the red blood cells by ficoll gradient centrifugation. Then, the hMSC's are separated from the other mononucleated cells (lymphocytes or monocytes) by plastic adherence in culture [128]. _____ 30

4 RESULTS AND DISCUSSION

- Figure 4.1** – Morphology of the PVDF microspheres obtained. A) and B) Microspheres only; C) High density concentration of microspheres electro sprayed in α -PVDF film; D) Low density concentration of microspheres electro sprayed in α -PVDF film. Scales: A) 2 μ m; B) 1 μ m; C) 10 μ m; D) 10 μ m. _____ 35
- Figure 4.2** – Microspheres size distribution obtained for the described electro spray conditions. _____ 36
- Figure 4.3** – FTIR spectra of the β -phase PVDF film and microspheres. _____ 38
- Figure 4.4** – DSC thermogram of the PVDF commercial film and of the PVDF microspheres obtained by electro spray method. _____ 39

Figure 4.5 – Overall cell morphology of hMSC's analyzed by SEM. A) and B) films with low density of PVDF microspheres; C) and D) films with high density of PVDF microspheres; E) alpha film; F) microspheres only.	41
Figure 4.6 – Confocal fluorescence microscopy images of hMSC's after 4 days of cell culture in A) glass covers, B) β -PVDF film C) films with high density of PVDF microspheres, D) films with low density of PVDF microspheres. The scale bar (100 μ m) is valid for all the images.	43
Figure 4.7 – Confocal fluorescence microscopy reconstructed 3D image of the hMSC's after 4 days of cell culture on the β -PVDF microspheres. Each green cross is distanced 50 μ m from the next one, as indicated by the scale bar.	44
Figure 4.8 – Schematic representation of how cell shape and RhoA signaling or cytoskeletal tension alters hMSC's commitment [138].	45
Figure 4.9 – Cell viability for cells seeded on the PVDF samples and cells seeded on glass covers (control +). Results are expressed as mean \pm standard deviation with n = 3. *P \leq 0.05, **P \leq 0.01 vs. Glass.	46
Figure 4.10 – Histograms of the hMSC's (passage 4) flow cytometry analysis at day 0 of cell culture.	47
Figure 4.11 – Histograms of cells seeded in TCPS at day 4 compared to: A – day 0 cells before seeding; B – cells seeded on β -PVDF film at day 4; C – cells seeded on HD-M film at day 4; D – cells seeded on LD-M film at day 4.	48
Figure 4.12 – Histogram of cells seeded in TCPS at day 4 compared to β -PVDF film. The color legend is the same as Figure 4.11.	50
Figure 4.13 – Histograms of cells seeded on TCPS at day 7 compared to cells seeded on TCPS at day 4 before OS medium introduction. A – Cells seeded in basal medium; B – cells seeded in OS medium.	51
Figure 4.14 – Histograms TCPS seeded cells at day 14 compared to TCPS seeded cells at day 4 with and without OS medium.	53
Figure 4.15 – Histograms TCPS seeded cells at day 14 compared materials' seeded cells at day 14. All samples and control were cultured with osteogenic medium. A – HD-M film; B – LD-M film; C – β -film.	54
Figure 4.16 – Confocal fluorescence microscopy images of cells after 14 days of cell culture in: A) glass; B) β -PVDF film; C) HD-M PVDF film; D) LD-M PVDF film. The scale bar (100 μ m) is valid for all images.	56
Figure 4.17 – Confocal fluorescence microscopy image of cells after 14 days of 3D cell culture on PVDF microspheres.	57

LIST OF TABLES

1 INTRODUCTION

Table 1.1 – Summary of the main characteristics of electronic and ionic EAPs. _____	3
Table 1.2 – Negative and Positive markers as proposed by the ISCT. Adapted from [71]. _____	14
Table 1.3 – Review of studies that have been done with PVDF as a suitable material for bone regeneration or osteogenic differentiation and their specific results. _____	20

3 MATERIALS & METHODS

Table 3.1 – Antibodies used against cell-surface antigens to characterize hMSC's. FITC - Fluorescein isothiocyanate; PE – Phycoerythrin; PerCP-Cy5.5 – Peridinin-chlorophyll protein-cyanine5.5; APC – Allophycocyanin. _____	33
Table 3.2 – Controls performed in flow cytometry analysis. The purpose of the controls at 7 and 14 days are to compare them to cells cultured on the PVDF samples, which are already growing under differentiation medium. _____	34

4 RESULTS AND DISCUSSION

Table 4.1 – Characteristic absorption FTIR bands of different PVDF phases [15]. _____	37
--	----

LIST OF ABBREVIATIONS

#

2D – Two dimension

3D – Three dimension

β and α -PVDF – beta and alpha phase

Polyvinylidene Fluoride

A

ALP – Alkaline Phosphatase

APC – Allophycocyanin

AR – Alizarin Red

AT – Adipose Tissue

ATR – Attenuated Total Reflectance

B

BM – Bone Marrow

BSA – Bovine Serum Albumin

C

CD – Cluster of Differentiation

D

DAPI – (4',6-diamidino-2-phenylindole)

DMEM – Dulbecco's Modified Eagle Medium

DPBS – Dulbecco's Phosphate-Buffered Saline

DSC – Differential Scanning Calorimetry

E

EAP – Electroactive Polymer

ECM – Extracellular Matrix

F

FC – Flow Cytometry

FE – Field Emission

FITC – Fluorescein isothiocyanate

FN – Fibronectin

FTIR – Fourier Transform Infrared Spectroscopy

G

GPI – Glycophosphatidylinositol

H

h - hour

HD-M – PVDF film electrosprayed with a high density of β -PVDF microspheres

HLA – Human Leukocyte Antigen

hMSC – human Mesenchymal Stem Cell

I

ISCT – International Society for Cellular Therapy

L

LD-M – PVDF film electrospayed with a low density of β -PVDF microspheres

M

MEM- α – Minimum Essential Medium Alpha

MHC – Major Histocompatibility Complex

min – minute

mm – millimeters

mM – millimolar

MS – Microspheres

MSC – Mesenchymal Stem Cell

MTS – (3-(4,5-dimethylthiazol-2-yl)-5-(3-carboxymethoxyphenyl)-2-(4-sulfophenyl)-2H-tetrazolium)

N

nm – nanometers

O

OS – Osteogenic Supplements

P

P/S – Penicillin-Streptomycin

PBMC's – Peripheral Blood Mononuclear Cells

PBS – Phosphate-Buffered Saline

PE – Phycoerythrin

PerCP-Cy5.5 – Peridinin chlorophyll protein-cyanine5.5

PVDF – Polyvinylidene Fluoride

R

Ref - Reference

RT – Room Temperature

rpm – revolutions per minute

S

s – second

SEM – Scanning Electron Microscopy

T

TCPS – Tissue Culture Polystyrene

TE – Tissue Engineering

TGF- β – Transforming Growth Factor Beta

U

UV – Ultraviolet

1 INTRODUCTION

Biomedical engineering has been defined as an extension of chemical engineering towards biomaterials [1]. Tissue Engineering (TE) is one of its main branches. Various disciplines, such as materials science, cell biology, reactor engineering, as well as clinical research contribute to tissue engineering.

The development in the TE field – in which new tissues are created from cultured cells and biomaterials – has been driven by the shortage of donor tissue, that limits the number of people who receive life-saving organ and tissue transplantations [2]. Biomaterials serve both as a transplant vehicle for the cells of interest and as template guiding tissue regeneration. These are named scaffolds and may also be utilized to deliver specific biological factors which will induce new tissue formation from cells already present in the surrounding tissue [3].

TE field relies extensively on the use of porous 3D scaffolds to provide the appropriate environment for the regeneration of tissues and organs. These scaffolds are seeded with cells and growth factors or subjected to biophysical stimuli in the form of a bioreactor – a device or system which applies different types of mechanical or chemical stimuli to cells (Figure 1.1) [4]. The extracellular matrix (ECM) secreted by the living cells will create a suitable environment, enhancing the native capacity of cells to integrate, proliferate and differentiate [5]. The addition of growth factors and other ECM components should also promote the intercellular communication and attachment of cells to the scaffold, inducing proliferation [6].

To fabricate these scaffolds, a variety of biomaterials, including synthetic polymers, ceramics and naturally derived proteins are being utilized. Also, biological materials such as collagen, proteoglycans, alginate-based substrates and chitosan have all been used in the production of scaffolds for tissue engineering [7]–[9]. They are biodegradable and so allow host cells to produce their own ECM over time and replace the degraded scaffold. Moreover, they are biologically active and promote excellent cell adhesion and growth. However, fabricating scaffolds from biological materials with homogeneous and reproducible structures presents a challenge. In addition, the scaffolds generally have poor mechanical properties, which limits their use [4].

Therefore, in the past few years, synthetic polymers are being increasingly used for therapeutics and it is believed that many further developments in medicine will be achieved thanks to such materials [10].

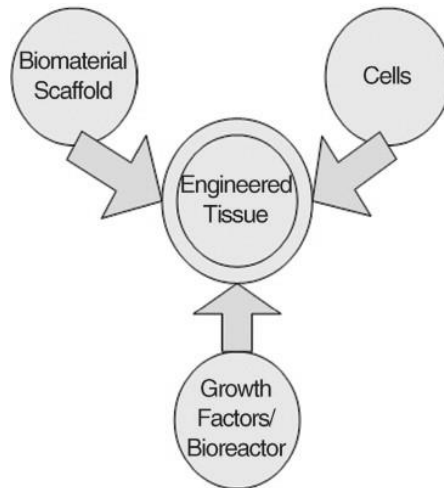


Figure 1.1 – Tissue engineering triad. Cells of interest, signals – provided chemically by growth factors or physically by a bioreactor – and the scaffold which acts as a template for tissue formation by allowing cells to migrate, adhere, and produce tissue [4].

1.1 ELECTROACTIVE POLYMERS AND “ACTIVE” TISSUE ENGINEERING

Polymers have attractive properties compared to inorganic materials. They are lightweight, inexpensive, fracture tolerant and easily processed and manufactured. They can be configured into complex shapes and their properties can be tailored according to demand [11]. A variety of synthetic polymers such as poly(lactic acid) (PLA), poly(glycolic acid) (PGA), poly(lactic-co-glycolic acid) (PLGA), poly(ethylene glycol) (PEG) and polycaprolactone (PCL) have been widely used to produce biomaterials/scaffolds for tissue engineering [12].

With the rapid advances in materials used in science and technology, various materials with intelligence embedded at the molecular level are being developed at a fast pace. These smart materials can sense variations in the environment, process the information and respond accordingly; in other words, they can respond to external stimuli – such as electrical field, pH, a magnetic field, and light – by changing shape or size [13]. These smart polymers can collectively be called *active* polymers.

Polymers that respond mechanically to electrical stimulation are called electroactive polymers (EAP) and are classified depending on the mechanism responsible for actuation. They are divided as electronic EAPs – which are driven by electric field or coulomb forces – or as ionic EAPs – which change shape by mobility or diffusion of ions and their conjugated substances [14]. Their electromechanical response, exhibiting large strain when subjected to electrical stimulation, makes them the human-made actuators that most closely imitate natural muscles. For this ability, EAP

materials have earned the name “artificial muscles” [11]. Their main characteristics are resumed in Table 1.1.

Table 1.1 – Summary of the main characteristics of electronic and ionic EAPs.

Electronic EAPs	<ul style="list-style-type: none"> ▪ Require high activation fields ($>100 \text{ V}\cdot\mu\text{m}^{-1}$), which are close to the electric breakdown level of the material; ▪ The applied electric field may induce a molecular conformation change as the dipoles are aligned with the field; ▪ Since the actuation does not involve diffusion of charge species, they are able to respond quite fast ($<10^{-3} \text{ s}$). ▪ Induces relatively large actuation forces; ▪ Can hold strain under DC activation.
Ionic EAPs	<ul style="list-style-type: none"> ▪ Can perform a much more pronounced deformation of the material; ▪ Require low driving voltages, nearly equal to 1–5 V; ▪ They must be operated in a wet state or in solid electrolytes; ▪ They have slow response characteristics when compared to electronic EAPs; ▪ High currents require rare earth electrodes such as gold or platinum; ▪ The majority aren't able to hold strain under DC voltage.

As polymers, EAP materials have a lot of attractive properties that are superior to other materials. EAP can be easily formed in various shapes and their properties can be engineered. They can be geometrically designed to bend, stretch or contract.

Integrating such molecular EAP materials into nanoscale and mesoscale devices, although a great challenge, can lead to new applications in the EAP field. Hence, these polymers are among the most interesting classes of polymers used as smart materials in numerous applications, such as sensors, actuators, energy and as biomaterials in the biomedical field, among others [15].

Piezoelectric materials are the most suitable for biomedical applications since they have also the interesting ability to vary surface charge when a mechanical load is applied, without the need for an external power source or connection wires [16]. Thus, the use of intrinsically charged piezoelectric polymers as tissue culture substrates can provide means of exposing cells directly to local time-varying electrical stimuli and enhance their response.

Fukada and Yasuda (1957) were the first to report bone piezoelectricity [17]. They have shown that the piezoelectric effect appears when the shearing force acts on the oriented collagen fibers so

that they slip past each other. Then, Basset (1968) [18] reviewed the biologic significance of piezoelectricity, reporting that DC current flow produces massive osteogenesis and bone formation. Also, it is known that electrical properties of bone are relevant not only for bone remodeling, but also as a stimulation for bone healing and repair [19], [20]. All of these studies proved that stressed bone exhibits electronegativity in areas of compression and that, upon fracture, the active metabolism and essentially the growing part of bone was also found to be negatively charged. This negative potential will produce current from the neighboring tissue [20].

A different approach was introduced by Fukada *et al.* (1975), where a piezoelectric material (electret) was implanted and tested. The results showed bone formation beneath the films and it was attributed to charges developed by deformation of the electret films [21], [22]. Additionally, it has been proved that a piezoelectric biological ceramic, hydroxyapatite and barium titanate was able to promote growth and repair of jawbones in dogs. Their chewing-promoted stress potential generated an electrical current that promoted osteogenesis [23]. Since then, many studies were performed and some of them proved that cell dynamic culturing and inherent piezoelectric materials enhanced proliferation and differentiation to osteogenic lineage, being more biomimetic than other used biomaterials, due to the electrical stimulation produced by mechanical stimulation with bioreactors, for instance. This concept can be called as “active” tissue engineering and has been successfully used in the past few years for bone formation, healing and regeneration (Figure 1.2) [24]. Basically, this approach completes the before mentioned tissue engineering triad by adding to the system physical stimulus provided by bioreactors, which attempt is to simulate *in vivo* physiological environment, as mentioned.

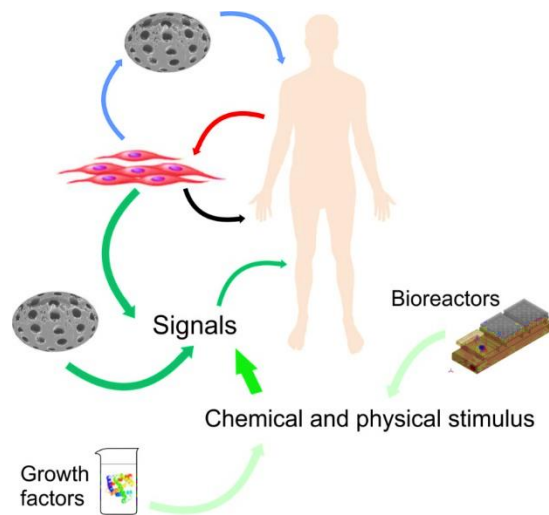


Figure 1.2 – Strategies for the new “active” tissue engineering concept with bioreactors [24].

1.2 POLY(VINYLIENEFLUORIDE) AS A POLYMER OF CHOICE: PROPERTIES AND HANDLING

From the short choice of piezoelectric polymers (including poly (L-lactic acid) (PLLA) and poly(hydroxybutyrate) (PHB)), poly(vinylidene fluoride) (PVDF) and its co-polymers are still the ones with the best electroactive performance, showing the largest piezo, pyro, and ferroelectricity responses [25]. The possibility of tailoring PVDF properties and microstructure, allows new and challenging applications in the biomedical area, not only in device applications but also induce targeted cell responses [26]. This semi-crystalline and biocompatible polymer shows a complex structure and can present five distinct crystalline phases (β -, α -, δ -, γ -, ϵ -) related to different chain conformations designed as all trans (TTT) planar zig-zag for the β -phase, TGTG' (trans-gauche–trans-gauche) for the α - and δ -phases and T₃GT₃G' for γ - and ϵ -phases [15].

Many of the interesting properties of PVDF, in particular those related with its use as sensor or actuator, are related to the strong electrical dipole moment of the PVDF monomer unit ($(5 - 8) \times 10^{-30}$ Cm) which is due to the electronegativity of fluorine atoms as compared to those of hydrogen and carbon atoms [27]. The polar β -, γ - and δ -phases have an overall dipolar contribution per unit cell, as the monomer units and therefore the dipolar moments are packed in a unique morphology (Figure 1.3-A). The β -phase has the strongest piezoelectric response found among polymers (highest dipolar moment per unit cell – 8×10^{-30} Cm), being the most electrically active phase, followed by the γ -phase [15].

Different strategies have been therefore developed to obtain the electroactive phases of PVDF, mainly focusing on the development of specific processing methods and the inclusion of specific fillers. The β -phase can be obtained by mechanical stretching of the α -phase; from melt under specific conditions such as high pressure, external electric field and ultra-fast cooling (Figure 1.3-B); from solvent casting; or by the addition of nucleating fillers such as BaTiO₃, clay, hydrated ionic salt, poly(methyl methacrylate) (PMMA), TiO₂ or nanoparticles such as ferrite, palladium or gold. Also, the development of PVDF copolymers such as poly(vinylidene fluoride-trifluoroethylene) (PVDF-TrFE) has allowed to obtain this material in the electroactive phase [15].

Usually, PVDF and other commonly used piezoelectric polymers are mechanically stretched followed by corona poling in order to induce a net dipole in the material [28].

Another important issue is that due to the similarity of β - and γ -phase specific conformations, their characteristic Fourier Transformed Infrared Spectroscopy (FTIR) bands and X-ray diffraction (XRD)

peaks (which are typically used for phase identification) either coincide or are very close to each other, making difficult to distinguish among both phases [15]. For that, a careful interpretation of the results provided by FTIR, XRD and Differential scanning calorimetry (DSC) should be enough to identify the correct phase of PVDF. Therefore, the combination of different techniques is needed in order to correctly identify α -, β - and γ -phases, since there is superposition of the peaks on each of the different techniques [29]–[31].

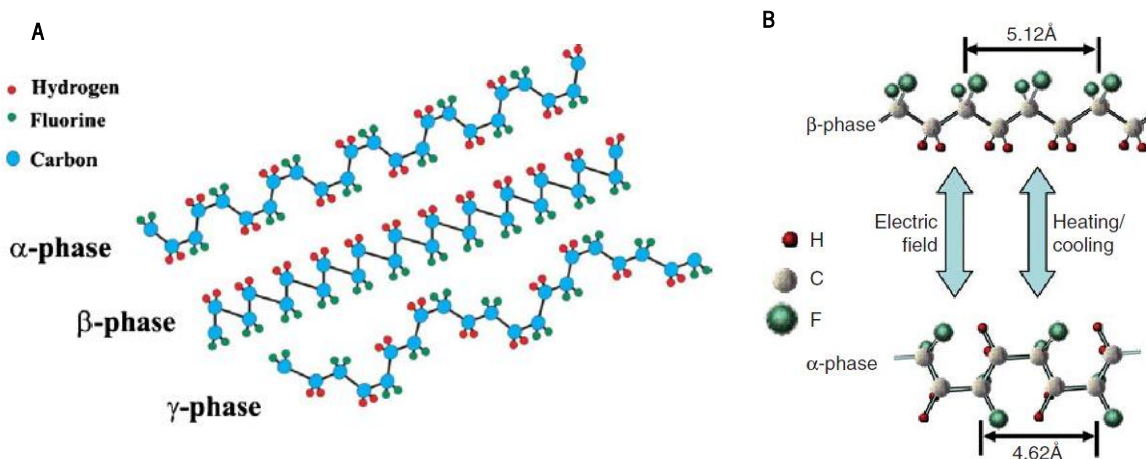


Figure 1.3 – A) Schematic representation of the chain conformation for the α , β and γ phases of PVDF [15]. B) Obtaining the β -phase conformation of PVDF. Schematic of the molecular shape change [14].

Additionally, this polymer has the appropriate mechanical, thermal and chemical properties for biomedical applications [32], since it can be produced in the form of fibers, films or porous structures allowing the production of materials with a customized microstructure for these applications [33]–[35].

1.3 DESIGN AND DEVELOPMENT OF SCAFFOLDS/BIOMATERIALS FOR TISSUE ENGINEERING APPLICATIONS

As mentioned above, in the last years, the potential of electroactive polymers has been recognized for biomedical applications. In this sense, these materials can be used as smart scaffolds to stimulate cell growth and compatibility, biosensors, mechanical sensors and actuators, among others [25]. Therefore, in tissue engineering, the polymeric scaffold material serves as a biomimetic template for cell adhesion, proliferation, differentiation and ECM formation and mineralization; thereby providing a favorable environment for rapid regeneration of tissue [36].

As a result, biocompatibility and biodegradability are the two main ideal properties required for these biomaterials [37]. They should not elicit any short- or long-term immune response. Similarly, polymers and their degradation products should not be toxic to cells or tissues or affect the normal physiological functions [38]. Implantation of inert biomaterials may lead the immune system to cause encapsulation of the implant in fibrogen and platelets as an attempt to remove the foreign material from the site of the tissue. This encapsulation can lead to further complications, since the thick layers of fibrous capsulation may prevent the implant from performing the desired functions [39].

So, the demand for an electroactive polymer to be used in TE that: (i) can be biocompatible, (ii) does not elicit unnecessary inflammatory response, (iii) does not demonstrate any adverse immune response or cytotoxicity, (iv) and that, similarly with all materials in contact with the human body, can be sterilizable to prevent infection, is a great challenge in the TE field. In addition, the mechanical properties of the polymeric scaffold must be compatible and should not collapse during surgical implantation or during the patient's regular activities [36].

1.3.1 Interaction between cells and biomaterials

Cells and materials interplay a central issue in tissue engineering, as the physicochemical properties of scaffold materials affects cell behavior. The compatibility and cell response are strongly influenced by the surface properties of the biomaterial, such as surface charge, chemical composition surface energy, morphology, hydrophobicity and roughness, which will have an effect on cells attachment, spreading, differentiation and maturation [40]. Accordingly, different cells may behave differently on materials, depending on their architecture: the cellular response is strongly influenced by the interconnectivity, pore size/curvature, microporosity and macroporosity [16]. Strong research efforts have been devoted to the tailoring of physicochemical properties of biomaterials: their chemical composition, wettability and topography, in order to induce appropriate cell responses [41]. Proving this concept, Huag *et al.* (2009) showed that two different cell lines cultured *in vitro*, osteoblast hFOB1.19 and fibroblast L929, exhibited different responses on different membranes: the hFOB1.19 cells showed an intensified cell proliferation with an increase of surface roughness, whereas the L929 cells demonstrated the opposite, preferring to attach and grow on a flat surface [42].

Additionally, an interconnected pore structure and high porosity will ensure cellular penetration, adequate diffusion of nutrients to cells within the construct and allows diffusion of waste

products out of the scaffold [4]. A successful scaffold should balance mechanical function with biofactor delivery, making a transition over time in which the regenerated tissue assumes function as the scaffold degrades. This balance often forces a choice between a denser scaffold providing better function and a more porous scaffold providing better biofactor delivery [43]. The role of porosity and pore size in 3D scaffolds was recently reviewed in [44].

Scaffolds can be prepared by different types of fabrication techniques. Since the biopolymer characteristics are determined by the chosen fabrication technique, it is important to be able to control it. The choice must always be done regarding the bulk and surface properties of the polymer and the proposed function of the scaffold. The main techniques for scaffolds fabrication include for example solvent casting, gas foaming, self-assembly, electrospinning, phase separation, fiber mesh, fiber bonding, melt molding, membrane lamination and freeze drying [45].

1.3.2 Electrospaying

It is possible to notice, by analyzing aforementioned recent tissue engineering studies with PVDF and so many others with different polymers (recently reviewed in [46], [47]), that electrospun polymer nanofibers are proper materials for cell culture. Their fine structures resemble natural extracellular matrices and can efficiently interact with cell surfaces and promote cell proliferation. However, the fabrication of 3D scaffolds from electrospun nanofibers is still very difficult due to the fibers continuous entangled form, limiting their application to 2D or single tube-like scaffolds [48].

To address this problem, the production of polymeric microspheres by electrospaying may be the most suitable method, since it has the potential to overcome limitations of the traditional emulsion-based techniques and can, additionally, provide reproducible nano- and microspheres [49]. Moreover, this technique has the potential to generate narrow size distributions of particles with low agglomeration or coagulation and convenient encapsulation with high yields [50].

In electrospinning, the viscosity of the polymer solution affects the morphology of the final product [51]. By decreasing viscosity, the polymer solution jet is gradually thinned and the diameter of the fiber becomes nonuniform, which results in a beaded fiber – an undesired product in electrospinning. In electrospaying, the viscosity is further decreased, so the polymer jet breaks up into tiny droplets and microspheres are obtained [52]. Simultaneously, the ambient humidity and volatility of the solvent affect the surface morphology of electrospun products. The difference between the

electrospinning and electrospaying techniques lies in the chain entanglement density of the polymer solution [53]. For this reason, the determination of a critical polymer concentration is of utmost importance, because it can dictate the behavior of electrospaying/electrospinning.

In the electrospaying process (Figure 1.4-A), a polymer solution is loaded into a syringe and infused at a constant rate using a syringe pump through a small but highly charged capillary. A collector is placed at a 7 to 30 cm distance from the capillary and the applied voltage is typically up to ± 30 kV. When the power supply is turned on, at the tip of the steel capillary two major electrostatic forces (electrostatic repulsion of like charges and Coulombic force of the external electric field) force the hemispherical surface of the droplet to distort into a conical shape known as the Taylor cone (Figure 1.4-B). Once droplets detach from the Taylor Cone, which is when the electrostatic forces counteract the surface tension, the solvent evaporates, generating dense and solid particles that end attached to the collector [49].

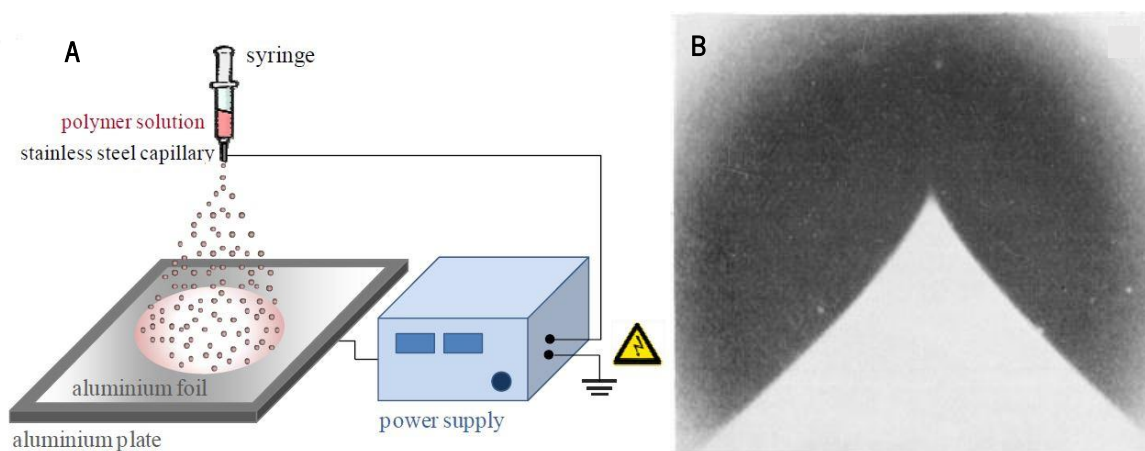


Figure 1.4 – A) Schematic of the typical electrospaying setup [49]. B) The Taylor Cone, from which a jet of charged particles emanates above a threshold voltage [54].

During the electrospay process, there are various parameters that need to be optimized according to the desired final product. These include: voltage, distance to collector, needle gauge, flow rate, polymer, drug, solvent, surfactant, protein/polymer ratio and organic/aqueous ratio [49]. Therefore, before proceeding to this technique, there must be an identification of key parameters responsible for particle size, distribution and morphology as a prelude to any further investigation.

1.4 MESENCHYMAL STEM CELLS

Since the first non-hematopoietic adult Mesenchymal Stem Cells, MSC's, description by Friedstein *et al.* (1966) [55], many studies have been carried out through the next years. They established that these cells derive from stromal compartment of bone marrow (BM) and that seeding of BM cell suspensions at clonal density results in establishment of colony-forming units [56]. The name "osteogenic stem cell" or "BM stem cell" came when Owen and Friedenstein carried out *in vivo* transplantation and recognized that bone, cartilage, adipose and fibrous tissue could be experimentally generated starting from a single BM stromal cell [57].

In this line of thought, MSC's are nowadays defined as multipotent cells that adhere to plastic, have a fibroblast-like morphology, express a specific set of surface antigens and have great interest in the scientific community due to their differentiation potential towards cells belonging to the musculoskeletal lineages, such as adipocytes, osteocytes and chondrocytes [58] (Figure 1.5).

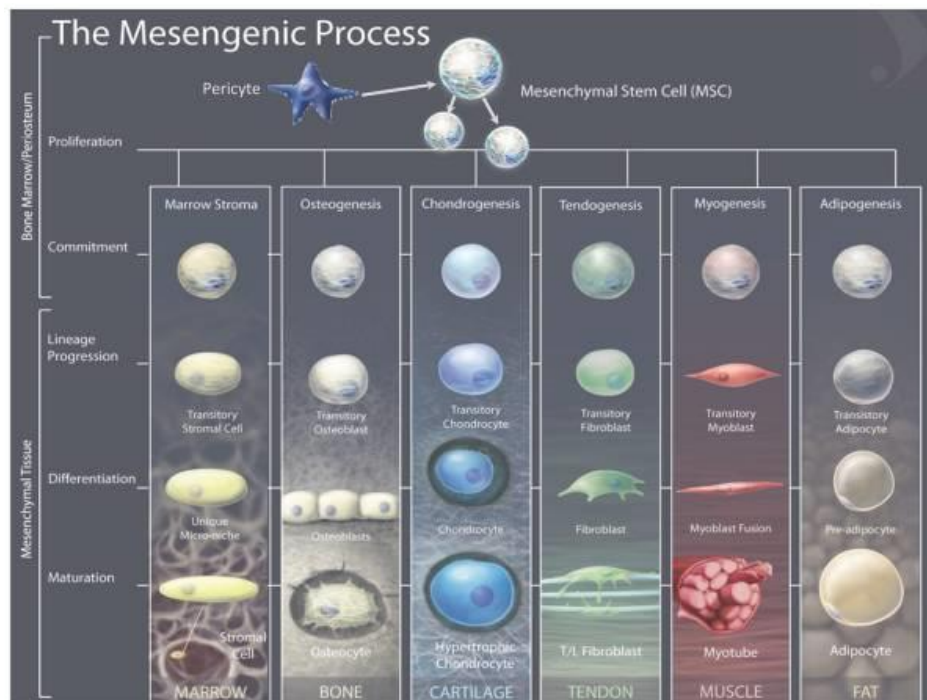


Figure 1.5 – The progeny of a MSC can be induced into one of the several mesenchymal lineage pathways [62].

Even though MSC are usually isolated from BM aspirate of the superior iliac crest of the pelvis in humans, MSC's have also been isolated from a number of other tissues including periosteum,

trabecular bone, adipose tissue (AT), synovium, skeletal muscle, scalp tissue, deciduous teeth, placenta and umbilical cord blood (UCB) [59], being the most common ones from BM, UCB and AT; a comparative analysis was carried out by Kern *et al.* (2006) [60].

Recently, a new insight was attributed to MSC's and they were named as *in vivo* "drugstores". Given that MSC's were revealed to be perivascular *in vivo* [61], Caplan and Correa (2011) proposed that MSC's leave their perivascular location during a local injury and secrete bioactive molecules that will help to regenerate tissue by creating a suitable microenvironment, thus regulating the local immune response [62].

So, these cells have an enormous potential for clinical use mainly due to: i) their ability to self-renew to a certain extent and differentiate; ii) displaying a variety of important cell functions in the organism, including migration and transport functions to damage sites, helping on their renewal; iii) avoiding allogenic rejection, being therefore, non-immunogenic [63].

It's important, however, to ensure that hMSC's (human MSC's) do not lose their potency during sub-culturing passages. This is one of the major challenges, since cells were found to decrease telomerase activity during *in vitro* expansion, which will result in an increase of the probability of malignant transformation and a decline in their multipotency [64]. Thus, culturing early hMSC's will be more reliable for *in vitro* culture purposes. Also, it has been shown that hMSC's obtained from young donors can undergo ± 40 population doublings *in vitro*, but the hMSC's obtained from older donors have a more compromised proliferative potential (± 24 population doublings) [65]. Despite the fact that a decrease in osteoblastic function was not noticed, it is still more reliable to culture cells with low population doublings to apply in *in vitro* proof-of-concepts.

1.4.1 Minimal criteria for defining mesenchymal stem cells

As MSC's lack a specific marker that can be used to isolate and characterize them, the International Society for Cellular Therapy (ISCT) proposed a series of standards to define MSC's [58]. One of the standards is that cells must have adherence to plastic when cultured in standard conditions. Moreover, they must have a specific surface antigen expression, specifically $\geq 95\%$ of the MSC's must express CD105, CD73 and CD90, and lack expression of CD45, CD34, CD14 or CD11b, CD19 or CD79 α and HLA (human leukocyte antigen) class II ($\leq 2\%$ positive). These have been widely used for identification of MSC's [66]–[70]. Finally, under standard differentiating conditions *in vitro*, they should

be able to differentiate onto adipocytes, osteoblasts and chondrocytes, showing multipotent differentiation potential.

There are various methods for MSC's identification, verification and characterization being the most used, flow cytometry. Immunofluorescence/Immunocytochemistry, western blot, protein arrays and real-time RT-PCR can also be employed and are the most common methods for identifying MSC's identity [71].

The markers that the ISCT proposed are the ones that enable researchers to distinguish MSC's from other cells present in the bone marrow (BM). Therefore, the positive markers are the surface antigens that hematopoietic stem cells (HSC's) do not express; and the negative markers are the antigens expressed by HSC's. Below, each one of the antigens as well as where they are expressed and which type of cells express them will be shortly explained.

As hMSC's process the HLA's corresponding to the major histocompatibility complex class I protein (MHC I) instead of MHC class II they have shown to have non-immunogenic surface antigens [72]. The HLA-DR, a class II HLA is only expressed by the MSC's when stimulated, e.g. by interferon gamma (IFN- γ) [73]. HLA's that correspond to the MHC class II are only present on antigen-presenting cells (APC's), such as B-cells, monocytes, macrophages and dendritic cells [74].

CD45 is an antigen encoded by the PTPRC gene, also known as protein tyrosine phosphatase, receptor type C. It is present on all nucleated hematopoietic cells and has an essential role in normal T and B-cell development and antigen receptor signaling [75].

CD14 acts as a co-receptor for mediating the innate immune response to bacterial lipopolysaccharide and it is mainly present in monocytes and macrophages, the most likely hematopoietic cells to be found in a MSC culture [76].

The B-lymphocyte antigen CD19 is a surface marker that, as the name indicates, is expressed early during pre-B-cell differentiation and its expression remains until final differentiation into plasma cells. It is expressed by all B-cells and follicular dendritic cells [77]. On mature B-cells, CD19 is a coreceptor molecule to the B-cell receptor (BCR), which is involved in signal transduction, processing of antigens and subsequent presentation of peptides to helper T-cells [78]. It may also adhere to MSC's in culture.

Hematopoietic progenitor cell antigen CD34 is a member of a family of single-pass transmembrane proteins and may play a role in attachment of stem cells to the BM extracellular matrix

or stromal cells, although the function of CD34 and its family members has not yet been fully determined. This antigen marks primitive hematopoietic progenitors and endothelial cells [79]. There is some controversy in having CD34 as a negative marker for characterization of MSC's; several groups have shown that MSC's express CD34, as reviewed elsewhere [72] and that lacking CD34 expression is likely a consequence of MSC's culturing instead of the real nature of these cells [80].

The ones that are certain to be positive biomarkers for MSC's are CD105, CD90 and CD73.

Endoglin or CD105 is a membrane protein that is part of the transforming growth factor beta (TGF- β) receptor complex. This molecule, expressed by MSC's and other cells within the BM, modulates the TGF- β signaling by interacting with activin and bone morphogenic protein in the presence of their respective ligand binding receptor [81]. Although it has not been clarified yet, it is thought that this molecule may play an functional role in stem cell differentiation, since it has been reported that members of the TGF- β family control MSC's differentiation [82]. A decrease in the expression of this marker has been related to multi-lineage differentiation of MSC's [83], [84].

CD90 or Thy-1 is conserved glycoposphatidylinositol (GPI) cell surface protein. It is expressed on thymocytes, peripheral T cells, fibroblasts, epithelial cells, neurons, MSC's and HSC's [85] and has a role in cell-cell and cell-matrix interactions as well as cell motility [86]. This molecule was considered to be a transient marker for early osteogenic differentiation of MSC's, since it has been proved its expression decreased while there was an increase of other osteogenic markers [83], [87].

Finally, CD73 also known as ecto-5'-nucleotidase is a GPI-linked membrane glycoprotein which catalyzes the conversion of extracellular nucleoside monophosphates into bioactive membrane permeable nucleosides, e.g. adenosine monophosphate (AMP) to adenosine [88]. Its loss has also been related to differentiation of MSC's into different lineages, specially onto chondrocytes and osteoblasts [83], [84].

A summary of the above mentioned markers and their roles is presented in Table 1.2.

Table 1.2 – Negative and Positive markers as proposed by the ISCT. Adapted from [71].

Negative Marker	HLA Class II	CD45	CD14	CD19	CD34
Used to exclude	APC's and lymphocytes	Leukocytes	Monocytes and macrophages	B-cells	Primitive hematopoietic cells and endothelial cells
Positive Marker	CD105		CD90		CD73
Biological Role	Catalyzes the production of extracellular adenosine from AMP		Wound repair; cell-cell and cell-matrix interactions		Vascular homeostasis; modulates TGF- β functions

1.4.2 Osteogenic differentiation

The osseous tissue has a unique capacity to heal and remodel without scarring. Bone formation or skeletal development and its regulation and homeostasis require a series of coordinated functions performed by multiple cell types and tissues. Its formation and renewal, called remodeling, is of utmost importance for the human body, since it provides skeletal support, serves as a reservoir for calcium and phosphate, maintaining the blood calcium levels, and provides a suitable niche for hematopoiesis [59].

Bone resorption is carried out by osteoclasts, which are derived from HSC's. Mature osteoblasts, derived from MSC's as before stated, can synthesize bone matrix that becomes mineralized, rebuilding the resorbed bone. These cells can further differentiate onto osteocytes (Figure 1.6) [89].

Although this is a natural mechanism, it is essential to understand bone formation, remodeling and its regulation in order to come up with additional bone-building treatments, since there are several conditions, both congenital and acquired, where bone replacement and treatment of bone defects are needed. Additionally, since the population aging continues to grow, these problems are expected to increase. The most used surgical procedure is autologous grafting, which is the “gold standard” in immunocompatibility. However, there are several disadvantages in this procedure: e.g. limited amount of tissue that can be harvested, requirement of a secondary surgery, recurrent pain, etc. [90]. Also, allografts or xenografts are optional treatments, although they bring other disadvantages including the possibility of graft rejection, risk of infections and transmission of donor pathogens.

To overcome these problems, tissue engineering and osteogenic differentiation performed on biomaterials is emerging as an appropriate alternative to grafts and to regenerate bone from MSC's of the host body.

As before mentioned (section 1.1), bone is known to have inherent piezoelectricity and therefore to react to mechanical and electrical stimuli. This reaction is responsible for maintaining bone health and integrity, since it has been proved that biophysical signals, including fluid shear stress, substrate strain, substrate topography and electromagnetic fields are transduced by MSC's and act on direct regulation of osteogenic differentiation, and, therefore to higher bone density and greater fracture resistance [91]. Specifically, osteocytes are known as mechano-sensing cells that act as transducers, converting the whole mechanical stimuli to chemical and biological signals for MSC recruitment, proliferation and differentiation.

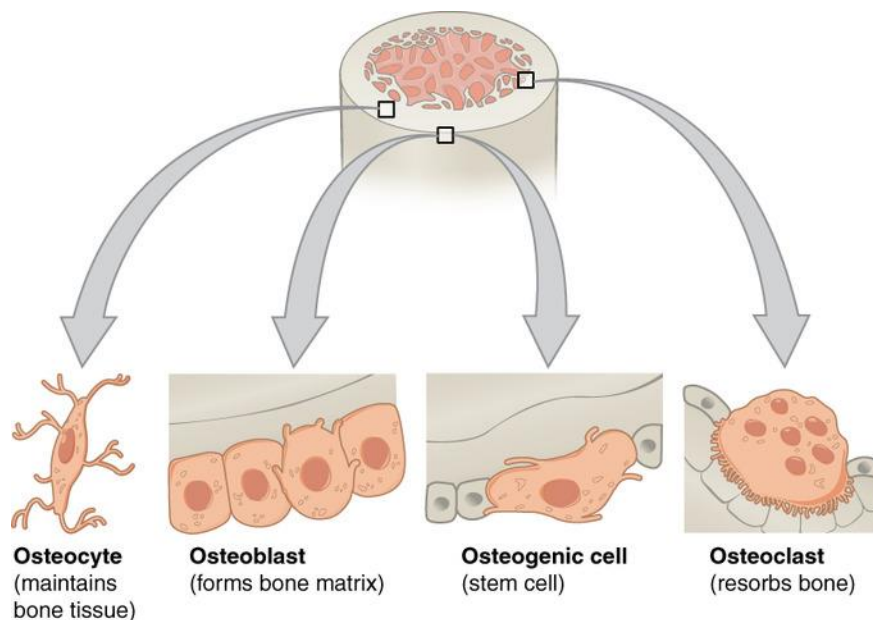


Figure 1.6 – The four types of cells found within the bone matrix. Osteogenic cells are undifferentiated and can develop to osteoblasts. Osteoblasts intervene in bone formation and when they get trapped within the self-calcified matrix, they become osteocytes, which have a different structure and function. They maintain the matrix mineral concentration via secretion of enzymes. Osteoclasts are very different in appearance from the other cells and develop from monocytes and macrophages. The latter resorb old bone [149].

Beyond biophysical signs, osteoblast differentiation from MSC's is also mediated via several signaling molecules such as morphogens, hormones, growth factors, cytokines, matrix proteins and transcription factors [59]. Runt-mediated transcription factor 2 (Runx2) and osterix, along with Wnt

signaling drive stem cells to differentiate onto pre-osteoblasts [92]. Alkaline phosphatase (ALP) expression starts to be noticed in committed pre-osteoblasts and so can be considered an early marker of osteogenic differentiation. Then, once they evolve to mature osteoblasts, a phenotypic change can be noticed: larger nucleus, enlarged Golgi, and extended endoplasmic reticulum. Additionally, this supports the idea of production of ECM and secretion of bone matrix proteins, such as collagen type I, which is dependent also on compressive and shear stresses [93]. When cell becomes finally differentiated into an osteocyte, they occupy a specific place in bone lacunae and also undergo phenotypic changes as the appearance of extensive filopodia, which allows connection with adjacent cells (Figure 1.6). Osteocytes can also regulate osteoblast and osteoclast activity and contribute to mineral metabolism [91]. When in this mineralization state phase, cells increase ALP activity and express late markers of differentiation such as osteocalcin and osteopontin and bone sialoprotein [94].

1.5 STATE-OF-ART

Now, it is known that many body tissues – such as bone, nervous and also muscle – react to mechanical and electrical stimuli. So, the use of electroactive films, membranes or scaffolds shows a novel and potentially interesting approach for tissue engineering applications, making piezoelectric polymers a physical template for cell adhesion and to carry electrical signals, thus improving tissue regeneration. In this line of thought, piezoelectric materials can provide a unique approach to mimic natural cell environment, allowing for electric or mechanic cues similar to the ones present in human body and therefore improving differentiation of hMSC's, to the osteogenic lineage, for instance [95].

1.5.1 Osteogenic differentiation on microspheres scaffolds

Recently, many studies have found applicability for numerous materials in microspheres scaffolds. They can be fabricated by several techniques including emulsification, solvent evaporation techniques, dissolution precipitation techniques and, recently, with electrospray. Also, they have several advantages comparing to conventional scaffolds and these will be reviewed in this section.

These are versatile, given that they can be engineered to modify composition, particle size, size distribution and morphology. Even porous microspheres have already been produced to be used as cell delivery carriers [96]. Also, microspheres have the ability to hold and release bioactive molecules

in a more controllable way than other materials, and as a result they are being widely used as a growth factor delivery system [97]. Their morphology allows them to respond to various stimuli from the surrounding environment, and can consequently perform triggered release by responding to external stimulation [98].

Furthermore, microspheres made of biocompatible polymers containing self-adhesive peptide sequences which can serve as a cell delivery vehicle either by inside cell encapsulation or attachment of the cells on their surface. Osteoblasts, as anchorage-dependent cells, can utilize these microspheres as an anchorage site, creating a suitable niche for new bone formation [98].

Additionally, there are two different ways in which these microspheres can be delivered to the target site: by sintering microspheres in a mould and then transfer it to the target site or by suspending the particles in an injectable delivery medium (suspensions and colloidal gels), and then inject it to the target site. The latter method is advantageous because it is minimally invasive and there is no need of surgery for insertion of the implant [99].

Among the large set of biomaterials employed on the manufacture of osteoinductive microspheres, here is a small review of studies that have been done in this area. So, microparticles or microspheres made of ceramics [100], calcium phosphate ceramics (CPCs) [101], [102], hybrid organic/inorganic compounds [103], [104], collagen [105], gelatin [106], alginate [107], chitosan [108], hydroxyapatite [109] and polymers, including PLG [110] and PLGA [111], [112] were reported as supports for cell studies of expansion and osteoblastic differentiation. Vascular endothelial growth factor A (VEGFA) loaded microspheres were reported to enhance osteogenic differentiation [113], as well as 17- β estradiol (E2) [111] and bone morphogenetic protein 2 (BMP2) loaded microspheres [106]; also, anti-BMP2 monoclonal antibodies encapsulation [107], dicalcium phosphate (CaHPO_4) and calcium carbonate (CaCO_3) composed microspheres [101], [104] have shown to help on this same differentiation pathway.

Polymer microspheres have been extensively fabricated for TE applications primarily because of their easy processing and versatility. Although natural polymers offer inherent cues for directing stem cell fate, their biological activity can be lost during processing and the body can react with an induced immune response. Therefore, and also for their reasonable costs and strong control over properties, synthetic polymers advanced as one of the most suitable materials for microspheres elaboration [98].

1.5.2 Osteogenic differentiation on poly(vinylidene fluoride)-based biomaterials

Some studies involving PVDF and other piezoelectric polymers have been reported regarding cell biocompatibility. Previous studies investigated the biocompatibility of PVDF films and demonstrated PVDF as a very promising material for biomedical applications [25]. Also, it is easily manipulated: studies have been done with fibers [114] and membrane bends [115] for bone tissue engineering applications. Thus, and also given its piezoelectric proprieties, PVDF has been used as a support for cell culturing and osteogenic differentiation, especially in the past few years.

In Table 1.3 is represented a review of the already accomplished studies of bone formation and osteogenic differentiation employing PVDF as biomaterial and their obtained results. Two of them have their ALP activity results below demonstrated (Figure 1.7).

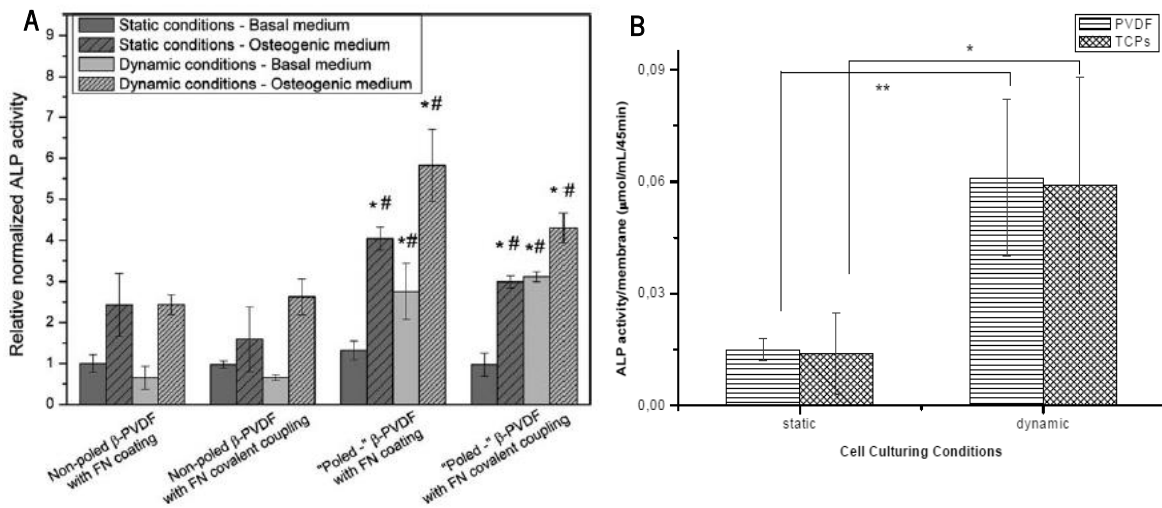


Figure 1.7 – Relative amounts of ALP activity of stem cells cultured on β-PVDF samples in two different studies. A) [116]; B) [117].

Ribeiro *et al.* (2015) [116] used stem cells isolated from adipose tissue and performed the experiments at passages 2-4. After 7 days of static culture, part of the cell-cultured samples was transferred to a bioreactor system in order to perform the dynamic cultures. In the latter, the culture plate was placed in a vertical vibration module at a frequency of 1 Hz. The results clearly showed a higher osteogenic differentiation on “poled –” PVDF samples under dynamic conditions (Figure 1.7-A). Given this, it can be concluded that osteogenic medium and piezoelectric cell stimulation increased this effect, i.e. the combination of biochemical and electromechanical stimulus is the one that has shown better results, proving the theoretical concepts reviewed in this chapter. Also, they were able to

prove that fibronectin is a “sticky” protein, since that no significant differences were found between adsorbed films and crosslinked films with fibronectin.

Also, Rodrigues *et al.* (2008) [117] isolated goat marrow stromal cells (GMC's) from the iliac crests of adult bone and the experiments were done at passage 3 with osteogenic medium. Two days after static culture, part of the cell-cultured samples were transferred to a lab rotator. They have shown that these cells proliferated fast regardless of the sample. However, in dynamic conditions cells cultures on PVDF presented high proliferation rate when compared to TCPS, which proves the potential of piezoelectricity on stem cells proliferation. Also, it's clear to see a huge increase on ALP activity when comparing static and dynamic conditions on the materials, which lead to the conclusion that mechanical stimulation really predisposed these cells to undergo osteogenic phenotype, which was then corroborated by the presence of calcium phosphates.

These studies, along with the ones present in Table 1.3, can prove all of the concepts revised in this chapter, specifically of piezoelectricity and electromechanical stimulation. Now it's possible to confirm that polarized materials have an influence on attachment and proliferation of cells. Most of all, these materials, like PVDF, are able to provide a similar environment to the one that exists in natural bone even under static conditions, enhancing, therefore, osteogenic differentiation. However, under dynamic conditions, these effects seem enhanced, mainly because these conditions mimic not only the electrical but also the mechanic stimulated environments existing in the body, and particularly, in bone, improving osteogenic differentiation and making this a suitable material to be explored in new bone regeneration strategies.

Table 1.3 – Review of studies that have been done with PVDF as a suitable material for bone regeneration or osteogenic differentiation and their specific results.

PVDF morphology, phase and fillers	Seeded Cells / Implant site	“Dynamic culture” equipment	Results	Ref.
Non-poled and poled β -PVDF monomorph films and bimorph films	Rabbit's femur diaphysis	-	The osteogenesis is only induced in piezoelectric films and it's greater in the bimorph films (which consists in sticking two of the monomorph films)	[118]
Non-poled β -PVDF and poled β -PVDF films	Rat's tibia and femur periosteum	-	More bone formation and periosteal reaction occurred in association with the piezoelectric β -PVDF implants	[119]
Electrospun β -PVDF (with different electrospinning voltages)	Mesenchymal Stem Cells	-	The PVDF fibers supported and promoted osteogenic differentiation. The highest voltage used (25kV) encouraged cell adhesion and, therefore, enhanced differentiation	[114]
Non-poled and “poled +” β -PVDF films with and without titanium layer	MC3T3-E1	Bioreactor 1 Hz	“Poled +” PVDF films promoted higher osteoblast adhesion and proliferation. Dynamic culture improved even more these effects	[16]
γ -PVDF/MT-4; α -PVDF/NaY-32	MSC's differentiated to osteoblasts	-	Zeolite and clay composites are biocompatible, increased cell culture proliferation and did not show significant <i>in vivo</i> pro-inflammatory effect, shown by controlled vascularization at the implanted site (dorsal skinfold)	[25]
β -PVDF membranes	Goat marrow cells (GMCs)	Lab Rotator	This material improved GMC's adherence and proliferation and enhanced osteogenic differentiation both in static and dynamic culture conditions (Figure 1.7-B)	[117]
Non-poled, “poled +” and “poled –” β -PVDF and α -PVDF films	MC3T3-E1	-	Samples with a surface density of electrical charges show higher cell density and viability when compared to the non-poled β -PVDF films	[26]
PVDF with printed silver electrodes on both surfaces and covered with PMMA	MC3T3-E1	AC: 5V at 1 & 3 Hz 15 min each. Once every 24 h	Cells cultured in the actuator showed increase cell viability and gene expression of osteoblasts. The same conditions were applied <i>in vivo</i> and total bone area and new bone area was higher when comparing to static controls [120]	[121]
Non-poled, “poled +” and “poled –” β -PVDF and α -PVDF films	Human Adipose Stem Cells	-	“Poled –” β -PVDF films exhibit highest total adhesion area and highest number of focal adhesions. Charged films exhibit a larger level of osteogenic differentiation	[122]
Non-poled and “poled –” β -PVDF films	Human Adipose Stem Cells	Bioreactor 1 Hz	The highest amount of osteogenic differentiation was obtained when culturing cells on “poled –” β -PVDF films, with osteogenic medium and under dynamic conditions (Figure 1.7-A)	[116]

1.6 STRUCTURE OF THE THESIS

Given all of the above explained topics, in this work, PVDF microspheres will be produced as a support by a novel method, electrospray, in order to evaluate the biological response of hMSC's for tissue engineering applications. Three different and new biomaterials will be generated, two of them with an irregular "2D" topography of microspheres: electrospray deposition will be done with different lengths of time, producing two concentrations of microspheres adsorbed on films. The other will be produced as a new 3D microspheres cell-involving system.

Briefly, chapter 2 will resume the main goals of this work. In chapter 3, the required materials and methods for the substrates production and characterization together with the required procedures for the isolation, expansion and differentiation of hMSC's will be described in detail. Next, in chapter 4, the results of the materials characterization will be presented and discussed, along with the results for cell response when seeded on different substrates and under different culture conditions. Finally, the last chapter will sum up this work, bringing the major conclusions and some final remarks about which one of the supports suits best for tissue engineering applications and for culture and differentiation of hMSC's in specific cell lines; future perspectives will also be discussed.

2 OBJECTIVES

The main goal of this thesis is to produce piezoelectric supports to evaluate the biological response of hMSC's under static conditions for tissue engineering applications.

During the development of the work, the main objectives are to:

- Produce and characterize piezoelectric substrates for tissue engineering: β -phase PVDF polymeric microspheres and films with microspheres adsorbed in the same conformational phase;
- Study the influence of processing conditions on phase content and crystallinity of the PVDF samples by FTIR and DSC, respectively;
- Isolate and expand hMSC's in cell culture conditions;
- Study the influence of these biomaterials in cell response: cell viability, cell morphology and existence of focal adhesions.
- Study the influence of this biomaterial on osteoblastic differentiation by flow cytometry and by an osteocalcin immunocytochemistry assay.
- Evaluate the relevance/effect of the different biomaterials on hMSC's differentiation.

3 MATERIALS & METHODS

3.1 PROCESSING OF POLY(VINYLIDENEFLUORIDE) MICROSPHERES

PVDF microspheres were obtained from electro spray method. For that, PVDF (Solef 1010, *Solvay*) was dissolved in N,N-dimethylformamide (DMF, *Merk*) with a concentration of 7% (w/w) in a magnetic stirrer with temperature control, at 60 °C. It has been shown by *Correia et al.* (2014) that this PVDF concentration favors the formation of microspheres by electro spray method [24].

The polymer solution was then placed in a plastic syringe (10 mL) fitted with a steel needle with inner diameter of 0.25 mm. A syringe pump (NE-1000, *Syringepump*) fed the polymer solution into the tip at a rate of 2 mL.h⁻¹. A foil was used as a collector. The distance between the tip of the needle and the collector was 20 cm, the needle being in horizontal position and the collector in vertical position, as shown in Figure 3.1. The experiment was conducted by applying a voltage of 20 kV with a high-voltage power supply (Glassman FC Series 120 W) and the electrodeposition time was about 60 min.

To recover the microspheres from the foil, ethanol was used. After evaporation, a powder of microspheres was obtained. These microspheres were then subjected to vacuum in a heated vacuum desiccator ("Vacuo-Temp", *Selecta*) at 40 °C and 10⁻² mmHg for 24 h, in order to remove residual solvent in the samples.

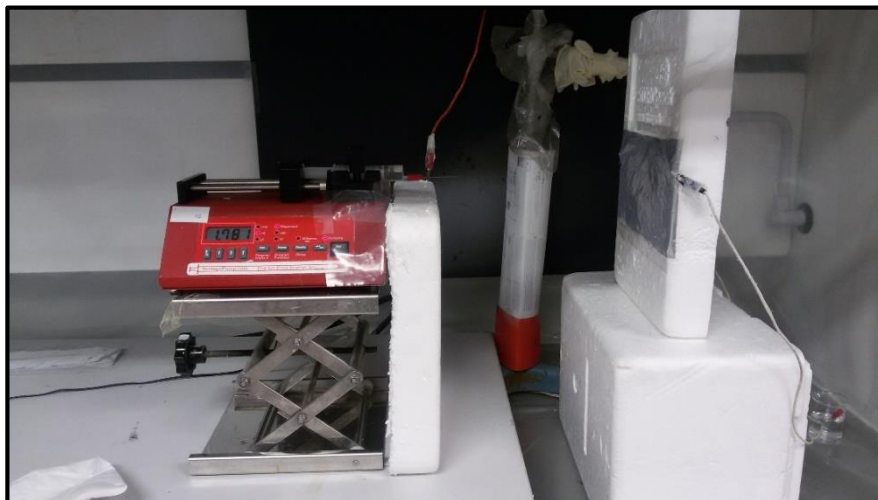


Figure 3.1 – Representation of the electro spray equipment installation utilized in this work.

3.2 PROCESSING OF POLY(VINYLIDENEFLUORIDE) MICROSPHERES FILMS

Films with adsorbed microspheres were also produced. For that, an α -phase PVDF film (*Measurement Specialities*) was subjected to electrospray, being the conditions equal to the ones used for microspheres processing. Two different concentrations of microspheres in the film were obtained: low concentration (15 min of microspheres deposition) and high concentration (45 min of microspheres deposition). "Poled –" β -phase flat PVDF films (*Measurement Specialities*) were used as control.

The films were cut in 8 mm diameter circles and placed on 48-well non-treated tissue culture polystyrene plates (TCPS) (*VRM*).

3.3 MATERIALS STERILIZATION

For sterilization purposes, the films were subjected to ultra violet (UV) light overnight and then washed 3 times for 10 min with Dulbecco's Phosphate-Buffered Saline (DPBS) (*ThermoFisher*). The microspheres were washed 2 times with 100% ethanol and 5 times with DPBS for 10 minutes each. Then, these were also subjected to UV light overnight.

3.4 FIBRONECTIN ADSORPTION

FN from human plasma (*Sigma-Aldrich*) was adsorbed onto the PVDF samples. The biomaterials were immersed in a FN solution of 20 $\mu\text{g}\cdot\text{mL}^{-1}$ for 1 h under constant shaking. After protein adsorption, the samples were rinsed in saline solution to eliminate the non-adsorbed protein.

3.5 CHARACTERIZATION OF POLY(VINYLIDENEFLUORIDE) SAMPLES

3.5.1 Field Emission Scanning Electron Microscopy

Electron microscopes use a beam of highly energetic electrons to probe objects on a very fine scale. Field emission (FE) is the emission of electrons from the surface of a conductor caused by a strong electric field. In this technique, a "cold" source is employed and a tungsten needle works as a cathode. The microscope is classified as a high vacuum instrument, allowing the electron movement along the column without scattering and helping to prevent discharges inside the gun zone. As the FE

source reasonably combines with scanning electron microscopes (SEM's) and because the electron beam produced by the FE source is about 1000 times smaller than that in a standard microscope with a thermal electron gun, the quality of the images will be noticeably improved [123].

Therefore, the FE scanning electron microscopy (FESEM) seemed to be the right tool to ensure high-resolution surface imaging of the micrometer PVDF spheres and to analyze PVDF's films surface.

Thus, electrosprayed samples were coated with a platinum layer using a sputter coating (EM MED020, *Leica*) and their morphology was observed by FESEM (FESEM, Model Ultra 55, *Zeiss*), with an accelerating voltage of 3 kV. Then, microspheres average diameter was measured with Image J to approximately 550 microspheres using the FESEM images.

3.5.2 Fourier Transform Infrared Spectroscopy

The influence of the processing conditions on the crystalline phase and the polymer phase content of the PVDF samples were analyzed by FTIR. This technique has already shown to be useful in previous studies to identify and quantify the different crystalline phases of PVDF [15], [30], [124], [125].

FTIR was performed at room temperature in a ThermoNicoletNexus apparatus in Attenuated Total Reflectance (ATR). The spectra was obtained from 4000 to 400 cm^{-1} , using 128 scans at a resolution of 8 cm^{-1} .

There are characteristic bands of each crystalline phase of PVDF, being the characteristic absorption bands for α - and β -phase at 766 and 840 cm^{-1} , respectively (these will be reviewed further on section 4.2) [15]. Since the achievement of the electroactive β -phase of this polymer was of utmost importance in this work, as explained earlier, the relative fraction of the β -phase in these samples was determined using eqn(1) [126].

$$F(\beta) = \frac{A_{\beta}}{(K_{\beta}/K_{\alpha})A_{\alpha} + A_{\beta}} \quad (1)$$

where $F(\beta)$ represents the β -phase content and A_{α} and A_{β} the absorbance at 766 and 840 cm^{-1} , respectively. Gregorio and Cestari (1994) have also calculated the absorption coefficients, K_{α} and K_{β} , at the respective wavenumber 766 and 840 cm^{-1} , which are 6.1×10^4 and $7.7 \times 10^4 \text{ cm}^2 \cdot \text{mol}^{-1}$,

respectively. It is assumed that FTIR absorption follows the Lambert-Beer law and that the samples are only composed of α - and β -PVDF [126].

3.5.3 Differential Scanning Calorimetry

In order to determine possible modifications in crystal structure and melting behavior, a DSC measurements were performed in the PVDF samples. This thermoanalytical technique measures the difference in amount of energy (or heat flow) required to maintain the sample and a predefined reference at the same temperature [127].

These measurements were performed in a PerkinElmer DSC 8000 apparatus using a heating rate of 20 °C.min⁻¹ under nitrogen purge. At first, it was necessary to calibrate the equipment with a predefined reference. The samples for the DSC studies were weighed and pieces of approximately 3.5 mg were placed into 30 μ L aluminum pans.

The process started at a minimum temperature of -80 °C and the sample was heated until it reached 200 °C at a heating rate of 20 °C.min⁻¹.

Ultimately, the degree of crystallinity (ΔX_c) of PVDF microspheres was calculated by measuring the melting enthalpy. Considering that the melting enthalpies for 100% crystalline samples of α - and β -phase PVDF are 93.07 J.g⁻¹ and 103.4 J.g⁻¹, respectively [124], the degree of crystallinity was determined using eqn(2):

$$\Delta X_c = \frac{\Delta H}{x\Delta H_\alpha + y\Delta H_\beta} \quad (2)$$

where ΔH is the enthalpy of the sample; ΔH_α and ΔH_β are the melting enthalpies of a 100% crystalline sample in the α - and β -phase; and the x and y the amount of the α - and β -phase present in the sample, respectively, that are obtained from the FTIR measurements [34].

3.6 EXTRACTION OF HUMAN MESENCHYMAL STEM CELLS AND PRIMARY CULTURE

3.6.1 Human bone marrow sample extraction

Human bone marrow was collected by the “Servicio de Hematología y Hemoterapia” in the Hospital La Fe, València. This procedure was performed according to established protocols after informed approval of the Local Ethics Committee of the Hospital La Fe.

The extraction of peripheral blood mononucleated cells (PBMC's) of BM was performed by ficoll density gradient centrifugation, which is explained below.

3.6.2 Density gradient centrifugation

The BM sample is diluted with DMEM (Dulbecco's Modified Eagle's Medium) (*ThermoFisher*) in proportion 1:2. After, 3 mL of Histopaque®-1077 (*Sigma-Aldrich*) were added to the sample and this mixture was centrifuged at $1000 \times g$ for 25 min at RT. At the end, the PBMC's at the interphase were collected by aspiration with a Pasteur pipette (Figure 3.2). The cells are then washed two times in DMEM by centrifuging them at $400 \times g$ for 10 min each.

Finally, the PBMC's were diluted on DMEM with 10% fetal bovine serum (FBS, South America PREMIUM, Labclinic, *Biowest*) and counted. Cells are then seeded on T 25 cm² (*Becton Dickinson*) flasks with DMEM culture media composed with 10% FBS, 100 U.mL⁻¹ penicillin-streptomycin (P/S) (*Invitrogen*) and 2.5 mg.L⁻¹ anfotericin B (*Sigma Aldrich*) at 37 °C in a 95% humidified air containing 5% CO₂.

After 48 h, the medium is changed and non-adherent cells are discarded.

3.6.3 Primary human mesenchymal stem cells culture

This method relies on the ability of hMSC's to adhere on plastic between 24-48 h, in contrast to the HSC's that also exist on the PBMC's “mix” (Figure 3.2) [128]. After this time (48 h), the non-adherent cells are discarded when the medium is changed. The next medium changes are performed every 4 days.

When 90% of confluence is reached, cells are trypsinized with trypsin supplemented with 0.25 % of EDTA (*Thermofisher*) for 8 min. Then, trypsin is neutralized with DMEM (10% FBS) in proportion 1:2 and it's finally centrifuged at $400 \times g$ for 10 min. The supernatant is discarded and the pellet (where

the cells are) is diluted in DMEM (10% FBS). Cells are then counted and seeded on new T25 cm² flasks, performing a new passage.

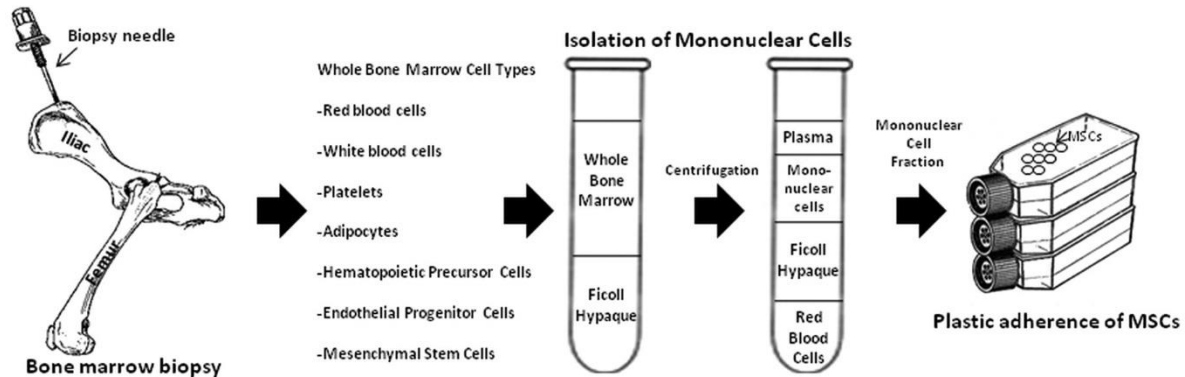


Figure 3.2 – Isolation of hMSC's from a BM biopsy. The whole BM is centrifuged and the mononucleated cells are separated from the red blood cells by ficoll gradient centrifugation. Then, the hMSC's are separated from the other mononucleated cells (lymphocytes or monocytes) by plastic adherence in culture [128].

3.7 CELL CULTURE CONDITIONS

The hMSC's were seeded in T75 cm² flasks (*Becton Dickinson*) with DMEM containing 1 g.L⁻¹ glucose supplemented with 0.5% amphotericin B, 1% P/S and 10% of FBS at 37 °C in a 95% humidified air containing 5% CO₂. The medium was changed every 3 days.

For cell culture, 10 mg of microspheres obtained by electrospray (7% w/v) and treated with fibronectin were placed in a 2 mL eppendorf. Then, after FN adsorption, the cells were mixed with the microspheres (1x10⁵ cells/eppendorf). Cell pellets without any microspheres were used as reference (positive control). Also, a density of 1x10⁴ cells/well was seeded onto each one of the films (β -PVDF films and PVDF films with high and low microspheres concentration). The medium was changed every 3 days. Cells were kept under expansion medium until confluence was reached.

The cells that were not used immediately in experiments were placed in cryovials (*Thermo Scientific*) and frozen in liquid nitrogen with FBS supplemented with 10% dimethyl sulfoxide (DMSO) after trypsinization and centrifugation at 400 \times g for 5 min.

Additionally, a differentiation culture media (osteogenic medium) was introduced after the hMSC's reached 100% confluence on the biomaterials. It was composed of DMEM medium containing 1 g.L⁻¹ glucose supplemented with 0.5% amphotericin B, 1% P/S, 10% FBS, 8 mM of β -Glycerophosphate

disodium salt hydrate (*Sigma Aldrich*), 10 nM of dexamethasone-water soluble (*Sigma Aldrich*) and 50 $\mu\text{g}\cdot\text{mL}^{-1}$ of L-Ascorbic acid 2-phosphate sesquimagnesium salt hydrate (*Sigma Aldrich*). The cell culture medium was replaced every 3 days during 14 days.

3.8 STUDY OF CELL VIABILITY

For quantification of viable cells in proliferation, after 4 days of cell seeding 3-(4,5-dimethylthiazol-2-yl)-5-(3-carboxymethoxyphenyl)-2-(4-sulfophenyl)-2H-tetrazolium (MTS) assay was carried out. The method is based on the reduction of MTS tetrazolium compound by NAD(P)H-dependent dehydrogenase enzymes in metabolically active cells to generate a colored formazan product that is soluble in cell culture media which can be quantified measuring the absorbance, therefore reflecting the number of viable cells.

Thus, cells were incubated with a 5:1 proportion of MTS (*Promega*) to DMEM without phenol red (*ThermoFisher*) for 3 h at 37 °C in dark. Then, the supernatant was used to determine the absorbance at 570 nm. For this study, only MTS+DMEM without phenol red was used as reference (blank) and cells cultured in 12 mm glass coverslips were considered to be the positive control.

All the quantitative results will be presented as mean \pm standard deviation (SD) of triplicate samples. Statistical differences were determined by ANOVA using Tukey test for the evaluation of different groups (Graphpad Prism 5.0, GraphPad Software). p values < 0.05 were considered to be statistically significant.

3.9 STUDY OF CELLS ADHESION

At the fourth day of culture, cells focal adhesions on the microspheres were accessed by immunocytochemistry methods. First, the cells were washed in DPBS and fixed with formalin (*Sigma Aldrich*) at 4 °C for 1 h. After, they were permeabilized with 0.5% Triton X-100 (*Sigma Aldrich*) in DPBS during 5 min at RT. After washing the samples with DPBS ++ (+calcium, +magnesium) (*Sigma Aldrich*), a protein solution of 5% bovine serum albumin (BSA) (*Sigma Aldrich*) and 0.1% Triton X-100 in DPBS was added. After 1 h at RT, the solution was removed and the samples were incubated with Anti-Vinculin antibody (*Sigma Aldrich*) at a 1:400 dilution in a solution of 5% BSA and 0.1% Triton X-100 in DPBS during 1 h at 37 °C. Then, the primary antibody was removed and the samples were washed

with 0.1% Triton X-100 in DPBS ++. At this point, samples were incubated with the secondary antibody antimouse Cy3 (*Jackson Research*), at a 1:200 dilution, together with Alexa Fluor® 488 phalloidin (*Invitrogen*), at a 1:100 dilution in the previously termed BSA solution during 1 h at 37 °C. Finally, the solution was removed and the samples were once again washed in 0.1% Triton X-100 in DPBS++ before being mounted in a microscope slide with aqueous mounting medium containing DAPI (*Vector Laboratories*).

For this study, cells cultured in 12 mm glass coverslips were used as a reference. Cell's focal adhesions were visualized using a confocal microscope (DMI8, *Leica*) and ImageJ, Photoshop and Leica Application Suite X softwares were used for treatment and analysis of the obtained images.

3.10 STUDY OF CELLS MORPHOLOGY

After 4 days of cells proliferation and at the day 14 of osteogenic medium introduction, the samples were fixed with formalin as described before. Following, the samples were washed in phosphate buffer (PB) (*ThermoFisher*) before being incubated with 1% osmium tetroxide (*Aname*) in PB for 45 min in dark. Then, the biomaterials were again washed to assure total removal of osmium tetroxide, before being dehydrated through a graded series of alcohol (50%, 60%, 70%, 80%, 96% and 100%) and submitted to critical-point drying (E3000, *Polaron*). The microspheres samples were before dispersed in 3% agarose (*Sigma Aldrich*) in water, making them suitable for critical-point drying procedure.

The dried samples were coated with a gold layer using a sputter coating (EM MED020, *Leica*) and their morphology was observed by SEM (JSM6300, *JEOL*), with an accelerating voltage of 10 kV.

3.11 FLOW CYTOMETRY STUDY

As mentioned, flow cytometry (FC) is the most employed method to MSC's identification and characterization. Therefore, this technique was employed in this work.

FC is a laser-based technique that measures and analyses diverse parameters of single particles, normally cells (e.g. particle's relative size, relative granularity or internal complexity, and relative fluorescence intensity), by suspending them in a stream of fluid. Then, this fluid transports the particles into a beam of light and, formerly, the optical system will distribute the light signals to

appropriate detectors. Finally, this will be transformed to electronic signals that can be computer processed. In this technique, the appropriate size ranges from 0.2 to 150 μm for any suspended particle or cell [129].

Therefore, before cell seeding onto the biomaterials, the freshly obtained and expanded hMSC's were characterized by FC in a FACSCanto-II cytometer (*Becton Dickinson*, San Jose, CA, USA). First, the cells were separated in 3 centrifuge tubes and centrifuged at 1400 rpm for 10 min. Then, the supernatant was removed and the pellet was resuspended in 80 μL of phosphate-buffered saline (PBS) (*ThermoFisher*). Next, 20 μL of FcR Blocking Reagent (*Miltenyl Biotec*) was added to each one of the tubes and the cell-surface antigens were marked with anti-human antibodies according to Table 3.1 in an incubation process that lasted 30 min at 2-8 $^{\circ}\text{C}$ in dark.

Table 3.1 – Antibodies used against cell-surface antigens to characterize hMSC's. FITC - Fluorescein isothiocyanate; PE – Phycoerythrin; PerCP-Cy5.5 – Peridinin-chlorophyll protein-cyanine5.5; APC – Allophycocyanin.

For each biomaterial sample...	FITC	PE	PerCP-Cy5.5	APC
Set 1	CD90 (<i>Miltenyl Biotec</i>)	CD105 (<i>Miltenyl Biotec</i>)	HLA-DR (<i>Becton Dickinson</i>)	CD73 (<i>Miltenyl Biotec</i>)
Set 2	CD19 (<i>Becton Dickinson</i>)	CD34 (<i>Becton Dickinson</i>)	CD45 (<i>Becton Dickinson</i>)	CD14 (<i>Becton Dickinson</i>)
Control	No antibodies added			

Succeeding, 2 mL of PBS was added to the tubes, before a 5 min centrifugation at 1400 rpm. The supernatant was removed and the cells were finally resuspended in 400 μL of PBS. Approximately 50.000 labelled cells were acquired and data was subsequently analyzed using Infinicyt™ software (*Cytognos S.L.*, Salamanca, Spain).

To analyze how the hMSC's markers evolve with time, cells that were cultured on the biomaterials were submitted to FC at day 4 of culture (when reaching 90% confluence) and at day 14, after differentiation medium introduction. With the purpose of having a suitable number of cells to perform FC analysis, biomaterials were cut in order to occupy all of the space in 6-well non-treated TCPS. Cells were seeded with the same density mentioned previously and, at the analysis day, they were trypsinized with 1 mL of trypsin for 5 min. Each one of the biomaterial-cultured cells were divided

in three groups and incubated with antibodies combinations according to Table 3.1. The following protocol was the same as described above for cells before seeding (day 0). Controls of cells seeded on TCPS were also submitted to FC analysis according to Table 3.2.

Table 3.2 – Controls performed in flow cytometry analysis. The purpose of the controls at 7 and 14 days are to compare them to cells cultured on the PVDF samples, which are already growing under differentiation medium.

Controls (done with)	Day 4	Day 7	Day 14
Expansion Medium	✓	✓	✓
Differentiation Medium	✗	✓	✓

3.12 OSTEOCALCIN IMMUNOCYTOCHEMISTRY

Mineralization of bone is characterized by the expression of late markers of differentiation such as osteocalcin (OC) and osteopontin [59], as referred in section 1.4.2. Accordingly, after 14 days of culture in differentiation medium, the content of bone-specific OC was measured by immunocytochemistry methods.

First, the cells were washed in DPBS and fixed with formalin at 4 °C for 1 h. After, MSC's were washed 3 times with DPBS ++ and permeabilized with 0.5% Triton X-100 in DPBS during 5 min at room temperature. After washing the samples with DPBS ++ (*Sigma Aldrich*), a protein solution of 5% BSA and 0.1% Triton X-100 in DPBS was added. After 30 min at 37 °C, the solution was removed and the samples were incubated with Anti-Osteocalcin antibody (*Abcam*) at a 1:200 dilution in a solution of 5% BSA and 0.1% Triton X-100 in DPBS during 1 h at 37 °C. Then, the primary antibody was removed and the samples were washed with 0.1% Triton X-100 in DPBS ++. At this point, the samples were incubated with the secondary goat antibody anti-rabbit Alexa 488® (*Invitrogen*), at a 1:200 dilution in the previously termed BSA solution during 1 h at 37 °C. Finally, the solution was removed and the samples were once again washed in 0.1% Triton X-100 in DPBS++ before being mounted in a microscope slide with aqueous mounting medium containing DAPI.

For this study, cells cultured in 12 mm glass coverslips were used as a reference. Cells relative content of OC was studied using a confocal microscope and ImageJ, Photoshop and Leica Application Suite X softwares were used for treatment and analysis of the obtained images.

4 RESULTS AND DISCUSSION

4.1 ELECTROSPRAYED MICROSPHERES MORPHOLOGY AND SIZE DISTRIBUTION

Previous studies have shown that with a polymer concentration of 5 % (w/v) till 10 % (w/v), microspheres with different size distributions are obtained, due to the solvent evaporation from the droplets before reaching the foil. That, together with polymer diffusion will generate dense and solid particles that end attached to the collector [124], [130].

Therefore, for PVDF electro spray at a concentration of 7% (w/v), spherical microspheres with diameters in a range between 0 – 6 μm were expected, when processed with the right parameters for achievement of PVDF microspheres by this technique, which were already studied by Correia *et al.* (2014) [124]. Figure 4.1 shows representative FESEM images of the PVDF microspheres and of the α -film adsorbed PVDF microspheres prepared by electro spray from a concentration of 7% (w/v) using DMF as solvent.

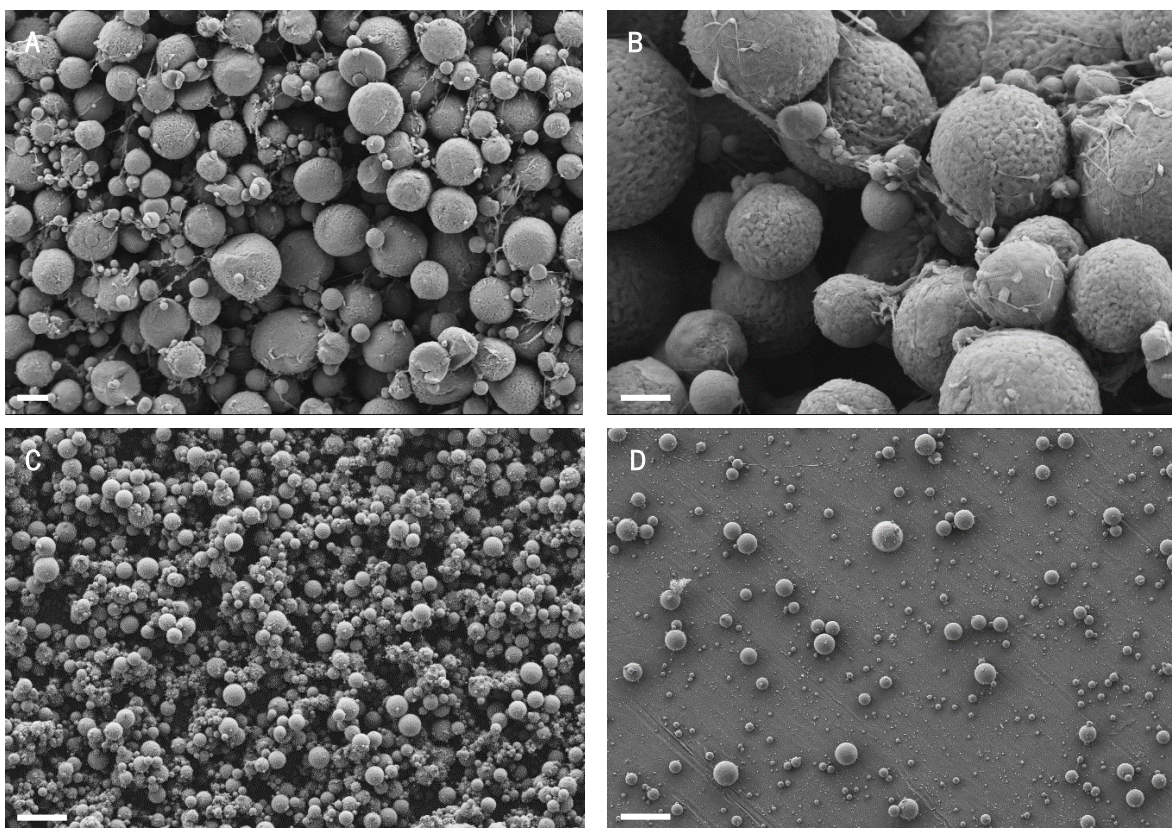


Figure 4.1 – Morphology of the PVDF microspheres obtained. A) and B) Microspheres only; C) High density concentration of microspheres electro sprayed in α -PVDF film; D) Low density concentration of microspheres electro sprayed in α -PVDF film. Scales: A) 2 μm ; B) 1 μm ; C) 10 μm ; D) 10 μm .

The spherical morphology of the obtained samples can be observed in Figure 4.1, along with a wide range for microspheres size. One thing that contributes to the microspheres surface roughness observed in Figure 4.1-A and B is the moisture present in the atmosphere when the electrospay is carried on, since the ambient parameters including temperature, humidity, and air velocity in the chamber contribute to different products of electrospay [131]. Indeed, mostly humidity and volatility of the solvent have shown to affect the surface of these products, showing submicron surface features with an increase in humidity [132].

The high and low concentration of PVDF microspheres adsorbed on films produced are shown in Figure 4.1-C and D, respectively. It can be seen that production of these biomaterials for cell seeding was successful, and the microspheres are within the same range of diameters.

The corresponding particle size distribution is shown in Figure 4.2. The microspheres average diameter was $3.04 \pm 1.70 \mu\text{m}$. Each column within the figure is identified with the mean of the of size values that it encloses, e.g. between 0 and 1 μm , the column is identified with 0.5 μm , and so on.

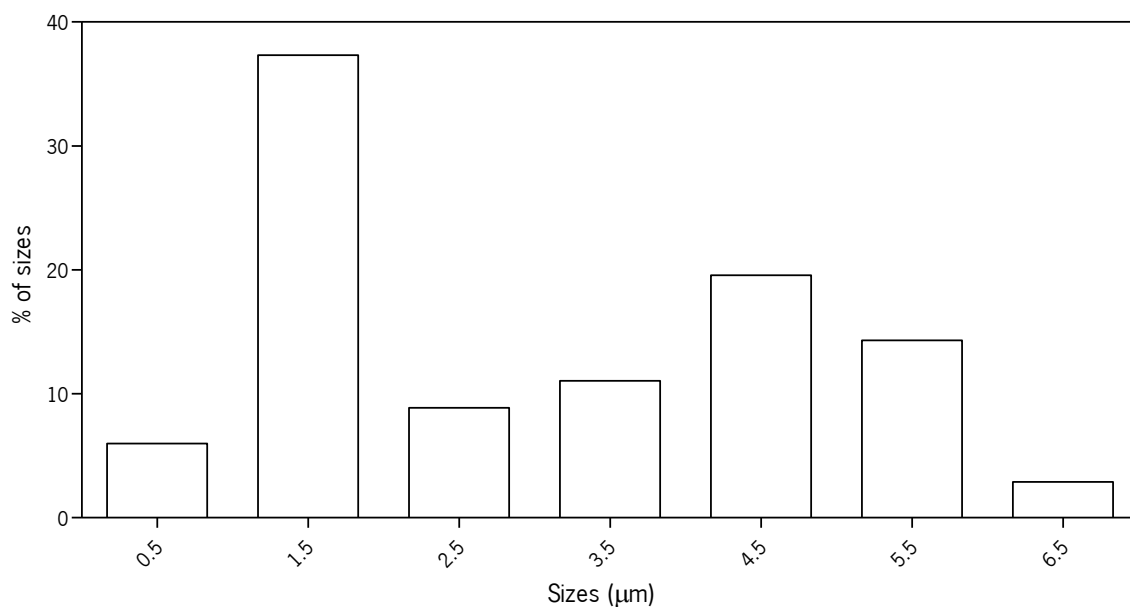


Figure 4.2 – Microspheres size distribution obtained for the described electrospay conditions.

4.2 POLY(VINYLDIFLUORIDE) PHASE CONTENT

In this work it was important to obtain the β - electroactive phase of PVDF, since it has shown very good results in cell culturing, as previously mentioned.

Also, as previously said, the characteristic FTIR bands of this polymer can provide an accurate confirmation that the β - electroactive phase was obtained, providing valuable information about the polymer phase structure [15]. It is known that PVDF is composed by the repetition unit $-\text{CH}_2-\text{CF}_2-$ along the polymer chain; therefore, with FTIR, some vibrational modes can be useful for the phase's identification. The characteristic FTIR absorption bands for α -, β - and γ -PVDF are represented in Table 4.1.

Table 4.1 – Characteristic absorption FTIR bands of different PVDF phases [15].

	α	β	γ
Wavenumber (cm⁻¹)	408	510	431
	532	840	512
	614	1279	776
	766		812
	795		833
	855		840
	976		1234

Although some bands for the β - and γ -phase are very close to each other, it has been recently accepted that the band at 840 cm⁻¹ is a strong band characteristic of the β -phase, whereas the characteristic absorption for the γ -phase appears as a shoulder at 833 cm⁻¹ [15]. The α -phase has also a characteristic strong absorption band at 766 cm⁻¹. Bormashenko *et al.* (2004) have summarized experimental and theoretical results for the vibrational spectrum of PVDF, being the band at 840 cm⁻¹ characteristic of the CH₂ group rocking, and the band at 766 cm⁻¹ of the CF₂ group bending and of the sceleate bending [133]. Figure 4.3 shows the FTIR-ATR spectra representative for PVDF microspheres and for the β -phase PVDF film for comparison.

The general appearance of the spectra is similar for the two samples. However, for the microspheres, some characteristic absorption modes for the α -phase (766 and 976 cm⁻¹) can be seen, along with the strong and characteristic band for β -phase at 840 cm⁻¹, common for the two samples.

The relative amount of α - and β -phase present in the different samples was calculated by eqn(1) as previously explained (section 3.5.2). The film presents a \cong 76% fraction of β -phase, while

the microspheres present a $\cong 71\%$, which is even higher than the one obtained by Correia *et al.* (2014) [124]. This decrease in the percentage of the electroactive phase is according to the most pronounced α -absorption bands present in the microspheres spectrum. The achievement of the β -phase in these microspheres is due to the low temperature solvent evaporation, given that electrospray is done at room temperature, which favors polymer crystallization in the electroactive phase. Also, electrospinning has been characterized as a technique that due to high electric fields employed and high stretching ratio of the jets, can form the β -PVDF phase without the need of any treatment after this procedure [15], which can also be applied to electrospray, given that the conditions are nearly equal.

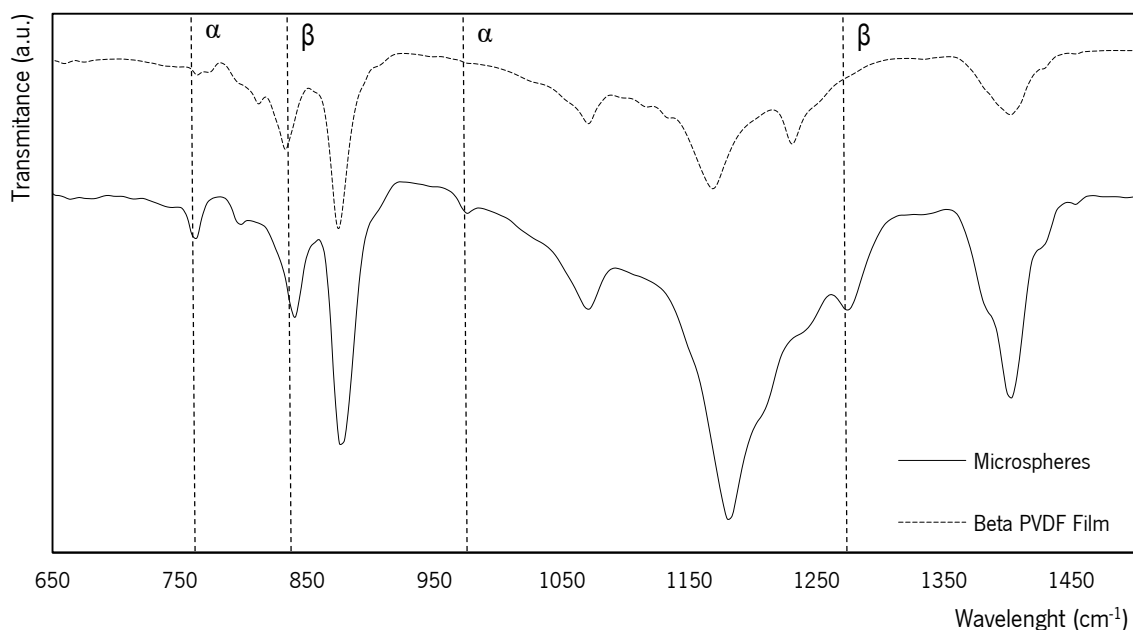


Figure 4.3 – FTIR spectra of the β -phase PVDF film and microspheres.

Comparatively to the previous Correia *et al.* (2014) [124] work with PVDF microspheres, there are no noteworthy differences. Although higher, the calculated value for the β -phase content of the microspheres is in the same interval of values and the characteristic bands of β - and α -phase PVDF present in the polymer microspheres spectra are very similar.

4.3 THERMAL CHARACTERIZATION

Complementary to the infra-red measurements, DSC was performed in order to identify and quantify the crystalline phase of PVDF samples. Because α - and β -PVDF have similar melting temperatures, this technique is not used for differentiation between the two phases [31]. The characteristic peaks depend not only on the crystalline phase but also on the morphology of the polymer. Therefore, it was accepted a melting temperature range for the α - and β -phase PVDF, which is from 167 °C to 172 °C [15].

The DSC thermogram obtained for the microspheres is represented in Figure 4.4. The samples show similar endothermic peaks. Comparing the microspheres to the PVDF film, the latter has higher melting enthalpy, which means that it contains higher crystallinity content.

The degree of crystallinity of each sample was determined from the DSC curves using eqn(2) as previously described (section 3.5.3). The degree of crystallinity for the film was \cong 58% and for the microspheres \cong 52%, according to the thermograms. The melting temperature was about 167 °C for the microspheres and 174 °C for the film, values that fall within the established temperature range for β -phase PVDF, taking in account the equipment error.

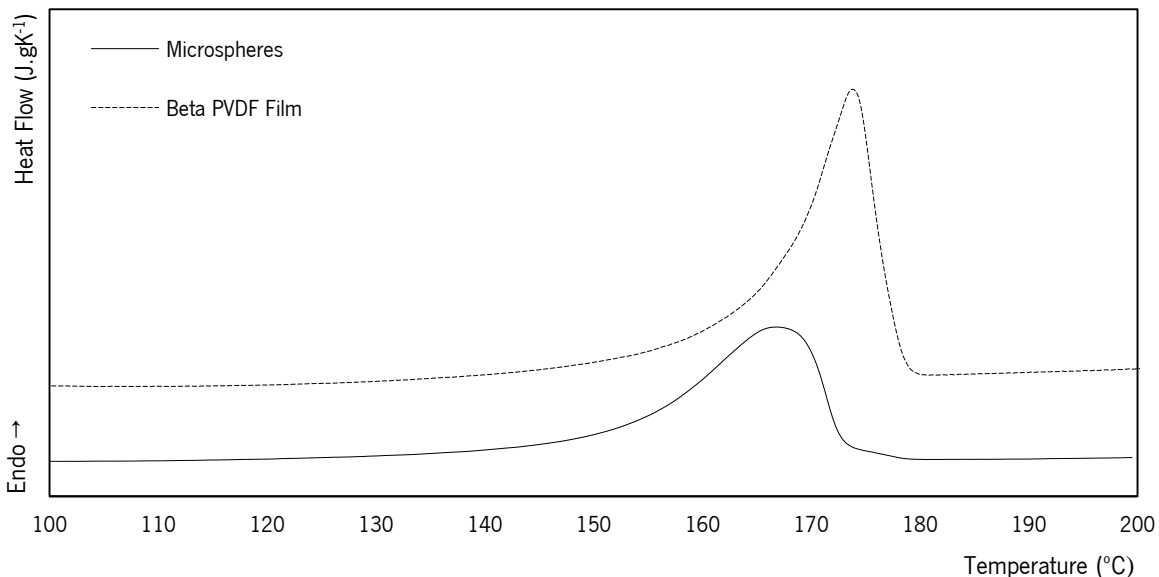


Figure 4.4 – DSC thermogram of the PVDF commercial film and of the PVDF microspheres obtained by electrospray method.

Comparing to the previous Correia *et al.* (2014) work with PVDF microspheres, there are no noteworthy differences in the melting temperature value neither in the degree of crystallinity [124].

4.4 CELL ATTACHMENT AND MORPHOLOGY

The overall morphology of the hMSC's seeded on the PVDF samples was visualized after 4 days of cell culture by SEM (Figure 4.5).

As said, FN was absorbed onto the biomaterials. This is a well-studied ECM glycoprotein able to bind to integrins, which are cell-surface receptors that link the ECM with the intracellular cytoskeleton [134]. Therefore, biomaterials surface modification with FN has already been performed and the results have shown to enhance cell attachment and proliferation [135]–[137]. Here, on Figure 4.5 and Figure 4.6 it's possible to see that, once more, FN enabled attachment and proliferation of cells seeded on the different PVDF biomaterials.

SEM images can reveal that cells cultured on the microspheres films seem to elongate their adhesion points in order to find a suitable place to hold on to. In the film with high density of microspheres, the cells became thinner and their body becomes less flatten and more elongated, compared to the film with low density of microspheres (LD-M). Figure 4.5-A and Figure 4.5-B also show that the cells are able to attach not only with their elongated filopodia but also show adhesion within the cell body to the film and microspheres. As there is no visible film in Figure 4.5-C and Figure 4.5-D, the high density microspheres film (HD-M) resembles a 3D environment, where the cells can only attach to the agglomerates of microspheres. Because of that, hMSC's adopt a particular shape, as can be seen.

Cells were also cultured on the α -PVDF film, as this film is the one that was coated with electrospayed microspheres for cell culture. It was important to verify the morphology adopted by hMSC's on this film, since it could improve the prediction of the behavior of cells cultured in LD-M films. In Figure 4.5-E it is possible to verify that cells spread and flatten much more, compared to the films with microspheres. As there is no impediment on their growth, MSC's adopt much larger shapes and have approximately twice the size.

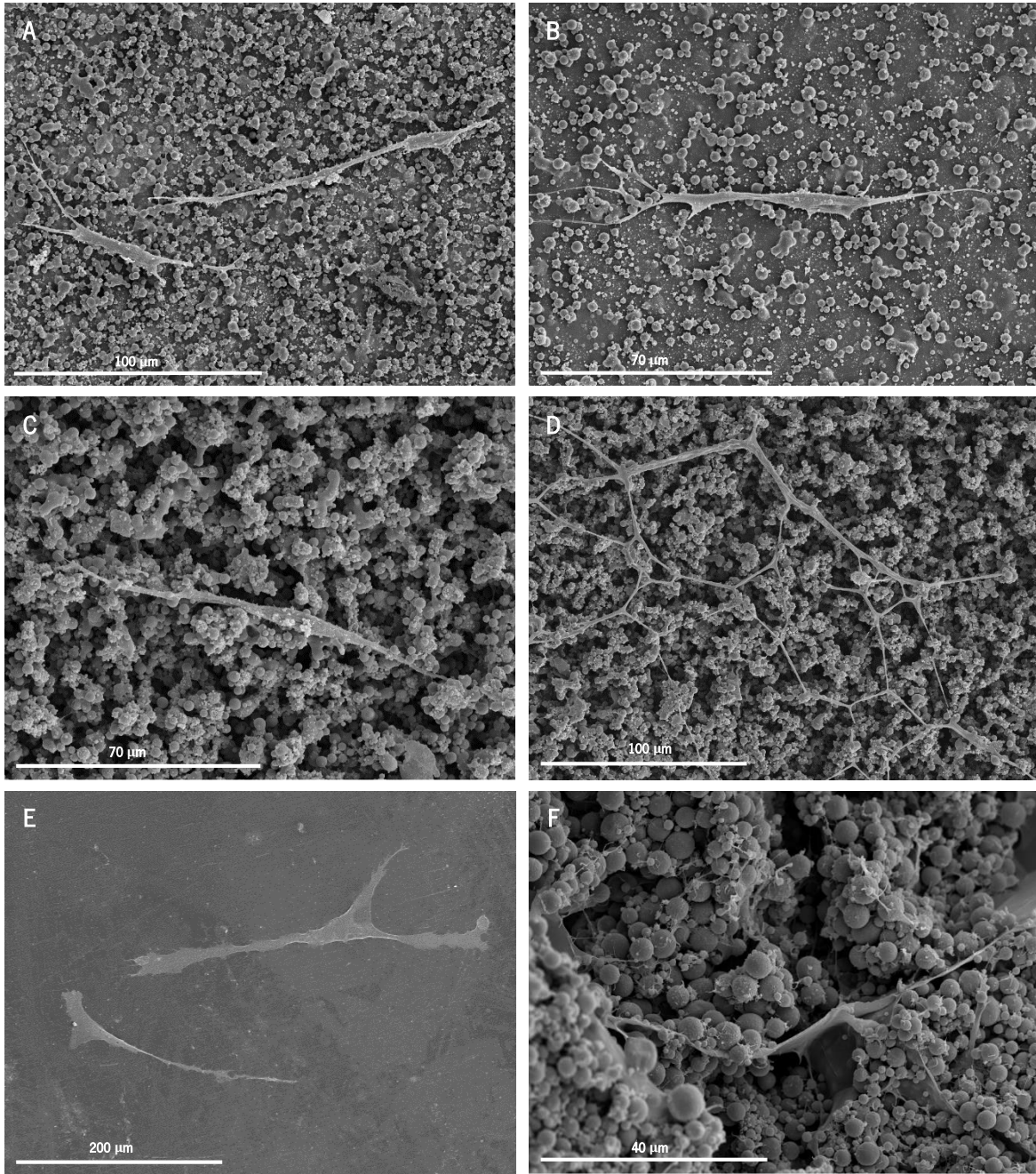


Figure 4.5 – Overall cell morphology of hMSC's analyzed by SEM. A) and B) films with low density of PVDF microspheres; C) and D) films with high density of PVDF microspheres; E) alpha film; F) microspheres only.

Finally, cells cultured in the 3D environment can be seen in Figure 4.5-F. It is possible to observe some cells within the microspheres agglomerate. These cells have a much more spread and large body and shorter filopodia compared with the cells cultured on the other samples, which resembles more to an osteoblast morphology [138]. As microspheres form an agglomerate, cells seem

to be continuously in contact with them, making this a suitable 3D environment for cell growth and culture. Additionally, microspheres have shown to break this agglomerate easily when submitted to low mechanical stress, so these may not confine cell growth or spreading. However, this substrate has its influence on cell shape: it's possible to see that – compared to the films with microspheres – these cells have no need to elongate their filopodia towards an attachment point; that happens because they are already surrounded by an appropriate niche that gives them support to grow and spread effortlessly.

Given this, it is possible to say that cells adopt diverse morphologies when cultured in the different substrates according to their surrounding niche. The “2 and a half” dimension substrate, which was considered to be the HD-M film, seemed to be similar to the 3D substrate, but it's now possible to verify that the cells behave and grow in a different way when cultured on these two substrates.

The overall cell attachment was also verified by confocal microscopy after actin-vinculin staining (Figure 4.6).

In the control (cells seeded on glass), cells were able to attach perfectly, as can be seen by the red dots that represent the focal adhesions. Cells have flattened and spread their body due to the ability to create more focal adhesions to this substrate.

Cells were also seeded on the β -PVDF film. This was carried out to evaluate differences of cell attachment and of cytoskeleton organization between the samples in the same piezoelectric conformational phase (β -phase), the flat film and the microspheres substrate, since this PVDF phase has proven to be the most suitable for cell culturing and differentiation [16], [33]. In this film it is possible to verify that there are cells that elongate more and seem to create specific adhesion points in the direction of cell growth, a fact that does not corroborate with cytoskeleton organization of the cells seeded on glass, meaning that substrate negative charge is influencing cell attachment, as seen in other studies done with stem cells seeded on flat β -phase films [122]

In the microspheres films, as cells were not cultured in flat surfaces, the images had to be stacked and assembled according to the different focused plans. For this reason, in Figure 4.6-C and 4.6-D focal adhesions are not as clear as seen in Figure 4.6-A and 4.6-B. However, their morphology is in concordance with the cytoskeleton orientation given that they adopt an elongated morphology, as seen in Figure 4.5. It is also possible to observe, in these both figures, focal adhesion points though the entire cell, indicating that cells are adhering to the microspheres. Additionally, their filopodia is

elongating towards the agglomerates of microspheres (according to Figure 4.5), in which it is possible to verify vinculin staining, creating very irregular shapes of hMSC's.

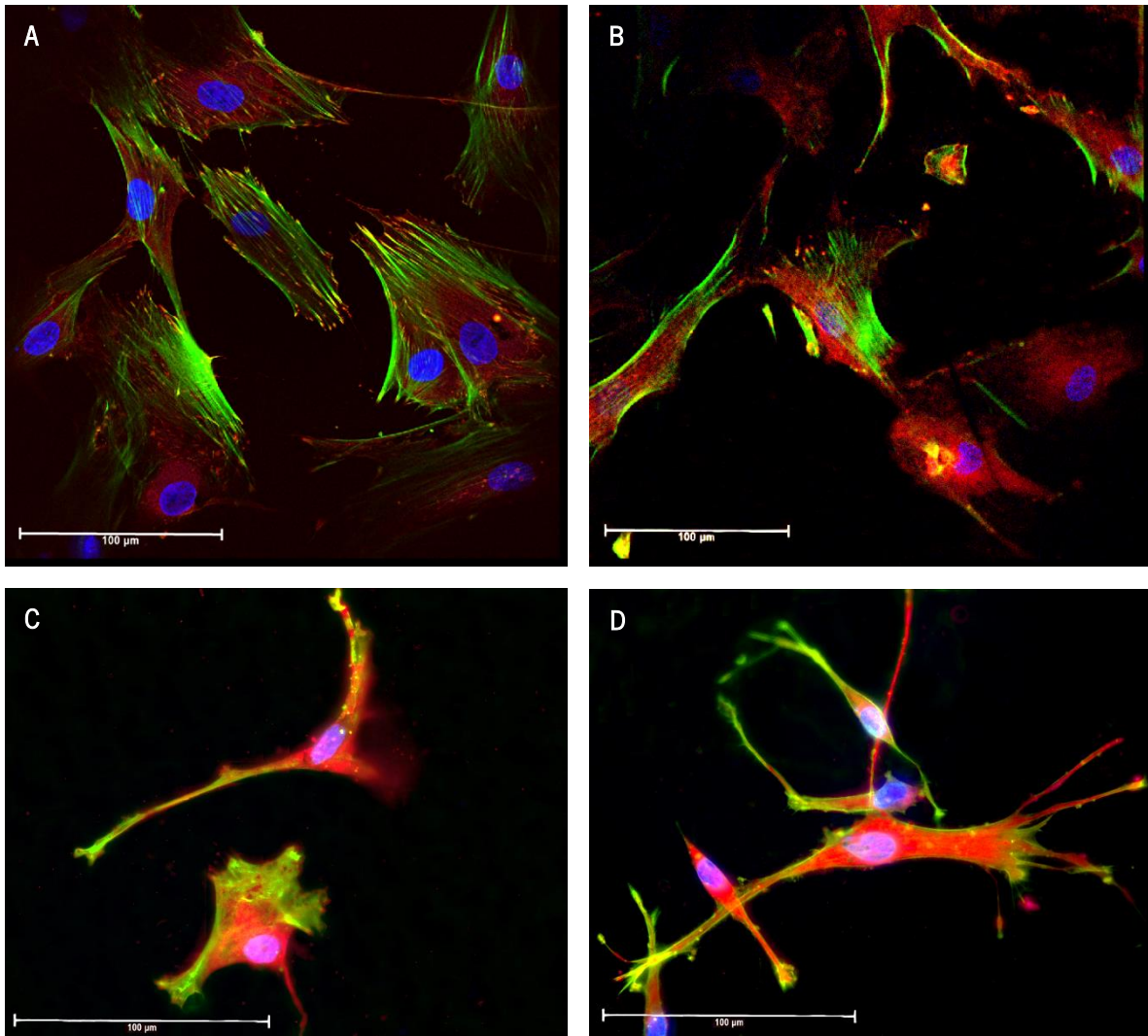


Figure 4.6 – Confocal fluorescence microscopy images of hMSC's after 4 days of cell culture in A) glass covers, B) β -PVDF film C) films with high density of PVDF microspheres, D) films with low density of PVDF microspheres. The scale bar (100 μ m) is valid for all the images.

For the microspheres only, a 3D image was assembled with the stacks of photos taken in confocal microscope using ImageJ software (Figure 4.7). It is possible to verify that cells have a unique morphology, and that is due to the disordered nature of the microspheres which do not induce any preferential cells orientation. Their cytoskeleton is highly elongated, being this 3D assembly an agglomerate of cells and microspheres. As microspheres are much smaller when compared to the

cells (Figure 4.5) and as they disrupt easily, it is not possible to observe them in this image. Also, these cells are smaller than the ones cultured in the other substrates and no vinculin staining can be seen. These two can be related with cell culture conditions, as medium changes always offer some mechanical stress to the seeded cells. This prevents cells to adhere to a specific set of microspheres and instead they are growing within dispersed groups of the substrate and adopting different morphologies, inhibiting focal adhesions.

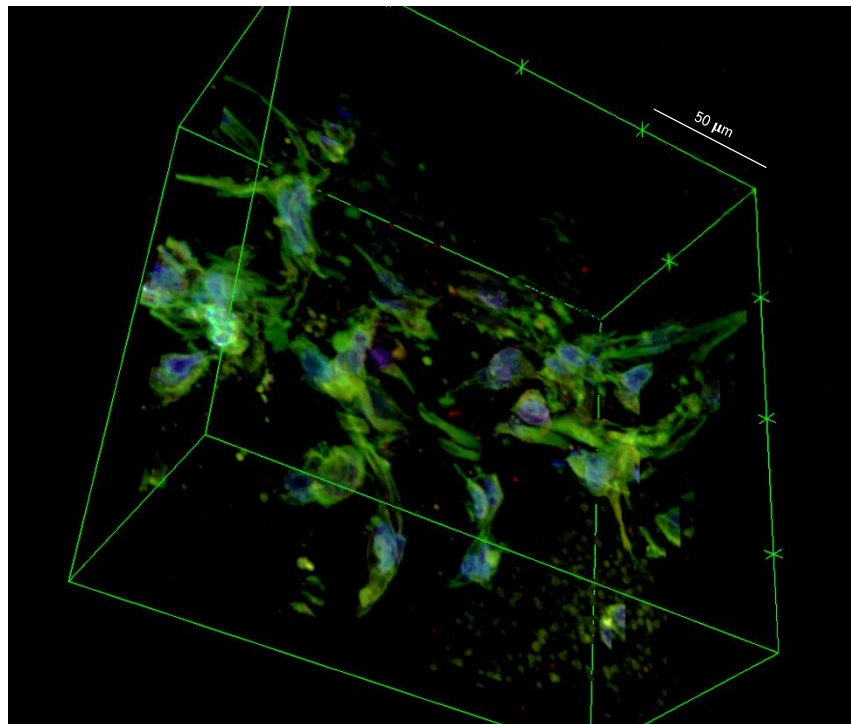


Figure 4.7 – Confocal fluorescence microscopy reconstructed 3D image of the hMSC's after 4 days of cell culture on the β -PVDF microspheres. Each green cross is distanced 50 μm from the next one, as indicated by the scale bar.

It has already been reported that disordered structures promotes MSC's to undergo osteogenic differentiation and that mechanotransductive events between the cell and the biomaterial were a key factor influencing cell fate [139]. In concordance, a study demonstrated that increased contractility of hMSC's leads preferentially to osteogenesis, while low contractility led to adipogenesis [140]. Matrix elasticity is also related to cell differentiation since Engler *et al.* (2006) showed that stiffer matrices increase cytoskeleton tension and thereby increase osteogenesis, while softer matrices led MSC's to differentiate towards alternative lineages [141]. Additionally, hMSC's that were allowed to grow without confinement demonstrated higher levels of bone cell markers when compared to those that grow under

standard culture conditions [142]. Through the years, researchers performed a series of studies which all demonstrated that cell culture conditions that increase cytoskeletal tension, promote osteogenesis; and other studies have linked cytoskeletal tension to cell spreading. Furthermore, McBeath *et al.* (2004) proved that changes in cell shape can alone influence in hMSC's commitment between osteogenic and adipogenic differentiation, and that RhoA – a small GTPase known to regulate the actin cytoskeleton in the formation of stress fibers – and its downstream effector

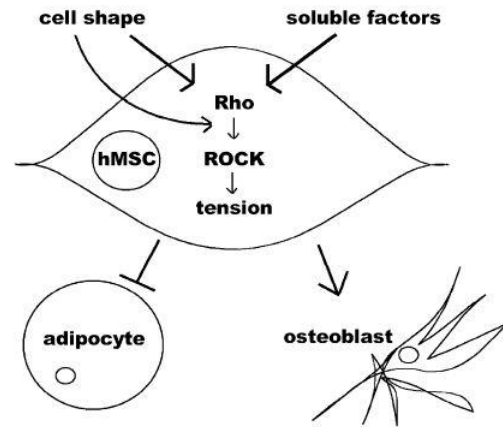


Figure 4.8 – Schematic representation of how cell shape and RhoA signaling or cytoskeletal tension alters hMSC's commitment [138].

ROCK, when inhibited, decrease expression of osteogenic markers (Figure 4.8), being their activity greatest when cells are sub confluent in osteogenic media [138]. Summing up, cell shape can alter commitment of hMSC's to adipocytes or osteocytes, given that adherent, flatten and spread cells undergo osteogenesis and round, non-spread cells undergo adipogenesis.

Thus, looking at this work results for cell attachment and morphology, the LD-M film seems to be the one that can provide the greatest body cell spreading and adherence. Additionally, this may be the stiffer substrate, and consequently the one that promotes the most cytoskeleton tension, likely making this the most suitable substrate for osteogenic differentiation. Attending to the HD-M film, it is possible to verify that it shares some of these LD-M film features, however this substrate does not seem to have the characteristic LD-M film stiffness, being a substrate that cannot have flatten and spread cells, theoretically reducing osteogenic potential.

As for the microspheres only, it can be seen that these cells can grow around the microspheres without having to remain attached and that they were able to create a 3D niche, which is the most suitable for mimicking *in vivo* bone marrow conditions of stem cell differentiation. Additionally, in Figure 4.5-F it can be seen that these cells spread more when compared to the cells seeded on the other samples. Also, their small size and unlike morphology can be justified by cytoskeleton tension produced when cells grow between the microspheres.

4.5 CELL VIABILITY

The viability of the attached cells on the PVDF samples after 4 days of culture is shown in Figure 4.9. This MTS assay has shown that PVDF is a suitable biomaterial for hMSC's growth and survival, since the samples have a $\cong 400\%$ increase (film and microspheres films) and a $\cong 300\%$ increase (microspheres only) in the measured absorbance compared to cells seeded on glass covers. There are not significant statistical differences among the PVDF samples. This result corroborates other cell studies that have been done with PVDF [16], [25], [26], [124].

However, it is possible to verify a lower number of cells when seeded on the PVDF microspheres, with a huge standard deviation. This is may be due to cell culture conditions that can vary greatly with medium changes or to the microspheres agglomeration, given that higher agglomeration state may give the hMSC's a more appropriate 3D culture niche, and consequently more cell viability. On other side, it has already been shown that proliferation is higher in flat surfaces than in 3D/porous ones. Additionally, it has been stated a genuine lack of proliferation ability of cells cultured in a 3D environment when comparing with those cultured in a monolayer [143].

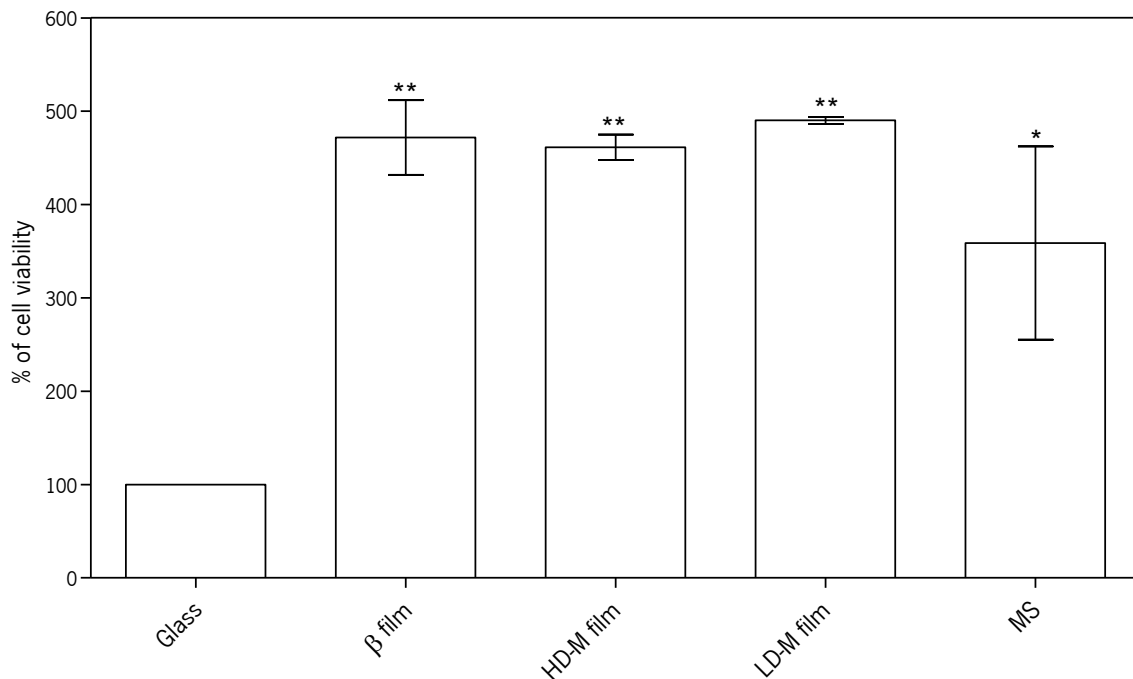


Figure 4.9 – Cell viability for cells seeded on the PVDF samples and cells seeded on glass covers (control +). Results are expressed as mean \pm standard deviation with $n = 3$. * $P \leq 0.05$, ** $P \leq 0.01$ vs. Glass.

4.6 FLOW CYTOMETRY ANALYSIS

hMSC's were submitted to FC in order to evaluate the loss or maintenance of the characteristic hMSC's markers.

In Figure 4.10, a histogram of the hMSC's at passage 4 is represented. It's possible to observe a logarithmic scale in the x-axis, which gives us an idea of the amount of antibodies that bound to the antigens of hMSC's, meaning that curves are more advanced in the logarithmic scale as cells express more markers (CD's). Each one of the 4 y-axis represent the antibodies (FITC, PE, PerCP and APC) used against the cell-surface antigens, as explained in Table 3.1. So, these cells revealed to be negative for hematopoietic markers CD19, CD34, CD45 and CD14, given that their blue representative curve is overlapping with the representative curve of the non-labeled cells, their autofluorescence, in green. These cells also revealed to be negative for HLA-DR and positive for CD90, CD105 and CD73, given that their pink curve is advanced in the "x" axis, when compared to the green curve of the non-labeled cells, which represents the positive labeling (Figure 4.10). So, according to Dominici *et al.* (2006) [58], these cells can be classified as mesenchymal stem cells.

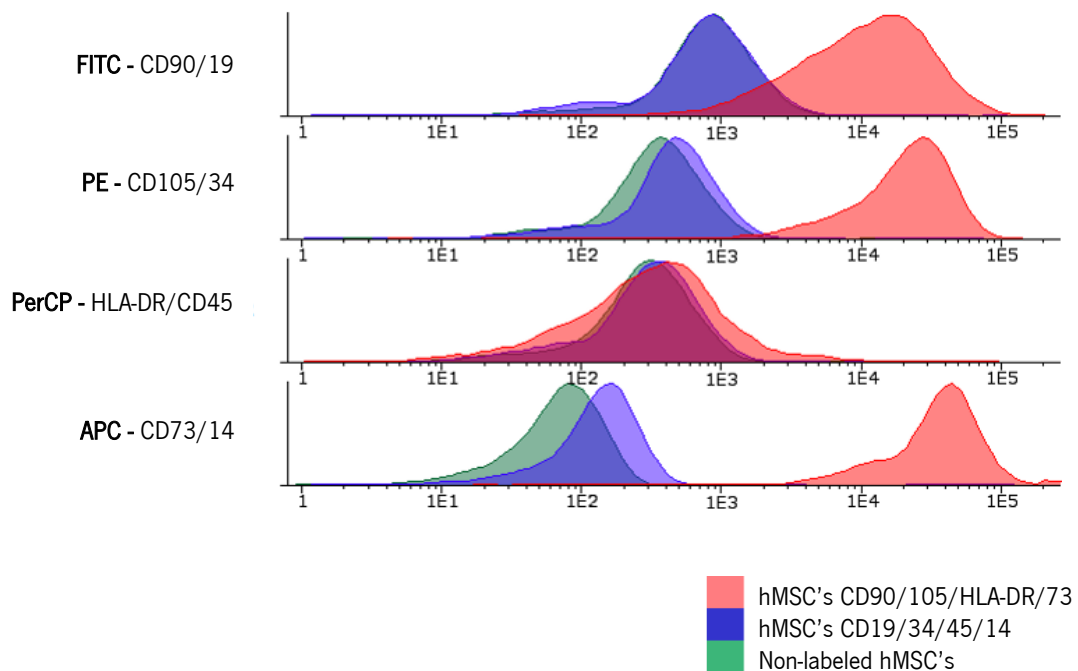


Figure 4.10 – Histograms of the hMSC's (passage 4) flow cytometry analysis at day 0 of cell culture.

At day 4 of cell culture, hMSC's were again analyzed. Now, cultured cells on the substrates were also evaluated. Due to the inability to separate hMSC's from the microspheres, cells cultured on

3D substrates could not pass through the cytometer fluidic system. Although microspheres were much smaller than hMSC's, they form huge agglomerates, which can, by one side, disturb the fluidics system and on the other side cover the coupled antibody signal. For this reason, the FC analysis of hMSC's cultured on 3D substrates has not been analyzed.

First, the cells seeded for 4 days in TCPS (control +) were compared with day 0 of cells (Figure 4.11-A). Then, day 4 of cells seeded on each one of the substrates (β -PVDF film, HD-M film and LD-M film) were also compared to day 4 of cells cultured in TCPS (Figure 4.11-B, 4.11-C and 4.11-D, respectively).

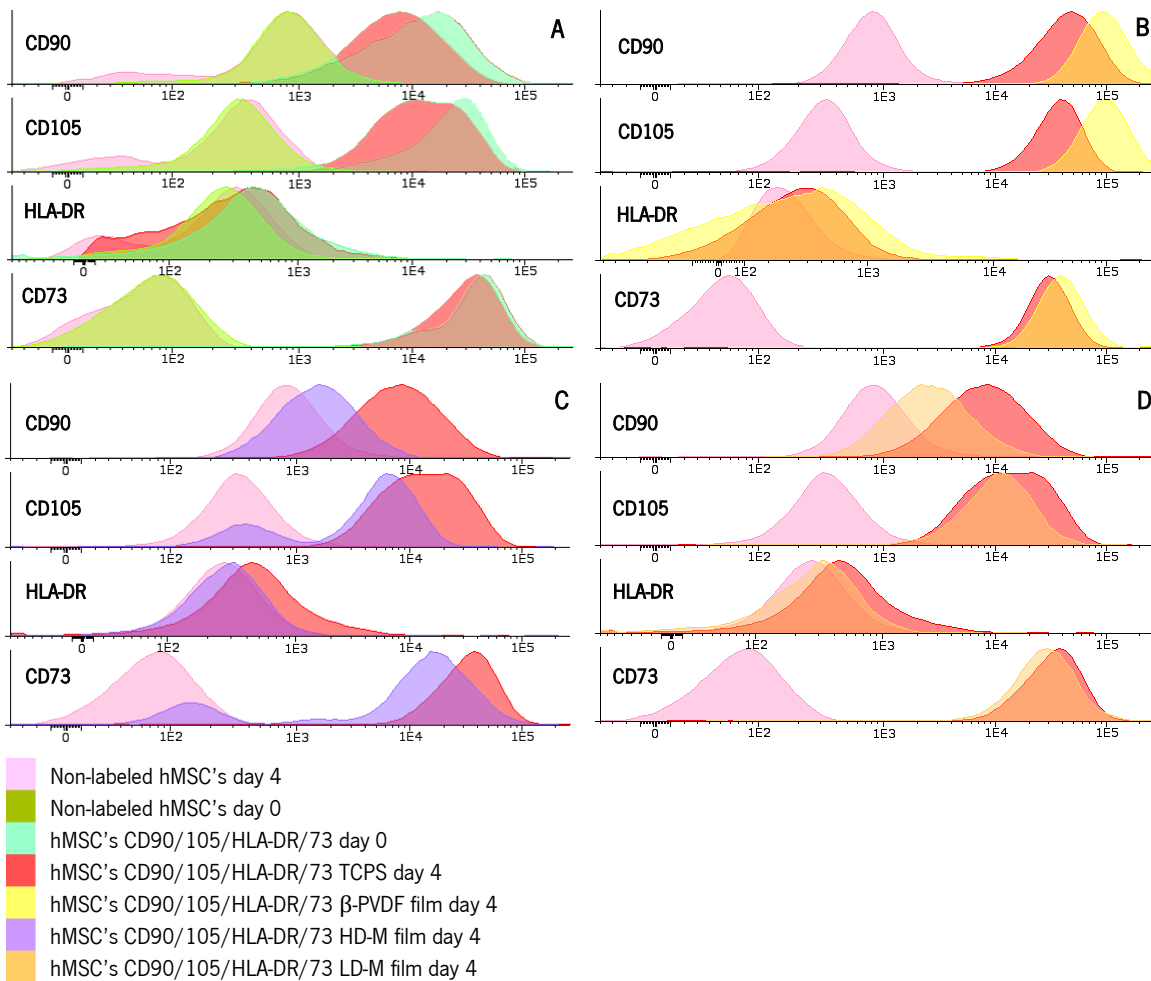


Figure 4.11 – Histograms of cells seeded in TCPS at day 4 compared to: A – day 0 cells before seeding; B – cells seeded on β -PVDF film at day 4; C – cells seeded on HD-M film at day 4; D – cells seeded on LD-M film at day 4.

When comparing cells before seeding and cells cultured on TCPS for 4 days (Figure 4.11-A), it can be observed that there was a great loss of CD90 and CD105. That is, the curves related to the

positive markers of cells cultured on TCPS at day 4 (dark pink) are displaced from the curves related to the cells at day 0 (light green). The first are closer to the non-labelled cells (green), and therefore with less amount of CD90 and CD105 in their surface, given that the non-labeled cells (green) represent the autofluorescence of the cells, in other words, the negative labeling.

In the same line of thought, CD73 also decreased expression but not as much as the other ones. As mentioned before, loss of these three hMSC's markers together was already reported to be related with their differentiation [83], [84]. The difference in the behavior of CD105 and CD90 on the one side and CD73 on the other might be relevant. The loss of CD105 expression was already related to multi-lineage differentiation of stem cells. On the other hand, it has been stated that hMSC's loss CD90 expression as cells mature towards osteoblastic-like cells [87]. Low down-regulation of CD73 could be explained because it has already been shown that CD73 generated adenosine promotes osteoblast differentiation and that it is expressed in mature osteoblasts [144], [145], so its expression may vary, as seen in H. J. Jin *et al.* (2009) [83], but not as much as the other positive markers, maybe because more time is still needed for these cells to become totally differentiated. Thus, in 4 days of cell culture it can be observed that cells already started to lose some of the MSC markers, when comparing day 0 with day 4 cells cultured on TCPS's, proving that cells have already started to differentiate.

Now, cells cultured in TCPS for 4 days will be compared to cells cultured in the different produced materials (β -phase PVDF films, HD-M films and LD-M films) also for 4 days in order to verify if these biomaterials were able to enhance differentiation.

Histogram B of Figure 4.11 demonstrates cells cultured on β -phase PVDF films. It can be seen that its positive markers are up-regulated in comparison to the day 4 control cells. That is, the curves related to the positive markers of cells cultured on β -phase PVDF films at day 4 (yellow) are displaced from the curves related to the cells cultured on TCPS at day 4 (dark pink). The first are more distant to the non-labelled cells (in light pink), and therefore with higher amount of CD90, CD105 and CD73 in their surface, given that the non-labeled cells (light pink) represent the autofluorescence of the cells, in other words, the negative labeling. That happened because, upon acquisition of day 4 seeded cells on these substrates, there is a lot of autofluorescence of the sample, which can be seen in Figure 4.12 (blue curves). This may happened because the cells used for this experiment were one passage ahead of those used to do the other FC studies on the samples. So, according to Wagner *et al.* (2008) this

phenomena can happen due to the accumulation of highly fluorescent lipofuscin at later passages and continuous increase in granularity and cell size, enhancing FC forward-scatter signal and increasing hMSC's autofluorescence [146]. Conversely, it can be seen that CD73 has a “standard” autofluorescence (in blue – Figure 4.12), only CD90 and CD105 increased it. So, according to CD90 and CD105 autofluorescence, cells loss almost totally

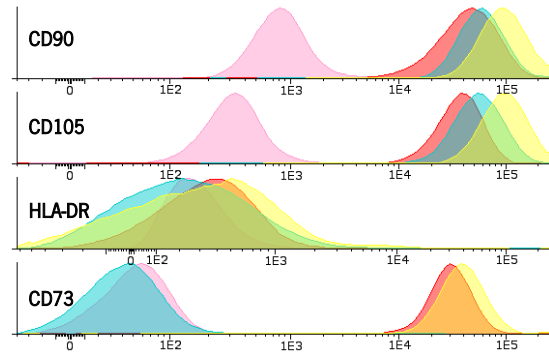


Figure 4.12 – Histogram of cells seeded in TCPS at day 4 compared to β -PVDF film. The color legend is the same as Figure 4.11.

these cell markers. However, it is not possible to support this conclusion, given that even the β -film autofluorescence histogram is up-regulated when compared to day 4 cells cultured on TCPS. Alternatively, this up-regulation can be a consequence of the material nature. Because this material has a superficial heterogeneous negative charge, it can be somehow influencing the mesenchymal stem cells and their labelling, having therefore consequences on FC analysis.

Histograms C and D of Figure 4.11 represent cells seeded on HD-M films and LD-M films, respectively. It can be observed that their positive markers decreased even more compared to TCPS seeded cells at the same day, meaning that these cells lost a lot of their typical hMSC's characteristics. This reports on the influence of these microspheres films on the differentiation of hMSC's. Additionally, on histogram C of Figure 4.11, in CD105 and CD73, a sub-population of cells can be seen overlapping the non-labeled cells, meaning that these subset of cells lost completely their markers expression. As seen in Figure 4.9, cells did not lose their viability on these supports, proving that these sub-populations of cells are not relative to dead cells. Also, the decrease in CD90 was greater in cells cultured on this HD-M film. This leads to the conclusion that this substrate, and this irregular topography, somehow leads cells to differentiate, more that when cultured on more flat surfaces, which is disagreeing with the first theoretical hypothesis of the LD-M film being the most suitable for differentiation.

Overall, it can be concluded that microspheres films, and particularly HD-M films give the cells the appropriate topography to induce their differentiation. Topography of biomaterials induces different cell shapes, and different shapes have shown to regulate indirectly differentiation onto the osteoblast phenotype [138]. Therefore, these substrates can be giving the cells a specific tension that directly stimulates osteoblastic differentiation.

4.7 ASSESSMENT OF HUMAN MESENCHYMAL STEM CELLS OSTEOGENIC DIFFERENTIATION

4.7.1 Flow Cytometry analysis

After 4 days of cell proliferation under basal medium, osteogenic supplemented (OS) medium was added, as previously mentioned, and cells were kept in this medium for 14 days. Therefore, FC analysis was continued in order to compare these to the previously obtained results in basal medium. First, a check-up control was performed at day 7. Finally, at day 14 samples and controls were also analyzed. From now on, days will be describe as if day 0 was the first day of OS medium introduction.

At day 7, two controls were analyzed and compared to day 4 TCPS seeded cells (before introducing OS medium). Both these controls were performed with cells cultured on TCPS, one with OS medium (Figure 4.13-B) and other with basal medium (Figure 4.13-A).

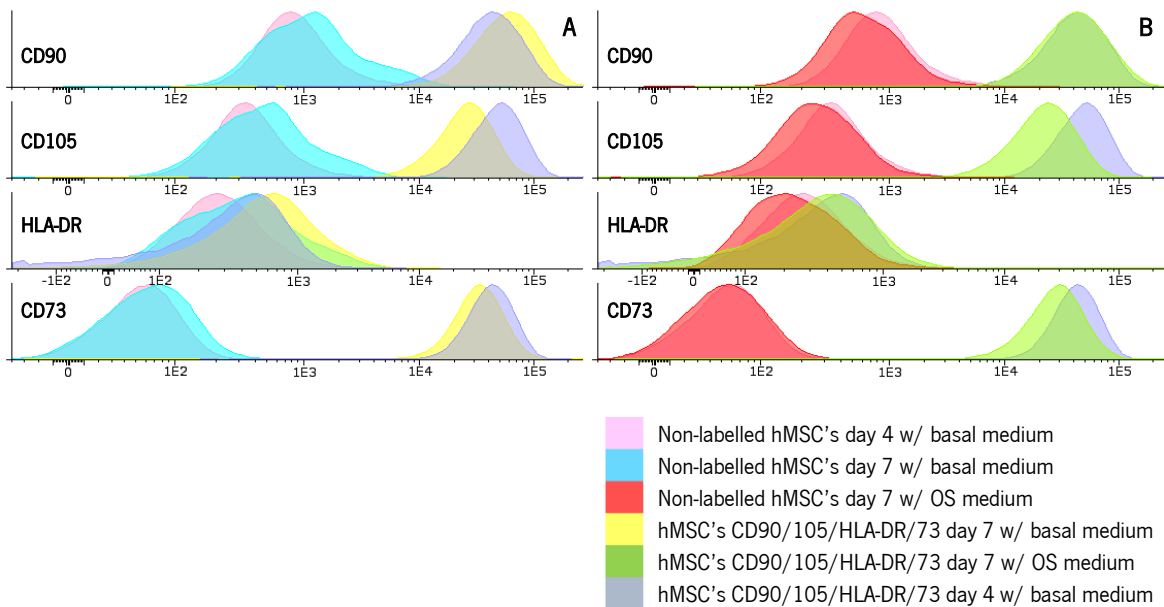


Figure 4.13 – Histograms of cells seeded on TCPS at day 7 compared to cells seeded on TCPS at day 4 before OS medium introduction. A – Cells seeded in basal medium; B – cells seeded in OS medium.

Analyzing and comparing these histograms, it can be observed that, in OS medium, the markers were down-regulated when compared to basal medium, but not markedly, which means that OS medium is starting to make some influence on markers down-regulation. That is, the curves related to the positive markers of cells cultured on TCPS at day 7 with OS medium (green) are displaced from the curves related to the cells cultured on TCPS at day 4 (grey). The first are closer to the non-labelled

cells (red), and therefore with less amount of CD90, CD105 and CD73 in their surface, given that the non-labeled cells (red) represent the autofluorescence of the cells, in other words, the negative labeling.

In the same line of thought, in histogram A of Figure 4.13, it can be seen that the curve related to CD90 of cells cultured on TCPS at day 7 with basal medium (yellow) was up-regulated when compared to the day 4 cells cultured on TCPS (grey), although CD105 and CD73 decreased expression, being closer to the non-labeled cells curve (blue). This differentiation study was done with a different subset of hMSC's that, at day 0, had the typical hMSC's markers but, as said, could have different sensibility to osteogenic medium or to the samples, and may have to be cultured for longer time to have the same results as those seen in Figure 4.11. However, these can be conclusive as well, because overall hMSC's are losing their specific markers even without OS medium, which means that cell's confluence achieved at the same time as medium change to OS had an influence on differentiation potential.

For control purposes, another FC analysis was performed at 14 days after osteogenic induction comparing cells cultured on TCPS with and without OS medium with cells cultured on TCPS at day 4 of cell culture without OS medium (Figure 4.14).

It can be seen that CD105 and CD73 markers decreased with culture time on TCPS, even without OS and that, with addition of the inductive media, all of the markers decreased expression. That is, the curves related to CD105 and CD73 of cells cultured on TCPS at day 14 with (blue) and without (light green) OS medium are displaced from the curves related to the cells cultured on TCPS at day 4 (purple). The first are closer to the non-labelled cells (dark green), and therefore with less amount of CD105 and CD73 in their surface, that is, closer to the negative labeling. However, in basal medium, CD90 slightly increased its expression, as also seen at 7 days of culture (their positive curve, in light green, is farther to the non-labeled cells than the cells cultured on TCPS at day 4, in purple) (Figure 4.14). That can be due to the nature of the TCPS, which prevents cells to lose expression of all markers and enter osteogenic differentiation as fast as cells cultured with OS medium, which lose all expression markers, even in TCPS, as can be observed.

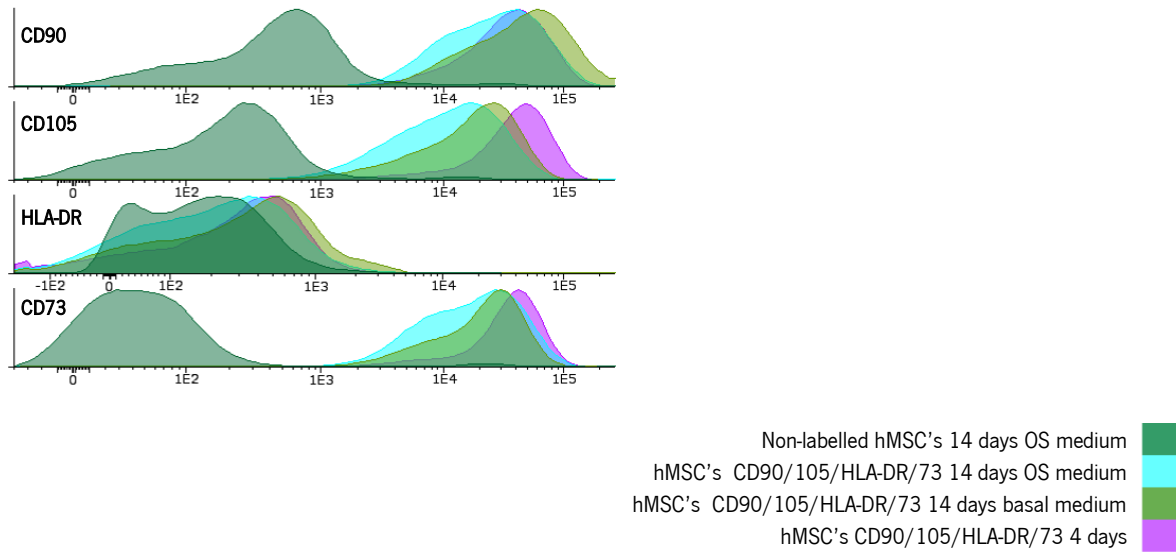


Figure 4.14 – Histograms TCPS seeded cells at day 14 compared to TCPS seeded cells at day 4 with and without OS medium.

A final FC analysis was performed at day 14 of osteogenic induction comparing cells cultured on TCPS to cells cultured on the samples. All samples presented in Figure 4.15 were analyzed at day 14 and all were induced to osteogenic differentiation upon addition of OS medium.

Till now, FC has proven that the biomaterial had influence on hMSC's markers, being down-regulated when cultured in these substrates. Also, OS medium has shown to decrease these same markers and confluence has also revealed some influence on their loss of expression.

Analyzing these graphs representing a 14 day culture, first it can be realized that non-labelled cells are up-regulated in all of them, being constant in β -phase PVDF film, compared to Figure 4.12. That is, the curves that correspond to the non-labeled cells cultured on the biomaterials, dark blue for the HD-M film, orange for the LD-M film and dark green for the β -phase film, are distanced from the non-labeled curve of cells cultured on TCPS (light pink), as if they have acquired labeling of CD90 and CD105, which is impossible. This supports the idea that autofluorescence increases in parallel with length of cell culture in these samples. This fact can also influence the analysis of the histograms, given that cells can be closer to loss of cell markers (closer to non-labelled cells curve) but still are on the same histogram place as cells cultured on TCPS, giving the illusion that these cells have not lost their pluripotentiality.

It is noteworthy that here, histograms are comparing cells seeded on the biomaterials with the cells seeded on TCPS with the same days of culture, and not with the beginning of culture time nor with cells seeded with no OS.

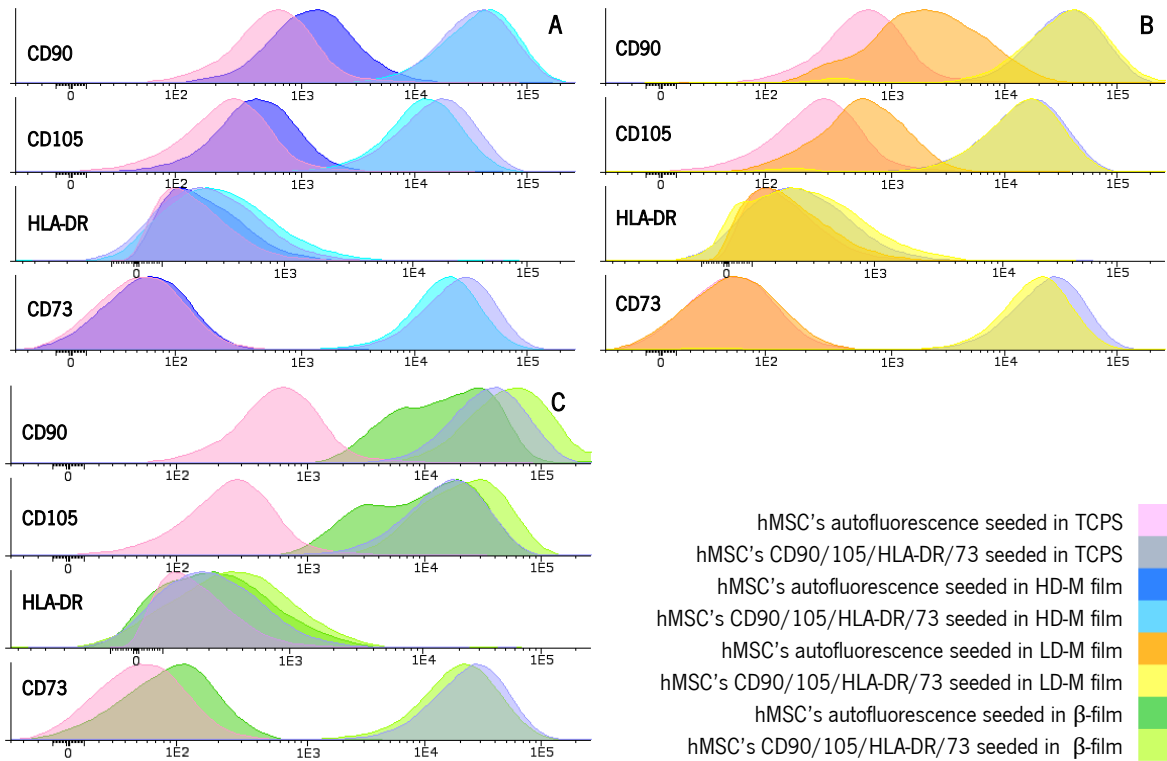


Figure 4.15 – Histograms TCPS seeded cells at day 14 compared materials' seeded cells at day 14. All samples and control were cultured with osteogenic medium. A – HD-M film; B – LD-M film; C – β -film.

So, having a closer look, and ignoring the up-regulation on the non-labelled cells, in histogram A and B of Figure 4.15, HD-M and LD-M film, respectively, the substrates seem to have only a slightly down-regulation on CD105 and CD73 markers. This can mean that TCPS are also osteoinductive and/or that osteogenic supplements (biochemical signals) and confluence (mechanical stress) had influence the behavior, shape, adhesion and, consequently, differentiation of human mesenchymal stem cells, in a manner that could mimic the topographical stress created by HD-M and LD-M films only at four days without OS. Also, it can be concluded that the stress and tension created by the microspheres films at the first days of culture, which lead hMSC's to lose expression of markers so fast, began to gain stability over time, and now it is clear that the difference is not so pronounced.

Besides, cells can present less down-regulation of markers, given that 4 days FC study was done with one subset of cells and the rest of the study was done with another set of unfrozen stem cells, but with origin on the same donor. It has been reported that hMSC's age influence cell-based therapies [147]. So, even all of the experiments were done with cells from passages 4-6, they can behave differently. Also, culture conditions may not be the same, for example it is also known that initial plating density alone can influence cell fate, independently of ahead transcriptional differentiation steps [138]. If cells are plated with high density, cell adhesion and spreading against the substrate decrease and cell-cell interaction increases. Although theoretically the same density was plated on PVDF substrates, manual cell counting can never be fully reliable. This also can happen because substrates are very irregular, particularly the HD-M film, and cells adopt different shapes and adhere differently even in the same substrate, influencing in this way FC analysis.

Finally, in histogram C of Figure 4.15, the same that happened in four days of culture can be observed. The β -PVDF film seeded cells had so much autofluorescence in CD90 and CD105 markers that, when compared to the positive markers curve, can be deduced a total loss of CD105 and CD90. However, this is not an accurate conclusion. Additionally, this phenomena is not common, as can be seen in H. J. Jin *et al.* (2009) histograms, where isotype controls did not have autofluorescence. So, the same conclusions taken for day 4 seeded cells with no OS can be applied to this time point, which in summary appoint to the influence of the heterogeneous negative surface charge on the behavior and differentiation of these cells, consequently influencing FC analysis. This is a phenomenon that has to be explored in further studies, especially on what is the effect produced on the MSC's by the superficial charge of these films.

4.7.2 Osteocalcin localization by immunocytochemistry

As said, osteocalcin is a major bone protein and has an important function in metabolism of mineralized tissues [148]. Therefore, to corroborate the results obtained by FC analysis, after 14 days of OS medium addition, an immunocytochemistry localization of osteocalcin was performed. The results for the different samples can be seen in Figure 4.16.

First, it is clear that cells cultured on glass do not express osteocalcin (Figure 4.16-A).

The β -phase PVDF film seems to have more osteocalcin staining when comparing to the microspheres films (Figure 4.16-B). This observation can lead to a different interpretation of the FC

results, since it is clear that these cells are expressing this major bone protein. So, it can be concluded that the autofluorescence phenomenon it's covering the down-regulation of cell markers on these flat beta phase PVDF films.

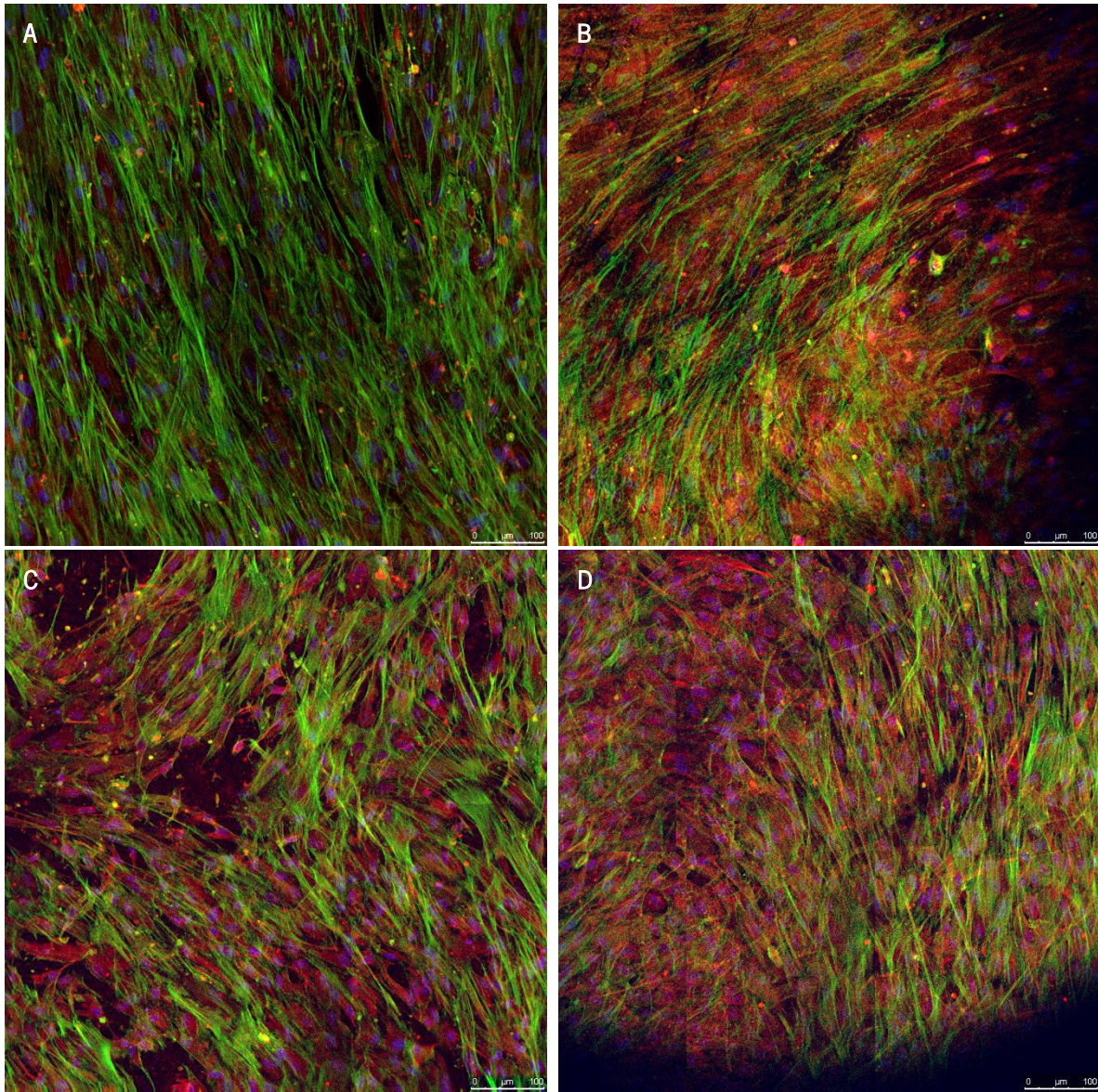


Figure 4.16 – Confocal fluorescence microscopy images of cells after 14 days of cell culture in: A) glass; B) β -PVDF film; C) HD-M PVDF film; D) LD-M PVDF film. The scale bar (100 μ m) is valid for all images.

Comparing the two PVDF microspheres samples, they have almost the same amount of osteocalcin staining. The morphology can also be visualized through actin green staining. It is

noteworthy that cells cultured on glass have a much more organized morphology, when compared to those cultured on PVDF samples, which seem to swirl. Also, in the HD-M film this effect seems enhanced, and that may be because cells are obligated to elongate and grow depending in where microspheres are placed. Given that these films have higher amounts of microspheres, cells do not have a flat surface to hold on and spread in parallel. So, even if FC studies at day 14 after OS introduction were doubtful, these results leave no place for it, confirming osteogenic differentiation by osteocalcin red staining.

PVDF microspheres only were also observed by confocal microscopy in order to localize osteocalcin within the cells (Figure 4.17). As seen, cells still wrapped up on the microspheres. The cell number decreased a lot, probably due to mechanical stress and medium changes through all culture time. It has also been shown that BM MSC's lack ability to proliferate in 3D environments and, as culture time increases, the number of cells in deeper layers decreases [143]. Osteocalcin red staining can be observed even though actin stands out. So, although very instable, 3D culture on microspheres was able to show some osteocalcin

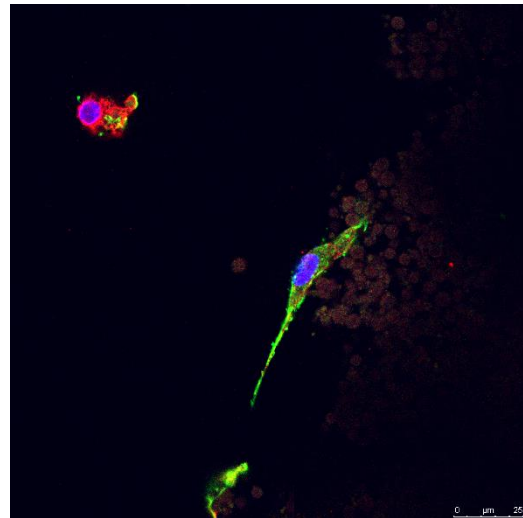


Figure 4.17 – Confocal fluorescence microscopy image of cells after 14 days of 3D cell culture on PVDF microspheres.

staining. Even though this was a promising substrate to improve hMSC's differentiation, further studies will have to be performed in order to find a reproducible way of culturing cells along with these microspheres for a long time. Also, a novel protocol for separation of microspheres and cells will be needed to perform FC analysis on these.

Overall, PVDF samples show a soft osteocalcin staining, which along with FC analysis confirms the hypothesis that these cells are entering the osteogenic differentiation pathway.

5 CONCLUSIONS, FINAL REMARKS & FUTURE PERSPECTIVES

Concluding, this new shaped PVDF microspheres topography was able to enhance hMSC's differentiation, proving the concept that morphology can really affect cell's adherence, which will result in a different shape adopted by them, and consequently different predisposition to differentiate onto distinct lineages. Controversially, this effect was greater at the first 4 days of culture without addition of osteogenic supplements. This proves that the support itself has the appropriate features to induce this differentiation state and that, with appropriate stimulation, this effect could have been greater at 14 days after osteogenic induction, instead of more stabilized, as seen. So, it can be concluded that mechanical signals or stress (provided by the substrate and by confluence itself) affects these hMSC's even more than biochemical signals (osteogenic supplements introduced).

Additionally, the negative heterogeneous charge has also affected the cells but in a different way. Even though cells seeded on β -phase PVDF films show greater staining on the osteocalcin immunocytochemistry, the FC analysis revealed an abnormal autofluorescence phenomena of the non-labelled cells, which did not happen with the cells seeded on TCPS's and happened at less extent with cells seeded on microspheres films. Additionally, this phenomenon happened only in two of the channel markers. Charge has already shown to influence stem cells behavior, but since this is a novel technique employed on the assessment of loss of cell markers to extrapolate differentiation potential, this has never been seen before. So, additional studies will have to be performed in order to understand what is really happening inside the cells, by evaluating downstream regulation of osteogenic transcription factors produced by external charge stimulation.

Regarding microspheres 3D culture, it can be stated that a suitable culture niche for the cells – involved in microspheres – was created, as seen in the confocal images. The shape and morphology adopted by these cells did not resemble the ones seeded on the other substrates, but this fact does not refute the hypothesis of these cells entering osteogenic differentiation pathways. However, additional assays will have to be performed to confirm the possible osteoinductive potential of this 3D substrate, particularly a method for separation of microspheres and cells, in order to become suitable for a flow cytometry analysis, such as incorporating magnetic nanoparticles in the PVDF solution before electrospray processing. At day 4, no focal adhesions were observed and cell-cell interactions can increase with time, mimicking *in vivo* environments. Additionally, in order to have a more stable culture, different techniques for medium changes will also have to be established. Perfusion culture plates have

been introduced in the past few years can be an appropriate alternative for this type of culture, since the cell culture stability will be increased and mechanical disturbance provided by medium changes will be eliminated.

Overall, since the β -PVDF phase is the one that has the highest piezoelectric proprieties, these cells could have an even more enhanced osteogenic response when cultured on electromechanically stimulated substrates, with a biorreator, which would result on a more biomimetic approach to these studies. This dynamic stimulation has already presented satisfactory results, as before reviewed.

So, substrates with superficial charge as β -phase PVDF and substrates that expose cells to a different topography, like the films with microspheres produced in this work, can enhance cells osteogenic differentiation potential. Therefore, the produced scaffolds could be implanted directly to facilitate bone regeneration *in vivo*. With the mechanical stimulation produced by body's natural movements, their piezoelectric response will be improved, and, consequently, this will give electric and mechanical stimulus to the cells, which together with biochemical stimulus, will increase tissue regeneration.

Also, since flow cytometry is a method based on cells specific markers and the standard protocol has few steps for elaboration, washing steps and incubation hours are diminished, when comparing to immunocytochemistry methods. Moreover, manual management associated errors are not so frequent. This technique gives a quantitative reliable analysis of the hMSC's-associated markers and how much these same markers lost expression. FC, till date, has not been used in assessment of differentiation potential of hMSC's seeded on biomaterials, but it has proven to be a very powerful and valuable technique for these studies. Additionally, these studies could be improved with a flow cytometry analysis performed in shorter time intervals, demonstrating what is the evolution of markers with time and how they lose their expression when entering different phases of differentiation, which could help scientist understanding what the potential of their scaffolds/biomaterials.

Summing up, the produced HD-M films have proven to be the most suitable for osteogenic differentiation. However, this same differentiation was achieved using the other produced biomaterials and a new technique was identified as valuable for these studies.

6 BIBLIOGRAPHY

- [1] N. A. Peppas and R. Langer, "Origins and development of biomedical engineering within chemical engineering," *AIChE J.*, vol. 50, no. 3, pp. 536–546, Mar. 2004.
- [2] D. J. Mooney, D. F. Baldwin, N. P. Suh, J. P. Vacanti, and R. Langer, "Novel approach to fabricate porous sponges of poly(d,l-lactic-co-glycolic acid) without the use of organic solvents," *Biomaterials*, vol. 17, no. 14, pp. 1417–1422, Jul. 1996.
- [3] R. Langer and J. P. Vacanti, "Tissue engineering.," *Science*, vol. 260, no. 5110, pp. 920–6, May 1993.
- [4] F. J. O'Brien, "Biomaterials & scaffolds for tissue engineering," *Mater. Today*, vol. 14, no. 3, pp. 88–95, Mar. 2011.
- [5] Y. Cao, T. I. Croll, J. G. Lees, B. E. Tuch, and J. J. Cooper-White, "Scaffolds, Stem Cells, and Tissue Engineering: A Potent Combination!," *Aust. J. Chem.*, vol. 58, no. 10, p. 691, Nov. 2005.
- [6] J. Jagur-Grodzinski, "Polymers for tissue engineering, medical devices, and regenerative medicine. Concise general review of recent studies," *Polym. Adv. Technol.*, vol. 17, no. 6, pp. 395–418, Jun. 2006.
- [7] P. X. Ma, "Scaffolds for tissue fabrication," *Mater. Today*, vol. 7, no. 5, pp. 30–40, May 2004.
- [8] J. A. Hubbell, "Biomaterials in Tissue Engineering," *Bio/Technology*, vol. 13, no. 6, pp. 565–576, Jun. 1995.
- [9] A. Vats, N. S. Tolley, J. M. Polak, and J. E. Gough, "Scaffolds and biomaterials for tissue engineering: a review of clinical applications," *Clin. Otolaryngol. Allied Sci.*, vol. 28, no. 3, pp. 165–172, Jun. 2003.
- [10] R. Duncan, "The dawning era of polymer therapeutics.," *Nat. Rev. Drug Discov.*, vol. 2, no. 5, pp. 347–60, May 2003.
- [11] Y. Bar-Cohen, *Electroactive polymer (EAP) actuators as artificial muscles: reality, potential, and challenges*. 2004.
- [12] X. Liu and P. X. Ma, "Polymeric Scaffolds for Bone Tissue Engineering," *Ann. Biomed. Eng.*, vol. 32, no. 3, pp. 477–486, Mar. 2004.
- [13] R. Samatham, K. J. Kim, D. Dogruer, H. R. Choi, M. Konyo, J. D. Madden, Y. Nakabo, J.-D. Nam, J. Su, S. Tadokoro, W. Yim, and M. Yamakita, "Active Polymers: An Overview," in *Electroactive Polymers for Robotic Applications*, K. J. Kim and S. Tadokoro, Eds. Springer London, 2007, pp. 1–36.
- [14] Y. Bar-Cohen and Q. Zhang, "Electroactive Polymer Actuators and Sensors," *MRS Bull.*, vol. 33, no. 03, pp. 173–181, Jan. 2011.
- [15] P. Martins, A. C. Lopes, and S. Lanceros-Mendez, "Electroactive phases of poly(vinylidene fluoride): Determination, processing and applications," *Prog. Polym. Sci.*, vol. 39, no. 4, pp. 683–706, Apr. 2014.
- [16] C. Ribeiro, S. Moreira, V. Correia, V. Sencadas, J. G. Rocha, F. M. Gama, J. L. Gómez Ribelles, and S. Lanceros-Méndez, "Enhanced proliferation of pre-osteoblastic cells by dynamic piezoelectric stimulation," *RSC Adv.*, vol. 2, no. 30, p. 11504, Oct. 2012.
- [17] E. Fukada and I. Yasuda, "On the Piezoelectric Effect of Bone," *J. Phys. Soc. Japan*, vol. 12, no. 10, 1957.

- [18] C. Bassett and L. Andrew, "Biologic significance of piezoelectricity," *Calcif. Tissue Res.*, vol. 1, no. 1, pp. 252–272, Dec. 1967.
- [19] J. J. Ficat, M. Thiechart, P. Ficat, C. Lacabanne, F. Micheron, and I. Bab, "Piezoelectric induction of bone formation: Ultrastructural observations," *Ferroelectrics*, vol. 60, no. 1, pp. 313–316, Feb. 1984.
- [20] C. T. Brighton, Z. B. Friedenberg, E. I. Mitchell, and R. E. Booth, "Treatment of nonunion with constant direct current.," *Clin. Orthop. Relat. Res.*, no. 124, pp. 106–23, May 1977.
- [21] E. Fukada, T. Takamatsu, and I. Yasuda, "Callus Formation by Electret," *Jpn. J. Appl. Phys.*, vol. 14, no. 12, pp. 2079–2080, Dec. 1975.
- [22] G. V. Cochran, M. W. Johnson, M. P. Kadaba, F. Vosburgh, M. W. Ferguson-Pell, and V. R. Palmieri, "Piezoelectric internal fixation devices: a new approach to electrical augmentation of osteogenesis.," *J. Orthop. Res.*, vol. 3, no. 4, pp. 508–13, Jan. 1985.
- [23] F. Jianqing, Y. Huipin, and Z. Xingdong, "Promotion of osteogenesis by a piezoelectric biological ceramic," *Biomaterials*, vol. 18, no. 23, pp. 1531–1534, Dec. 1997.
- [24] C. Ribeiro, V. Sencadas, D. M. Correia, and S. Lanceros-Méndez, "Piezoelectric polymers as biomaterials for tissue engineering applications," *Colloids Surfaces B Biointerfaces*, vol. 136, pp. 46–55, Dec. 2015.
- [25] R. Costa, C. Ribeiro, A. C. Lopes, P. Martins, V. Sencadas, R. Soares, and S. Lanceros-Mendez, "Osteoblast, fibroblast and in vivo biological response to poly(vinylidene fluoride) based composite materials.," *J. Mater. Sci. Mater. Med.*, vol. 24, no. 2, pp. 395–403, Feb. 2013.
- [26] C. Ribeiro, J. A. Panadero, V. Sencadas, S. Lanceros-Méndez, M. N. Tamaño, D. Moratal, M. Salmerón-Sánchez, and J. L. Gómez Ribelles, "Fibronectin adsorption and cell response on electroactive poly(vinylidene fluoride) films.," *Biomed. Mater.*, vol. 7, no. 3, p. 035004, Jun. 2012.
- [27] E. Giannetti, "Semi-crystalline fluorinated polymers," *Polym. Int.*, vol. 50, no. 1, pp. 10–26, Jan. 2001.
- [28] N. Weber, Y.-S. Lee, S. Shanmugasundaram, M. Jaffe, and T. L. Arinze, "Characterization and in vitro cytocompatibility of piezoelectric electrospun scaffolds.," *Acta Biomater.*, vol. 6, no. 9, pp. 3550–6, Sep. 2010.
- [29] M. Benz and W. B. Euler, "Determination of the crystalline phases of poly(vinylidene fluoride) under different preparation conditions using differential scanning calorimetry and infrared spectroscopy," *J. Appl. Polym. Sci.*, vol. 89, no. 4, pp. 1093–1100, Jul. 2003.
- [30] S. Lanceros-Méndez, J. F. Mano, A. M. Costa, and V. H. Schmidt, "FTIR and DSC Studies of Mechanically Deformed β -VDF Films," *J. Macromol. Sci. Phys.*, vol. 40, no. 3–4, pp. 517–527, 2001.
- [31] R. Gregorio, "Determination of the α , β , and γ crystalline phases of poly(vinylidene fluoride) films prepared at different conditions," *J. Appl. Polym. Sci.*, vol. 100, no. 4, pp. 3272–3279, May 2006.
- [32] F. Liu, N. A. Hashim, Y. Liu, M. R. M. Abed, and K. Li, "Progress in the production and modification of PVDF membranes," *J. Memb. Sci.*, vol. 375, no. 1–2, pp. 1–27, Jun. 2011.
- [33] P. M. Martins, S. Ribeiro, C. Ribeiro, V. Sencadas, A. C. Gomes, F. M. Gama, and S. Lanceros-Méndez, "Effect of poling state and morphology of piezoelectric poly(vinylidene fluoride) membranes for skeletal muscle tissue engineering," *RSC Adv.*, vol. 3, no. 39, p. 17938, Sep. 2013.
- [34] C. Ribeiro, V. Sencadas, J. L. G. Ribelles, and S. Lanceros-Méndez, "Influence of Processing

- Conditions on Polymorphism and Nanofiber Morphology of Electroactive Poly(vinylidene fluoride) Electrospun Membranes,” *Soft Mater.*, vol. 8, no. 3, pp. 274–287, Sep. 2010.
- [35] A. California, V. F. Cardoso, C. M. Costa, V. Sencadas, G. Botelho, J. L. Gómez-Ribelles, and S. Lanceros-Mendez, “Tailoring porous structure of ferroelectric poly(vinylidene fluoride-trifluoroethylene) by controlling solvent/polymer ratio and solvent evaporation rate,” *Eur. Polym. J.*, vol. 47, no. 12, pp. 2442–2450, Dec. 2011.
- [36] R. Ravichandran, S. Sundarajan, J. R. Venugopal, S. Mukherjee, and S. Ramakrishna, “Advances in polymeric systems for tissue engineering and biomedical applications.,” *Macromol. Biosci.*, vol. 12, no. 3, pp. 286–311, Mar. 2012.
- [37] S. Sethuraman, L. S. Nair, S. El-Amin, R. Farrar, M.-T. N. Nguyen, A. Singh, H. R. Allcock, Y. E. Greish, P. W. Brown, and C. T. Laurencin, “In vivo biodegradability and biocompatibility evaluation of novel alanine ester based polyphosphazenes in a rat model.,” *J. Biomed. Mater. Res. A*, vol. 77, no. 4, pp. 679–87, Jun. 2006.
- [38] M. S. Taylor, A. U. Daniels, K. P. Andriano, and J. Heller, “Six bioabsorbable polymers: in vitro acute toxicity of accumulated degradation products.,” *J. Appl. Biomater.*, vol. 5, no. 2, pp. 151–7, Jan. 1994.
- [39] K. C. Dee, D. A. Puleo, and R. Bizios, *An Introduction To Tissue-Biomaterial Interactions*. 2003.
- [40] Y. Chen, M. R. Cho, A. F. T. Mak, J. S. Li, M. Wang, and S. Sun, “Morphology and adhesion of mesenchymal stem cells on PLLA, apatite and apatite/collagen surfaces.,” *J. Mater. Sci. Mater. Med.*, vol. 19, no. 7, pp. 2563–7, Jul. 2008.
- [41] B. J. Papenburg, E. D. Rodrigues, M. Wessling, and D. Stamatialis, “Insights into the role of material surface topography and wettability on cell-material interactions,” *Soft Matter*, vol. 6, no. 18, p. 4377, Sep. 2010.
- [42] H.-S. Huag, S.-H. Chou, T.-M. Don, W.-C. Lai, and L.-P. Cheng, “Formation of microporous poly(hydroxybutyric acid) membranes for culture of osteoblast and fibroblast,” *Polym. Adv. Technol.*, vol. 20, no. 12, pp. 1082–1090, Dec. 2009.
- [43] S. J. Hollister, “Porous scaffold design for tissue engineering.,” *Nat. Mater.*, vol. 4, no. 7, pp. 518–24, Jul. 2005.
- [44] Q. L. Loh and C. Choong, “Three-dimensional scaffolds for tissue engineering applications: role of porosity and pore size.,” *Tissue Eng. Part B. Rev.*, vol. 19, no. 6, pp. 485–502, Dec. 2013.
- [45] B. Subia, J. Kundu, and S. C. Kundu, “Biomaterial Scaffold Fabrication Techniques for Potential Tissue Engineering Applications,” *Tissue Eng.*, Mar. 2010.
- [46] L. Jin, T. Wang, M.-L. Zhu, M. K. Leach, Y. I. Naim, J. M. Corey, Z.-Q. Feng, and Q. Jiang, “Electrospun fibers and tissue engineering.,” *J. Biomed. Nanotechnol.*, vol. 8, no. 1, pp. 1–9, Mar. 2012.
- [47] V. Shabafrooz, M. Mozafari, D. Vashae, and L. Tayebi, “Electrospun nanofibers: from filtration membranes to highly specialized tissue engineering scaffolds.,” *J. Nanosci. Nanotechnol.*, vol. 14, no. 1, pp. 522–34, Jan. 2014.
- [48] M. Ikeuchi, R. Tane, and K. Ikuta, “Electrospray deposition and direct patterning of polylactic acid nanofibrous microcapsules for tissue engineering.,” *Biomed. Microdevices*, vol. 14, no. 1, pp. 35–43, Mar. 2012.
- [49] N. Bock, M. A. Woodruff, D. W. Hutmacher, and T. R. Dargaville, “Electrospraying, a Reproducible Method for Production of Polymeric Microspheres for Biomedical Applications,” *Polymers (Basel)*, vol. 3, no. 4, pp. 131–149, Jan. 2011.
- [50] C. H. Park and J. Lee, “Electrosprayed polymer particles: Effect of the solvent properties,” *J.*

- Appl. Polym. Sci.*, vol. 114, no. 1, pp. 430–437, Oct. 2009.
- [51] H. Fong, I. Chun, and D. . Reneker, “Beaded nanofibers formed during electrospinning,” *Polymer (Guildf.)*, vol. 40, no. 16, pp. 4585–4592, Jul. 1999.
- [52] A. Jaworek, “Micro- and nanoparticle production by electro-spraying,” *Powder Technol.*, vol. 176, no. 1, pp. 18–35, Jul. 2007.
- [53] S. L. Shenoy, W. D. Bates, H. L. Frisch, and G. E. Wnek, “Role of chain entanglements on fiber formation during electrospinning of polymer solutions: good solvent, non-specific polymer–polymer interaction limit,” *Polymer (Guildf.)*, vol. 46, no. 10, pp. 3372–3384, Apr. 2005.
- [54] G. Taylor, “Disintegration of Water Drops in an Electric Field,” *Proc. R. Soc. A Math. Phys. Eng. Sci.*, vol. 280, no. 1382, pp. 383–397, Jul. 1964.
- [55] A. J. Friedenstein, I. I. Piatetzky-Shapiro, and K. V Petrakova, “Osteogenesis in transplants of bone marrow cells.,” *J. Embryol. Exp. Morphol.*, vol. 16, no. 3, pp. 381–90, Dec. 1966.
- [56] A. J. Friedenstein, R. K. Chailakhjan, and K. S. Lalykina, “The development of fibroblast colonies in monolayer cultures of guinea-pig bone marrow and spleen cells,” *Cell Prolif.*, vol. 3, no. 4, pp. 393–403, Oct. 1970.
- [57] M. Owen and A. J. Friedenstein, “Stromal stem cells: marrow-derived osteogenic precursors.,” *Ciba Found. Symp.*, vol. 136, pp. 42–60, Jan. 1988.
- [58] M. Dominici, K. Le Blanc, I. Mueller, I. Slaper-Cortenbach, F. Marini, D. Krause, R. Deans, A. Keating, D. Prockop, and E. Horwitz, “Minimal criteria for defining multipotent mesenchymal stromal cells. The International Society for Cellular Therapy position statement.,” *Cytotherapy*, vol. 8, no. 4, pp. 315–7, Jan. 2006.
- [59] Z.-L. Deng, K. A. Sharff, N. Tang, W.-X. Song, J. Luo, X. Luo, J. Chen, E. Bennett, R. Reid, D. Manning, A. Xue, A. G. Montag, H. H. Luu, R. C. Haydon, and T.-C. He, “Regulation of osteogenic differentiation during skeletal development.,” *Front. Biosci.*, vol. 13, pp. 2001–21, Jan. 2008.
- [60] S. Kern, H. Eichler, J. Stoeve, H. Klüter, and K. Bieback, “Comparative analysis of mesenchymal stem cells from bone marrow, umbilical cord blood, or adipose tissue.,” *Stem Cells*, vol. 24, no. 5, pp. 1294–301, May 2006.
- [61] M. Crisan, S. Yap, L. Casteilla, C.-W. Chen, M. Corselli, T. S. Park, G. Andriolo, B. Sun, B. Zheng, L. Zhang, C. Norotte, P.-N. Teng, J. Traas, R. Schugar, B. M. Deasy, S. Badylak, H.-J. Buhring, J.-P. Giacobino, L. Lazzari, J. Huard, and B. Péault, “A perivascular origin for mesenchymal stem cells in multiple human organs.,” *Cell Stem Cell*, vol. 3, no. 3, pp. 301–13, Sep. 2008.
- [62] A. I. Caplan and D. Correa, “The MSC: an injury drugstore.,” *Cell Stem Cell*, vol. 9, no. 1, pp. 11–5, Jul. 2011.
- [63] J. M. Ryan, F. P. Barry, J. M. Murphy, and B. P. Mahon, “Mesenchymal stem cells avoid allogeneic rejection.,” *J. Inflamm. (Lond.)*, vol. 2, p. 8, Jul. 2005.
- [64] I. Ullah, R. Baregundi Subbarao, and G.-J. Rho, “Human Mesenchymal Stem Cells - Current trends and future prospective.,” *Biosci. Rep.*, vol. 35, no. 2, Mar. 2004.
- [65] K. Stenderup, J. Justesen, C. Clausen, and M. Kassem, “Aging is associated with decreased maximal life span and accelerated senescence of bone marrow stromal cells.,” *Bone*, vol. 33, no. 6, pp. 919–26, Dec. 2003.
- [66] M. E. Bernardo, N. Zaffaroni, F. Novara, A. M. Cometa, M. A. Avanzini, A. Moretta, D. Montagna, R. Maccario, R. Villa, M. G. Daidone, O. Zuffardi, and F. Locatelli, “Human bone marrow derived mesenchymal stem cells do not undergo transformation after long-term in vitro culture and do

- not exhibit telomere maintenance mechanisms.," *Cancer Res.*, vol. 67, no. 19, pp. 9142–9, Oct. 2007.
- [67] E. L. Spaeth, J. L. Dembinski, A. K. Sasser, K. Watson, A. Klopp, B. Hall, M. Andreeff, and F. Marini, "Mesenchymal stem cell transition to tumor-associated fibroblasts contributes to fibrovascular network expansion and tumor progression.," *PLoS One*, vol. 4, no. 4, p. e4992, Jan. 2009.
- [68] A. Schellenberg, R. Ross, G. Abagnale, S. Jousen, P. Schuster, A. Arshi, N. Pallua, S. Jockenhoevel, T. Gries, and W. Wagner, "3D non-woven polyvinylidene fluoride scaffolds: fibre cross section and texturizing patterns have impact on growth of mesenchymal stromal cells.," *PLoS One*, vol. 9, no. 4, p. e94353, Jan. 2014.
- [69] K. E. Schwab and C. E. Gargett, "Co-expression of two perivascular cell markers isolates mesenchymal stem-like cells from human endometrium.," *Hum. Reprod.*, vol. 22, no. 11, pp. 2903–11, Nov. 2007.
- [70] S. Kidd, E. Spaeth, J. L. Dembinski, M. Dietrich, K. Watson, A. Klopp, V. L. Battula, M. Weil, M. Andreeff, and F. C. Marini, "Direct evidence of mesenchymal stem cell tropism for tumor and wounding microenvironments using in vivo bioluminescent imaging.," *Stem Cells*, vol. 27, no. 10, pp. 2614–23, Oct. 2009.
- [71] R&D Systems, "Markers & Methods to Verify Mesenchymal Stem Cell Identity, Potency, & Quality," *Minireviews*, 2013. [Online]. Available: <https://www.rndsystems.com/resources/articles/markers-and-methods-verify-mesenchymal-stem-cell-identity-potency-and-quality>.
- [72] P. Mafi, S. Hindocha, R. Mafi, M. Griffin, and W. S. Khan, "Adult mesenchymal stem cells and cell surface characterization - a systematic review of the literature.," *Open Orthop. J.*, vol. 5, no. Suppl 2, pp. 253–60, Jan. 2011.
- [73] R. Romieu-Mourez, M. Francois, M.-N. Boivin, J. Stagg, and J. Galipeau, "Regulation of MHC Class II Expression and Antigen Processing in Murine and Human Mesenchymal Stromal Cells by IFN- γ , TGF- β , and Cell Density," *J. Immunol.*, vol. 179, no. 3, pp. 1549–1558, Jul. 2007.
- [74] E. Ulvestad, K. Williams, L. Bø, B. Trapp, J. Antel, and S. Mørk, "HLA class II molecules (HLA-DR, -DP, -DQ) on cells in the human CNS studied in situ and in vitro.," *Immunology*, vol. 82, no. 4, pp. 535–41, Aug. 1994.
- [75] N. D. Huntington and D. M. Tarlinton, "CD45: direct and indirect government of immune regulation.," *Immunol. Lett.*, vol. 94, no. 3, pp. 167–74, Jul. 2004.
- [76] D. L. Simmons, S. Tan, D. G. Tenen, A. Nicholson-Weller, and B. Seed, "Monocyte antigen CD14 is a phospholipid anchored membrane protein.," *Blood*, vol. 73, no. 1, pp. 284–9, Jan. 1989.
- [77] L.-J. Zhou, D. Ord, S. Omori, and T. Tedder, "Structure of the genes encoding the CD19 antigen of human and mouse B lymphocytes," *Immunogenetics*, vol. 35, no. 2, Jan. 1992.
- [78] D. C. Otero, A. N. Anzelon, and R. C. Rickert, "CD19 Function in Early and Late B Cell Development: I. Maintenance of Follicular and Marginal Zone B Cells Requires CD19-Dependent Survival Signals," *J. Immunol.*, vol. 170, no. 1, pp. 73–83, Jan. 2003.
- [79] J. S. Nielsen and K. M. McNagny, "Novel functions of the CD34 family.," *J. Cell Sci.*, vol. 121, no. Pt 22, pp. 3683–92, Nov. 2008.
- [80] C.-S. Lin, H. Ning, G. Lin, and T. F. Lue, "Is CD34 truly a negative marker for mesenchymal stromal cells?," *Cytotherapy*, vol. 14, no. 10, pp. 1159–63, Nov. 2012.
- [81] W. L. Parker, M. B. Goldring, and A. Philip, "Endoglin is expressed on human chondrocytes and

- forms a heteromeric complex with betaglycan in a ligand and type II TGFbeta receptor independent manner.," *J. Bone Miner. Res.*, vol. 18, no. 2, pp. 289–302, Feb. 2003.
- [82] B. A. J. Roelen and P. ten Dijke, "Controlling mesenchymal stem cell differentiation by TGFbeta family members.," *J. Orthop. Sci.*, vol. 8, no. 5, pp. 740–8, Jan. 2003.
- [83] H. J. Jin, S. K. Park, W. Oh, Y. S. Yang, S. W. Kim, and S. J. Choi, "Down-regulation of CD105 is associated with multi-lineage differentiation in human umbilical cord blood-derived mesenchymal stem cells.," *Biochem. Biophys. Res. Commun.*, vol. 381, no. 4, pp. 676–81, Apr. 2009.
- [84] B. Delorme, J. Ringe, N. Gallay, Y. Le Vern, D. Kerboeuf, C. Jorgensen, P. Rosset, L. Sensebé, P. Layrolle, T. Häupl, and P. Charbord, "Specific plasma membrane protein phenotype of culture-amplified and native human bone marrow mesenchymal stem cells.," *Blood*, vol. 111, no. 5, pp. 2631–5, Mar. 2008.
- [85] X. D. Chen, H. Y. Qian, L. Neff, K. Satomura, and M. C. Horowitz, "Thy-1 antigen expression by cells in the osteoblast lineage.," *J. Bone Miner. Res.*, vol. 14, no. 3, pp. 362–75, Mar. 1999.
- [86] T. A. Rege and J. S. Hagood, "Thy-1 as a regulator of cell-cell and cell-matrix interactions in axon regeneration, apoptosis, adhesion, migration, cancer, and fibrosis.," *FASEB J.*, vol. 20, no. 8, pp. 1045–54, Jun. 2006.
- [87] A. Wiesmann, H.-J. Bühring, C. Mentrup, and H.-P. Wiesmann, "Decreased CD90 expression in human mesenchymal stem cells by applying mechanical stimulation.," *Head Face Med.*, vol. 2, p. 8, Jan. 2006.
- [88] S. P. Colgan, H. K. Eltzschig, T. Eckle, and L. F. Thompson, "Physiological roles for ecto-5'-nucleotidase (CD73).," *Purinergic Signal.*, vol. 2, no. 2, pp. 351–60, Jun. 2006.
- [89] S. Harada and G. A. Rodan, "Control of osteoblast function and regulation of bone mass.," *Nature*, vol. 423, no. 6937, pp. 349–55, May 2003.
- [90] J. C. Reichert, S. Saifzadeh, M. E. Wullschleger, D. R. Epari, M. A. Schütz, G. N. Duda, H. Schell, M. van Griensven, H. Redl, and D. W. Huttmacher, "The challenge of establishing preclinical models for segmental bone defect research.," *Biomaterials*, vol. 30, no. 12, pp. 2149–63, Apr. 2009.
- [91] P. M. Govey, A. E. Loisel, and H. J. Donahue, "Biophysical regulation of stem cell differentiation.," *Curr. Osteoporos. Rep.*, vol. 11, no. 2, pp. 83–91, Jun. 2013.
- [92] K. Nakashima, X. Zhou, G. Kunkel, Z. Zhang, J. M. Deng, R. R. Behringer, and B. de Crombrughe, "The novel zinc finger-containing transcription factor osterix is required for osteoblast differentiation and bone formation.," *Cell*, vol. 108, no. 1, pp. 17–29, Jan. 2002.
- [93] D. T. Nguyen and K. J. L. Burg, "Bone tissue engineering and regenerative medicine: Targeting pathological fractures," *J. Biomed. Mater. Res. Part A*, vol. 103, no. 1, pp. 420–429, Jan. 2015.
- [94] B. R. Olsen, A. M. Reginato, and W. Wang, "Bone development.," *Annu. Rev. Cell Dev. Biol.*, vol. 16, pp. 191–220, Jan. 2000.
- [95] S. Kustra and C. J. Bettinger, "Smart polymers and interfaces for dynamic cell-biomaterials interactions," *MRS Bull.*, vol. 37, no. 09, pp. 836–846, Sep. 2012.
- [96] T. K. Kim, J. J. Yoon, D. S. Lee, and T. G. Park, "Gas foamed open porous biodegradable polymeric microspheres.," *Biomaterials*, vol. 27, no. 2, pp. 152–9, Jan. 2006.
- [97] M. Biondi, F. Ungaro, F. Quaglia, and P. A. Netti, "Controlled drug delivery in tissue engineering.," *Adv. Drug Deliv. Rev.*, vol. 60, no. 2, pp. 229–42, Jan. 2008.
- [98] H. Wang, S. C. G. Leeuwenburgh, Y. Li, and J. A. Jansen, "The use of micro- and nanospheres

- as functional components for bone tissue regeneration.," *Tissue Eng. Part B. Rev.*, vol. 18, no. 1, pp. 24–39, Feb. 2012.
- [99] N. Yu, A. Schindeler, D. G. Little, and A. J. Ruys, "Biodegradable poly(alpha-hydroxy acid) polymer scaffolds for bone tissue engineering.," *J. Biomed. Mater. Res. B. Appl. Biomater.*, vol. 93, no. 1, pp. 285–95, Apr. 2010.
- [100] S.-J. Hong, H.-S. Yu, and H.-W. Kim, "Preparation of porous bioactive ceramic microspheres and in vitro osteoblastic culturing for tissue engineering application.," *Acta Biomater.*, vol. 5, no. 5, pp. 1725–31, Jun. 2009.
- [101] A. Chatterjea, H. Yuan, E. Fennema, R. Burer, S. Chatterjea, H. Garritsen, A. Renard, C. A. van Blitterswijk, and J. de Boer, "Engineering new bone via a minimally invasive route using human bone marrow-derived stromal cell aggregates, microceramic particles, and human platelet-rich plasma gel.," *Tissue Eng. Part A*, vol. 19, no. 3–4, pp. 340–9, Feb. 2013.
- [102] S. Samavedi, A. R. Whittington, and A. S. Goldstein, "Calcium phosphate ceramics in bone tissue engineering: a review of properties and their influence on cell behavior.," *Acta Biomater.*, vol. 9, no. 9, pp. 8037–45, Sep. 2013.
- [103] A. C. Jayasuriya and A. Bhat, "Fabrication and characterization of novel hybrid organic/inorganic microparticles to apply in bone regeneration.," *J. Biomed. Mater. Res. A*, vol. 93, no. 4, pp. 1280–8, Jun. 2010.
- [104] A. Champa Jayasuriya and A. Bhat, "Mesenchymal stem cell function on hybrid organic/inorganic microparticles in vitro.," *J. Tissue Eng. Regen. Med.*, vol. 4, no. 5, pp. 340–8, Jul. 2010.
- [105] B. P. Chan, T. Y. Hui, M. Y. Wong, K. H. K. Yip, and G. C. F. Chan, "Mesenchymal Stem Cell–Encapsulated Collagen Microspheres for Bone Tissue Engineering," *Tissue Eng. Part C Methods*, vol. 16, no. 2, pp. 225–235, Apr. 2010.
- [106] L. Solorio, C. Zwolinski, A. W. Lund, M. J. Farrell, and J. P. Stegemann, "Gelatin microspheres crosslinked with genipin for local delivery of growth factors.," *J. Tissue Eng. Regen. Med.*, vol. 4, no. 7, pp. 514–23, Oct. 2010.
- [107] A. Moshaverinia, S. Ansari, C. Chen, X. Xu, K. Akiyama, M. L. Snead, H. H. Zadeh, and S. Shi, "Co-encapsulation of anti-BMP2 monoclonal antibody and mesenchymal stem cells in alginate microspheres for bone tissue engineering.," *Biomaterials*, vol. 34, no. 28, pp. 6572–9, Sep. 2013.
- [108] C. A. Custódio, V. E. Santo, M. B. Oliveira, M. E. Gomes, R. L. Reis, and J. F. Mano, "Functionalized Microparticles Producing Scaffolds in Combination with Cells," *Adv. Funct. Mater.*, vol. 24, no. 10, pp. 1391–1400, Mar. 2014.
- [109] L. Xiong, J. Zeng, A. Yao, Q. Tu, J. Li, L. Yan, and Z. Tang, "BMP2-loaded hollow hydroxyapatite microspheres exhibit enhanced osteoinduction and osteogenicity in large bone defects.," *Int. J. Nanomedicine*, vol. 10, pp. 517–26, Jan. 2015.
- [110] H. E. Davis, B. Y. K. Binder, P. Schaecher, D. D. Yakoobinsky, A. Bhat, and J. K. Leach, "Enhancing osteoconductivity of fibrin gels with apatite-coated polymer microspheres.," *Tissue Eng. Part A*, vol. 19, no. 15–16, pp. 1773–82, Aug. 2013.
- [111] L. Hong, Y. Krishnamachari, D. Seabold, V. Joshi, G. Schneider, and A. K. Salem, "Intracellular release of 17- β estradiol from cationic polyamidoamine dendrimer surface-modified poly (lactico-glycolic acid) microparticles improves osteogenic differentiation of human mesenchymal stromal cells.," *Tissue Eng. Part C. Methods*, vol. 17, no. 3, pp. 319–25, Mar. 2011.
- [112] C. M. Rogers, D. J. Deehan, C. A. Knuth, F. R. A. J. Rose, K. M. Shakesheff, and R. A.

- Oldershaw, "Biocompatibility and enhanced osteogenic differentiation of human mesenchymal stem cells in response to surface engineered poly(d,l-lactic-co-glycolic acid) microparticles.," *J. Biomed. Mater. Res. A*, vol. 102, no. 11, pp. 3872–82, Nov. 2014.
- [113] T. Miao, K. S. Rao, J. L. Spees, and R. A. Oldinski, "Osteogenic differentiation of human mesenchymal stem cells through alginate-graft-poly(ethylene glycol) microsphere-mediated intracellular growth factor delivery.," *J. Control. Release*, vol. 192C, pp. 57–66, Jun. 2014.
- [114] S. M. Damaraju, S. Wu, M. Jaffe, and T. L. Arinzeh, "Structural changes in PVDF fibers due to electrospinning and its effect on biological function," *Biomed. Mater.*, vol. 8, no. 4, p. 045007, Aug. 2013.
- [115] L. Marques, L. A. Holgado, R. D. Simões, J. D. A. S. Pereira, J. F. Floriano, L. S. L. S. Mota, C. F. O. Graeff, C. J. L. Constantino, M. A. Rodriguez-Perez, M. Matsumoto, and A. Kinoshita, "Subcutaneous tissue reaction and cytotoxicity of polyvinylidene fluoride and polyvinylidene fluoride-trifluoroethylene blends associated with natural polymers.," *J. Biomed. Mater. Res. B. Appl. Biomater.*, vol. 101, no. 7, pp. 1284–93, Oct. 2013.
- [116] C. Ribeiro, J. Pärssinen, V. Sencadas, V. Correia, S. Miettinen, V. P. Hytönen, and S. Lanceros-Méndez, "Dynamic piezoelectric stimulation enhances osteogenic differentiation of human adipose stem cells.," *J. Biomed. Mater. Res. A*, vol. 103, no. 6, pp. 2172–5, Jun. 2015.
- [117] M. T. Rodrigues, M. E. Gomes, J. F. Mano, and R. L. Reis, " β -PVDF Membranes Induce Cellular Proliferation and Differentiation in Static and Dynamic Conditions," *Mater. Sci. Forum*, vol. 587–588, pp. 72–76, 2008.
- [118] J. J. Ficat, G. Escourrou, M. J. Fauran, R. Durroux, P. Ficat, C. Lacabanne, and F. Micheron, "Osteogenesis induced by bimorph polyvinylidene fluoride films," *Ferroelectrics*, vol. 51, no. 1, pp. 121–128, Mar. 1983.
- [119] A. A. Marino, J. Rosson, E. Gonzalez, L. Jones, S. Rogers, and E. Fukada, "Quasi-static charge interactions in bone," *J. Electrostat.*, vol. 21, no. 2–3, pp. 347–360, Sep. 1988.
- [120] J. Reis, C. Frias, C. Canto e Castro, M. L. Botelho, A. T. Marques, J. A. O. Simões, F. Capela e Silva, and J. Potes, "A New Piezoelectric Actuator Induces Bone Formation In Vivo: A Preliminary Study," *J. Biomed. Biotechnol.*, vol. 2012, pp. 1–7, Jan. 2012.
- [121] C. Frias, J. Reis, F. Capela e Silva, J. Potes, J. Simões, and A. T. Marques, "Polymeric piezoelectric actuator substrate for osteoblast mechanical stimulation.," *J. Biomech.*, vol. 43, no. 6, pp. 1061–6, Apr. 2010.
- [122] J. Pärssinen, H. Hammarén, R. Rahikainen, V. Sencadas, C. Ribeiro, S. Vanhatupa, S. Miettinen, S. Lanceros-Méndez, and V. P. Hytönen, "Enhancement of adhesion and promotion of osteogenic differentiation of human adipose stem cells by poled electroactive poly(vinylidene fluoride)," *J. Biomed. Mater. Res. Part A*, vol. 103, no. 3, pp. 919–928, Mar. 2015.
- [123] J. Pawley, "The development of field-emission scanning electron microscopy for imaging biological surfaces.," *Scanning*, vol. 19, no. 5, pp. 324–36, Aug. 1997.
- [124] D. M. Correia, R. Gonçalves, C. Ribeiro, V. Sencadas, G. Botelho, J. L. G. Ribelles, and S. Lanceros-Méndez, "Electrosprayed poly(vinylidene fluoride) microparticles for tissue engineering applications," *RSC Adv.*, vol. 4, no. 62, p. 33013, Jul. 2014.
- [125] V. Sencadas, R. Gregorio, and S. Lanceros-Méndez, " α to β Phase Transformation and Microstructural Changes of PVDF Films Induced by Uniaxial Stretch," May 2009.
- [126] R. Gregorio and M. Cestari, "Effect of crystallization temperature on the crystalline phase content and morphology of poly(vinylidene fluoride)," *J. Polym. Sci. Part B Polym. Phys.*, vol. 32, no. 5, pp. 859–870, Apr. 1994.

- [127] V. A. Bershtein and V. M. Egorov, *Differential Scanning Calorimetry of Polymers: Physics, Chemistry, Analysis, Technology*. Ellis Horwood, 1994.
- [128] A. R. Williams and J. M. Hare, "Mesenchymal stem cells: biology, pathophysiology, translational findings, and therapeutic implications for cardiac disease.," *Circ. Res.*, vol. 109, no. 8, pp. 923–40, Sep. 2011.
- [129] BD Biosciences, "Introduction to Flow Cytometry: A Learning Guide," in *Manual Part Number: 11-11032-01*, Becton and Dickinson Company, 2000, p. 52.
- [130] M. Nasir, H. Matsumoto, T. Danno, M. Minagawa, T. Irisawa, M. Shioya, and A. Tanioka, "Control of diameter, morphology, and structure of PVDF nanofiber fabricated by electrospray deposition," *J. Polym. Sci. Part B Polym. Phys.*, vol. 44, no. 5, pp. 779–786, Mar. 2006.
- [131] J. Doshi and D. H. Reneker, "Electrospinning process and applications of electrospun fibers," *J. Electrostat.*, vol. 35, no. 2–3, pp. 151–160, Aug. 1995.
- [132] C. L. Casper, J. S. Stephens, N. G. Tassi, D. B. Chase, and J. F. Rabolt, "Controlling Surface Morphology of Electrospun Polystyrene Fibers: Effect of Humidity and Molecular Weight in the Electrospinning Process," *Macromolecules*, vol. 37, no. 2, pp. 573–578, Jan. 2004.
- [133] Y. Bormashenko, R. Pogreb, O. Stanevsky, and E. Bormashenko, "Vibrational spectrum of PVDF and its interpretation," *Polym. Test.*, vol. 23, no. 7, pp. 791–796, Oct. 2004.
- [134] R. Pankov, "Fibronectin at a glance," *J. Cell Sci.*, vol. 115, no. 20, pp. 3861–3863, Oct. 2002.
- [135] D. M. Kalaskar, J. E. Downes, P. Murray, D. H. Edgar, and R. L. Williams, "Characterization of the interface between adsorbed fibronectin and human embryonic stem cells.," *J. R. Soc. Interface*, vol. 10, no. 83, p. 20130139, Jun. 2013.
- [136] J.-H. Kim, D. W. Jekarl, M. Kim, E.-J. Oh, Y. Kim, I. Y. Park, and J. C. Shin, "Effects of ECM protein mimetics on adhesion and proliferation of chorion derived mesenchymal stem cells.," *Int. J. Med. Sci.*, vol. 11, no. 3, pp. 298–308, Jan. 2014.
- [137] H.-S. Hung, C.-M. Tang, C.-H. Lin, S.-Z. Lin, M.-Y. Chu, W.-S. Sun, W.-C. Kao, H. Hsien-Hsu, C.-Y. Huang, and S. Hsu, "Biocompatibility and favorable response of mesenchymal stem cells on fibronectin-gold nanocomposites.," *PLoS One*, vol. 8, no. 6, p. e65738, Jan. 2013.
- [138] R. McBeath, D. M. Pirone, C. M. Nelson, K. Bhadriraju, and C. S. Chen, "Cell shape, cytoskeletal tension, and RhoA regulate stem cell lineage commitment.," *Dev. Cell*, vol. 6, no. 4, pp. 483–95, Apr. 2004.
- [139] M. J. Dalby, N. Gadegaard, R. Tare, A. Andar, M. O. Riehle, P. Herzyk, C. D. W. Wilkinson, and R. O. C. Oreffo, "The control of human mesenchymal cell differentiation using nanoscale symmetry and disorder.," *Nat. Mater.*, vol. 6, no. 12, pp. 997–1003, Dec. 2007.
- [140] K. A. Kilian, B. Bugarija, B. T. Lahn, and M. Mrksich, "Geometric cues for directing the differentiation of mesenchymal stem cells.," *Proc. Natl. Acad. Sci. U. S. A.*, vol. 107, no. 11, pp. 4872–7, Mar. 2010.
- [141] A. J. Engler, S. Sen, H. L. Sweeney, and D. E. Discher, "Matrix elasticity directs stem cell lineage specification.," *Cell*, vol. 126, no. 4, pp. 677–89, Aug. 2006.
- [142] D. Zhang and K. A. Kilian, "The effect of mesenchymal stem cell shape on the maintenance of multipotency.," *Biomaterials*, vol. 34, no. 16, pp. 3962–9, May 2013.
- [143] C. M. Antolinos-Turpín, R. M. Morales Román, J. Ródenas-Rochina, J. L. G. Ribelles, and J. A. Gómez-Tejedor, "Macroporous thin membranes for cell transplant in regenerative medicine," *Biomaterials*, vol. 67, pp. 254–263, Jul. 2015.
- [144] A. Ode, J. Schoon, A. Kurtz, M. Gaetjen, J. E. Ode, S. Geissler, and G. N. Duda, "CD73/5'-ecto-nucleotidase acts as a regulatory factor in osteo-/chondrogenic differentiation of mechanically

- stimulated mesenchymal stromal cells.," *Eur. Cell. Mater.*, vol. 25, pp. 37–47, Jan. 2013.
- [145] M. Takedachi, H. Oohara, B. J. Smith, M. Iyama, M. Kobashi, K. Maeda, C. L. Long, M. B. Humphrey, B. J. Stoecker, S. Toyosawa, L. F. Thompson, and S. Murakami, "CD73-generated adenosine promotes osteoblast differentiation.," *J. Cell. Physiol.*, vol. 227, no. 6, pp. 2622–31, Jun. 2012.
- [146] W. Wagner, P. Horn, M. Castoldi, A. Diehlmann, S. Bork, R. Saffrich, V. Benes, J. Blake, S. Pfister, V. Eckstein, and A. D. Ho, "Replicative senescence of mesenchymal stem cells: a continuous and organized process.," *PLoS One*, vol. 3, no. 5, p. e2213, Jan. 2008.
- [147] A. Stolzing, E. Jones, D. McGonagle, and A. Scutt, "Age-related changes in human bone marrow-derived mesenchymal stem cells: consequences for cell therapies.," *Mech. Ageing Dev.*, vol. 129, no. 3, pp. 163–73, Mar. 2008.
- [148] H. I. Roach, "Why does bone matrix contain non-collagenous proteins? The possible roles of osteocalcin, osteonectin, osteopontin and bone sialoprotein in bone mineralisation and resorption.," *Cell Biol. Int.*, vol. 18, no. 6, pp. 617–28, Jun. 1994.
- [149] Boundless, "Cell Types in Bones," *Boundless Biology*, 2015. [Online]. Available: <https://www.boundless.com/biology/textbooks/boundless-biology-textbook/the-musculoskeletal-system-38/bone-216/cell-types-in-bones-816-12058/>.